When Governments Look Away: Extremist Violence in the West Bank*

Adriano Amati

ETH Zürich

Abstract

Why do governments fail to restrain non-state violence when they can? Existing accounts emphasize weak capacity, direct state organization of violence, or strategic relationships with armed groups. They say less about decentralized violence enabled through enforcement choices. I develop a theory of institutional forbearance: governments may relax enforcement when violence advances goals they value, and anticipated leniency weakens deterrence. I test the argument in the West Bank, where radical settlers pursue territorial objectives partly shared by members of the Israeli government. Trump's 2016 election sharply reduced U.S. pressure on Israel, lowering external costs of forbearance. Using difference-in-differences, I compare changes across locations differing in pre-election suitability for settlement expansion. Settler violence against Palestinians rises disproportionately in high-suitability locations, increasing sharply in January 2018 and remaining elevated through 2023. Institutional forbearance thus enables non-state violence through selective enforcement without requiring centralized direction or an explicit agreement.

JEL Classification: C21, C31, D72, D74, F51, Z13
Keywords: Political violence, institutional forbearance, settler violence, territorial conflict, Israeli-Palestinian conflict, satellite data, diplomatic shocks, difference-in-differences

*I am grateful to Marco Di Cataldo, Giovanni Mastrobuoni, Juan Vargas, Livia Schubiger, Paolo Buonanno, Ruben Durante, Belal Fallah, Sergi Martínez, Jonathan Elkobi, Claudia Marangon, Matteo Machiorlatti, Gianmarco Torchetti, Francisco Tomás-Valiente Jordá and Luca Scotti for helpful comments and discussions. I also thank conference and seminar participants at the European Public Choice Society (EPCS), the IRDS and ICR research groups at ETH Zürich, the London School of Economics, and Sapienza University of Rome for valuable feedback. I owe a particular debt to Dror Etkes for the time he generously devoted to this project and for the data he shared. Finally, this research project would not have been possible without the work of Peace Now, B'Tselem, Yesh Din, and Kerem Navot. All remaining errors are my own.

Email address: adriano.amati@gess.ethz.ch (Adriano Amati)

1. Introduction

The standard explanation for why states fail to restrain violent non-state actors is that they cannot: the state lacks the capacity to police its territory, and violence fills the vacuum (Fearon and Laitin, 2003; Migdal, 1988; Herbst, 2000). Yet enforcement also fails where capacity is abundant, and existing work explains such tolerance mainly through organization and exchange: governments delegate violence to militias and armed auxiliaries to obtain information, manpower, and deniability (Carey et al., 2013; Jentzsch et al., 2015); tolerate paramilitaries in exchange for electoral or security benefits (Acemoglu et al., 2013); strike wartime bargains with insurgent organizations (Staniland, 2012) or calibrate repression in ongoing confrontations with criminal groups (Lessing, 2015, 2018). In each account the state commands the perpetrators, bargains with them, or is repaid for its tolerance.

Some episodes fit neither account. In Bolsonaro-era Brazil, permissive environmental politics coincided with Amazon land grabbing (Caetano, 2021; Nunes et al., 2024); in BJP-era India, cow-protection politics accompanied vigilante violence against Muslims and Dalits (Human Rights Watch, 2019; Maskara, 2021). In these cases capacity is not the binding constraint, and the perpetrators are not state agents or formal militias: no order directs them and no bargain binds them. They are private actors whose violence advances objectives that political elites might share. The question is therefore why a government with extensive coercive and administrative authority enforces the law selectively, that is, why it looks away.

This paper studies exactly this configuration. When privately initiated violence advances objectives the government partly shares, political authorities can benefit from it without directing or organizing it, simply by choosing how strongly to enforce the law against its perpetrators. Non-state actors—I refer to them as *aligned actors*—decide whether to use violence by weighing its expected returns against the punishment they expect to face, and enforcement is what sets that punishment. I formalize this argument in a simple model of *institutional forbearance*, borrowing the term from Holland (2016).

In the model, the government moves first and chooses how strongly to enforce the law against aligned non-state actors. It values some of the political or territorial gains their actions can produce, but bears the legal, diplomatic, institutional, and domestic costs of tolerating them. The actors then observe this enforcement environment and decide whether to use violence. Their decision depends on three elements: their underlying willingness to use violence, the punishment they expect to face, and the local productivity of violence, i.e. the extent to which violent action can generate material or strategic gains.

The model therefore yields a simple set of predictions. Greater forbearance lowers expected punishment and increases violence. The effect should also be stronger where violence is more productive, since tolerance is more valuable both to the actors who use violence and to a government that partly values the gains it produces. The costs of tolerance are generated by the political and institutional constraints on forbearance—domestic accountability pressures and external diplomatic pressure that make non-enforcement costly for the government. These constraints enter only through the government's problem: for instance, an external political shift that weakens them lowers the cost of tolerance, increases equilibrium forbearance and, through it, violence. An extension of the model endogenizes these constraints: tolerated radical action builds the institutional leverage of the constituency it benefits, which relaxes future constraints in turn. A temporary external shock can therefore leave forbearance and violence persistently above their pre-shock levels, and, when the feedback is strong enough, move the system to a durably more permissive and violent equilibrium (Appendix F.7).

The West Bank provides a unique setting to test these predictions. Israeli authority in the territory is extensive, making a lack of capacity argument unlikely. The relevant aligned actors are radical settlers associated with unauthorized outposts—sites established without the approvals required under the legal and administrative regime Israel applies in Area C (Supreme Court of Israel, sitting as the High Court of Justice, 2014, 2011; Kurtzer, 2016).[1] Their expansion can generate territorial gains that Israeli governments have often valued,[2] and the gains require no act of authorization: tolerated encroachment creates facts on the ground by itself. Moreover, the model's other central components are largely fixed in the relevant time-period: the same Netanyahu government remained in office from 2015 through 2019, the argument does not require radical settlers' underlying preferences to change, and the geographic characteristics determining

[1]"Authorized" throughout means authorized within that Israeli-administered regime, not lawful under international law. The ICJ, the ICRC, and the UN Security Council regard the West Bank, including East Jerusalem, as occupied and Israeli settlement policy as contrary to Article 49(6) of the Fourth Geneva Convention (International Court of Justice, 2024; International Committee of the Red Cross, 2024; United Nations Security Council, 2016); Israel disputes both (Ministry of Foreign Affairs, State of Israel, 2015). Israel's Supreme Court applies the law of belligerent occupation to the military commander but has generally avoided ruling on the legality of settlements as a class (Supreme Court of Israel, sitting as the High Court of Justice, 2005).

[2]Weymouth (2013); Ynetnews (2015); Heilman (2015); Israel Hayom (2017)

where territorial expansion is feasible are predetermined. What changes is an important external component of the government's cost of tolerance.

Donald Trump's unexpected election in November 2016 provides that change. The election was plausibly exogenous with respect to local violence and outpost expansion in the West Bank, and it marked a sharp reversal from the Obama administration's opposition to settlement expansion. The shift was reinforced by subsequent policy decisions, most visibly the December 2017 recognition of Jerusalem as Israel's capital. In the language of the model, this change reduced the diplomatic cost to Israeli political elites of tolerating radical settler activity, and a clear prediction follows: violence should rise after the political shift, and most where radical action can produce larger territorial gains.

Testing this prediction requires separating exposure to the radical frontier from the endogenous placement of outposts themselves, which emerge where geography, land access, and proximity to the existing settler network make encroachment feasible, the same features that may independently shape violence. I therefore construct a pre-determined measure of exposure from a model of outpost expansion estimated on pre-election data alone, combining local geography with the dynamics of the pre-2016 outpost network. The resulting suitability measure captures where territorial encroachment was most feasible on the eve of the shock. I then compare the monthly evolution of violence across a fine spatial grid between cells with high and low pre-determined suitability, tracing the dynamic response through the Trump's election, his inauguration, the Jerusalem Declaration and other relevant events.

The findings are consistent with the model. Violence rises significantly more in high-suitability areas after Trump's election, with the sharpest escalation following the December 2017 Jerusalem Declaration, and the effects persist through 2023. The effect is sizable: settler violence increases roughly 10-fold in high suitability areas from the pre-election baseline. An agnostic structural-break procedure that dates the shift from the data rather than imposing it recovers the same staged pattern: a first, modest break in April 2017, the main escalation in January 2018, and no comparable break in Palestinian violence against settlers until 2022. The response is also asymmetric: settler violence rises sharply and remains elevated over the long run, while Palestinian violence initially concentrates against the Israeli security apparatus rather than civilians. This timing is difficult to reconcile with a simple symmetric retaliation story and instead suggests an initial activation of radical settlers, followed by a slower and more generalized conflict dynamic. Moreover, the long-run persistence is consistent with the dynamic extension: a temporary shock shifts the system to a durably more violent equilibrium.

The geography of the response provides a more informative test of the theory. The increase concentrates at the radical outpost frontier rather than near established settlements more generally, indicating that it is not a simple by-product of Israelis and Palestinians living close to one another. More importantly, conditional on where outposts already stood before 2016, settler violence still rises after the shock in the places where further expansion was most feasible. Palestinian violence against settlers shows the opposite pattern: it follows where outposts already stood, not where expansion was feasible. The two margins identify different kinds of violence. Palestinian violence tracks presence because it is directed at an adversary who must be there to be attacked; settler violence tracks *opportunity*. This pattern is consistent with an encroachment dynamic in which violence is deployed where territory can still be taken rather than in defense of ground already held. The territorial gains subsequently materialize: after the Jerusalem Declaration, new outposts appear disproportionately in the same high-opportunity locations where violence rises, completing the sequence the model describes: permissiveness has its strongest effects where violence can produce durable territorial gains.

The descriptive evidence on how settler violence was received completes the picture. ACLED-recorded IDF–settler confrontations, a narrow proxy for one visible component of coercive enforcement, remain rare and do not scale with increases in settler violence. I also gather Knesset speeches in the 15-day window following each fatality event—a Palestinian killing a settler or vice versa—and document that right-wing blocs condemn and demand enforcement for killings by Palestinians far more readily than for comparable killings by settlers. Forbearance itself is not directly observable, but these are its observable traces on the two margins the model identifies: observable coercive enforcement that does not track the violence it should respond to, and a domestic constraint on forbearance that is persistently weak. External diplomatic pressure constituted an important additional constraint on tolerating radical settlers. The U.S. reversal relaxed precisely this constraint, providing the weakening of political constraints on forbearance that the model highlights.

The paper contributes to the literature on state and non-state violence by identifying a distinct way governments can benefit from privately initiated violence without organizing it. Existing work shows that political incentives shape whether governments protect civilians from communal violence (Wilkinson, 2004; Nellis et al., 2016), and that governments may tolerate or cooperate with organized armed groups that provide electoral, military, or political benefits (Acemoglu et al., 2013; Staniland, 2015; Dube and Naidu, 2015). The mechanism here is different. Aligned actors pursue their own ideological objectives and initiate violence independently; political authorities need neither explicitly direct them (Yanagizawa-Drott, 2014) nor bargain or reach tacit accommodations with them to benefit from the outcomes they produce (Staniland, 2012).[3] Their instrument is enforcement itself. By deciding how costly privately initiated violence will be, governments can encourage or restrain actions that advance objectives they partly share while remaining formally separate from those who carry them out. Extending Holland (2016), the object of non-enforcement is not informal redistribution but violence: looking away changes the expected price of violent action. The paper shows theoretically and empirically when this form of indirect political support becomes consequential—when the outcomes produced by aligned violence are sufficiently valuable to political authorities.

The argument also relates to research on elite signaling and norm erosion. Political shocks can change behavior by altering the social sanctions attached to previously stigmatized views and actions (Bursztyn et al., 2020; Giani and Méon, 2021; Müller and Schwarz, 2023; Albornoz et al., 2022; Alvarez-Benjumea and Valentim, 2024). This paper points to a different sanctioning institution. When the relevant behavior is illegal, political authorities themselves determine an important component of its expected cost through enforcement. Political change can therefore affect private behavior not only by changing what others are willing to condone (Bursztyn et al., 2020; Giani and Méon, 2021), but also by changing what the state is willing to punish. The contribution here is to study this latter margin in a setting where private actors' actions can themselves advance objectives valued by political authorities.

Finally, the paper offers a new lens on the Israeli-Palestinian conflict, where empirical work has focused on the strategic behavior of recognized actors or the economic effects of occupation (Durante and Zhuravskaya, 2018; Jaeger et al., 2012; Calì and Miaari, 2018; Adnan, 2015). It does so by assembling a novel fine-grained spatial dataset that combines geo-referenced violent events, comprehensive mappings of Israeli settlements, outposts, and Palestinian communities, satellite-based detection of outpost emergence,

[3] This characterization applies primarily to the period studied here. Since the coalition formed at the end of December 2022, and especially after the events of October 7 2023, the boundary between state and settler violence has become increasingly blurred (Office of the United Nations High Commissioner for Human Rights, 2023).

and Knesset parliamentary speeches, connecting shifts in external political constraints to local violence on the ground.

The remainder of the paper proceeds as follows. Section 2 presents the formal model. Section 3 provides historical and political context. Section 4 describes the data and Section 5 the empirical strategy. Section 6 presents the main findings. Section 7 examines the geography of the response, separating territorial opportunity from radical presence. Section 8 provides additional evidence on outpost expansion and the reception of settler violence. Section 9 presents robustness checks and Section 10 concludes.

2. Theoretical Framework

This section develops a model of enforcement forbearance from which the paper's empirical predictions derive. I adapt Holland (2016)'s concept of *forbearance*: intentional and revocable non-enforcement, in which the state retains the capacity to sanction a legal violation but chooses not to do so. As in Holland (2016), non-enforcement is therefore a political choice rather than evidence of limited state capacity. The difference lies in what makes that choice valuable. Holland (2016) studies forbearance as distributive policy, through which politicians tolerate illegal activity in order to benefit constituencies and obtain electoral support or rents. Here, the government instead partially values the political gains generated by non-state actors' actions. The model formalizes the interaction between private actors' incentives, government enforcement decisions, and the political and institutional constraints on forbearance.[4]

Primitives and payoffs Consider locations indexed by $i = 1, \ldots, N$. In each location, a radical non-state actor chooses violence $v_i \geq 0$. A government or political executive chooses local enforcement or forbearance,

$$f_i \in [0, 1],$$

where $f_i = 0$ denotes full enforcement and $f_i = 1$ full tolerance. Under full enforcement, radical actors face the full expected punishment cost. More generally, f_i captures the permissiveness of the enforcement environment faced by the actor, including expected

[4]The framework could be extended to distinguish between aligned and non-aligned radical actors, and to allow the state to choose direct force against the latter. This richer setting is beyond the scope of the paper.

intervention, prosecution, or other sanctions. In the empirical analysis, this is the latent enforcement margin the supporting evidence seeks to characterize.

The political and institutional environment is summarized by S. Higher values of S correspond to weaker scrutiny: a more permissive environment in which tolerance carries lower diplomatic, legal, political, or institutional costs.[5]

Each location has local opportunity $E_i \geq 0$, which captures the extent to which violence can produce strategic gains in location i. The strategic return to violence is $\pi(E_i)$, with $\pi(E_i) \geq 0$ and $\pi_E(E_i) > 0$. Thus, violence is more productive in high-opportunity locations. In the empirical analysis, this object maps to the geographic scope for territorial expansion. Forbearance determines how much of this local opportunity the radical actor can exploit.

Given f_i, the radical actor chooses violence to maximize

$$U_i^R(v_i; f_i) = [r_i + f_i\pi(E_i) - (1 - f_i)L]\, v_i - K_i(v_i),$$

where r_i is the actor's intrinsic return to violence, $L > 0$ is the punishment or enforcement cost under full enforcement, and $K_i(v_i)$ is a strictly convex private cost of violence.

The government partially internalizes the political or territorial gains generated by radical action. This is summarized by $\lambda \in [0, 1]$, which captures the extent to which the government values gains produced through violence by aligned non-state actors. I treat λ as fixed with respect to S, so changes in permissiveness operate through the cost of tolerating radical action rather than through government preferences. In the empirical analysis, $\lambda > 0$ corresponds to settings in which privately generated territorial or political gains overlap with government objectives.

For any induced level of violence v_i, the government's local payoff is

$$U_i^G(f_i, v_i; S) = \lambda f_i \pi(E_i) v_i - C_i(f_i, v_i; S).$$

The term $f_i\pi(E_i)v_i$ is realized violent output and λ the extent to which the government values these gains.[6] The cost function $C_i(f_i, v_i; S)$ collects the legal, diplomatic, institutional, and public-order costs of tolerating radical violence. I assume $C_i^f(f_i, v_i; S) \geq$

[5] S affects the government's cost of tolerance, not the underlying preferences of either the government or the radical actor.

[6] When $\lambda = 0$, the government derives no benefit from these gains.

0, with strict inequality for $f_i > 0$, and $C_i^v(f_i, v_i; S) \geq 0$. Weaker political constraints lower the relevant marginal costs, so $C_i^{fS}(f_i, v_i; S) \leq 0$ and $C_i^{vS}(f_i, v_i; S) \leq 0$.[7] Thus, a higher S lowers the marginal cost of tolerating radical action. The cost function bundles constraints of different origin, including domestic accountability pressures, such as parliamentary scrutiny, electoral backlash, judicial oversight, and media attention, as well as external diplomatic pressure. The empirical analysis considers evidence on both margins.

Timing and equilibrium The game unfolds sequentially. First, S is realized. Second, the government chooses local forbearance f_i. Third, the radical actor observes f_i and chooses violence v_i. Forbearance is an observable enforcement stance that remains operative while the actor acts. I solve the model by backward induction.

The radical actor is inactive when the net marginal payoff from violence is too low. On the active branch, i.e. $v_i^* > 0$, the best response satisfies

$$v_i^*(f_i) = (K_i')^{-1}\left(r_i - L + f_i[\pi(E_i) + L]\right).$$

Thus, forbearance increases violence because it lowers expected punishment and allows radical actors to exploit local opportunity. On the active branch, the radical actor's best response is increasing in f_i.

Anticipating this best response, the government chooses f_i to solve

$$f_i^* \in \arg\max_{f_i \in [0,1]} \left\{\lambda f_i \pi(E_i) v_i^*(f_i) - C_i\left(f_i, v_i^*(f_i); S\right)\right\}.$$

If several choices maximize the government's payoff, I select the largest. At an interior optimum, the government balances the additional political gains from radical action against the additional costs of tolerating it. A more permissive political environment lowers the relevant marginal costs, making greater forbearance more attractive. Equilibrium forbearance and violence therefore cannot decrease: greater tolerance can activate violence or raise its level where actors are already active. This response operates through enforcement rather than through changes in actors' underlying preferences or in the government's valuation of their political goals.[8] The framework delivers two main empirical predictions.

[7] At least one inequality is strict in the relevant interior region.

[8] Appendix F establishes global monotonicity and provides a stylized numerical illustration.

Prediction 1: Political permissiveness increases violence. Weaker political constraints on forbearance lower the marginal cost of non-enforcement. In schematic form,

$$S \uparrow \quad \Rightarrow \quad \text{marginal cost of forbearance} \downarrow \quad \Rightarrow \quad f_i^* \uparrow \quad \Rightarrow \quad v_i^* \uparrow .$$

The government tolerates more radical action, and radical actors respond by increasing violence.[9]

Prediction 2: Effects are stronger in high-opportunity locations. Other things equal, greater permissiveness should have its largest effects where violence can generate larger strategic gains. On the active branch,

$$\frac{\partial v_i^*}{\partial f_i} = \frac{\pi(E_i) + L}{K_i''(v_i^*)}.$$

Higher E_i raises the potential gains from a relaxation in enforcement through $\pi(E_i)$. It can also lower the level of forbearance required for violence to become privately worthwhile. Under the conditions stated in Appendix F, higher opportunity therefore facilitates activation and amplifies the response once actors are active.[10] Empirically, this predicts a larger increase in violence where the scope for territorial expansion is greater.

Dynamic extension The static model explains the activation of violence but does not let violence reshape the environment in which enforcement decisions are made. In Appendix F.7 I endogenize part of that environment by allowing tolerated violence that produces material gains to increase leverage over the institutions governing future enforcement. This creates a feedback: weaker constraints raise forbearance and violence today, while successful tolerated violence weakens those constraints tomorrow. A temporary shock can therefore leave forbearance and violence elevated after external conditions revert and, when the feedback is strong enough, push the system past a threshold beyond which the political environment remains durably more permissive. Non-enforcement remains revocable throughout—the state retains the capacity to enforce—but the political conditions governing whether that capacity is exercised need not return to their initial

[9]The last two arrows are weak in general and strict at regular active interior optima with a strict marginal-cost reduction.

[10]The ranking holds locally at active interior equilibria under quadratic private costs and the government-response complementarity condition in Appendix F.

configuration.[11]

3. Background

3.1. Historical Context

The Israeli-Palestinian conflict is one of the most protracted disputes in modern history. A major turning point came with the 1967 Six-Day War, when Israel occupied the West Bank, the Gaza Strip, the Golan Heights, and Sinai. Following the occupation, Israeli citizens began establishing civilian settlements in the West Bank, the Golan Heights and, for a time, in the Gaza Strip.[12] The ICJ, the ICRC, and the Security Council regard Israeli settlement policy in the occupied Palestinian territory, including East Jerusalem, as contrary to international law.[13] Settlement construction began under left-wing governments and intensified after 1977 with the Likud party's victory (Pappe, 2017; Hirsch-Hoefler and Mudde, 2020).[14] The 1993 Declaration of Principles then initiated an interim framework for Palestinian self-government and permanent-status negotiations, and the 1995 Interim Agreement, known as Oslo II, divided the West Bank into Areas A, B and C (Government of Israel and Palestine Liberation Organization, 1993, 1995). The Palestinian Authority assumed civil affairs and public order in Areas A and B and internal security in Area A, while Israel retained external security, the security of Israelis, overriding security responsibility in Area B and, in Area C—roughly 60% of the territory—all powers not transferred to it. Some redeployments occurred, but the process was never completed: the 2000 Camp David summit collapsed, the Second Intifada followed, and Area C remained under Israeli control and became the central arena of settlement expansion.

Beginning in the early 1990s, unauthorized structures known as *outposts* began to emerge throughout the West Bank. These are small clusters of structures, often established by ideologically motivated settlers without all the required governmental and

[11] This feedback is inspired by the decentralized-violence extension in Bisin et al. (2026), in which greater political weight for a violent group reduces police enforcement and increases private violence.

[12] Settlements in the Gaza Strip were dismantled in 2005 as part of Israel's unilateral disengagement plan.

[13] United Nations Security Council (1979a, 2016); International Committee of the Red Cross (1949); International Court of Justice (2024); International Committee of the Red Cross (2024). Israeli settlement in the Golan Heights is addressed separately by United Nations Security Council (1981).

[14] Likud (Hebrew for 'Consolidation') is the major center-right to right-wing political party in Israel. Its 1977 electoral victory ended nearly three decades of left-wing political dominance.

planning approvals, that have proliferated over the last decades (Peace Now, 2017b).[15] Typically located on hilltops, they often begin as temporary encampments and evolve into agricultural or shepherding farms that enable control over large surrounding areas (B'Tselem, 2021), and their expansion has been facilitated by political authorities at times permissive or ambivalent toward their presence (Peace Now, 2017a; B'Tselem, 2021). Figure 1 shows that after an increase around the 2nd Intifada (2000–2005) and a period of stability, outpost creation rises again from 2017–2018 and remains high through 2023.

Figure 1: Outposts in the Occupied West Bank

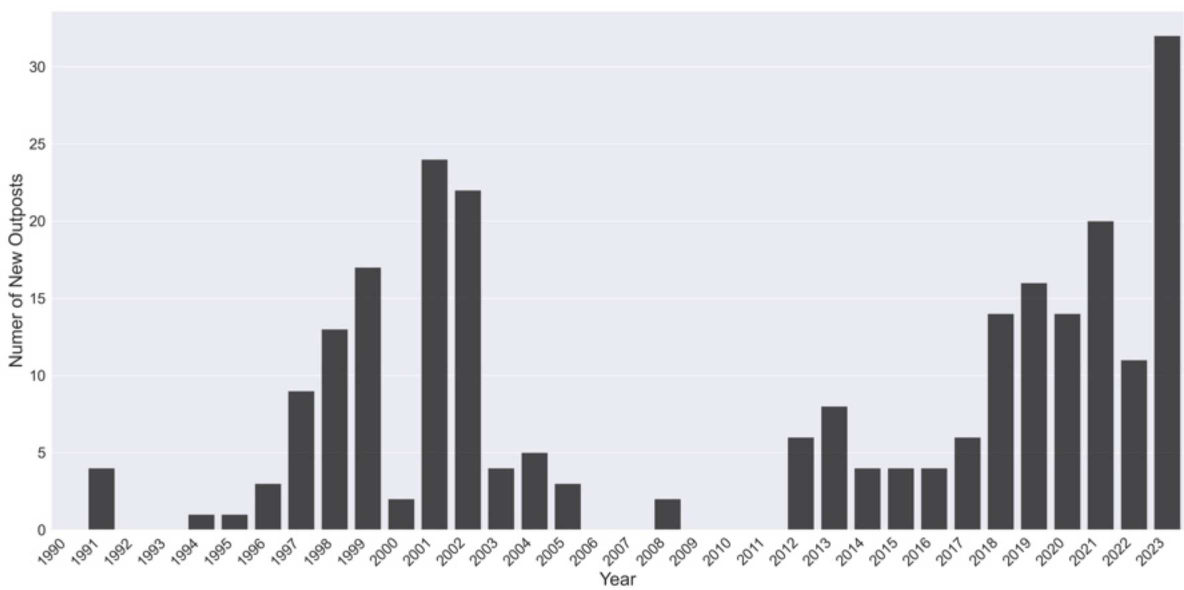

Notes: Number of new outposts created over time. Source B'Tselem (2024) and Peace Now (2024).

Outposts are closely associated with the "hilltop youth"—loosely organized settlers, often from second- or third-generation settler families, who operate in small, loosely autonomous groups and reject formal authority (Shalom Hartman Institute, 2022; Koplewitz, 2025). Their activities center on creating "facts on the ground": asserting territorial claims, pre-empting future concessions, and displacing Palestinian communities (Koplewitz, 2025; Peace Now, 2017a). This combination of ideological motivation, decentralized organization, and weak external constraint makes the outpost frontier particularly rele-

[15]Status varies across sites and over time, and some outposts are later granted recognition or planning authorization. The Migron and Amona judgments (Supreme Court of Israel, sitting as the High Court of Justice, 2011, 2014) concern particular outposts built on privately owned Palestinian land.

vant for understanding localized violence.[16] By contrast, government-authorized settlements mainly draw residents who are not ideologically motivated and who move largely because of housing costs and other cost-of-living considerations.[17]

3.2. Trump's Election & the Jerusalem Declaration

The Trump-era shift marked a break from the preceding U.S. policy environment. The Obama administration consistently opposed settlement expansion and described continued settlement activity as illegitimate. In December 2016 the United States abstained, allowing the adoption of Security Council Resolution 2334, which stated that the establishment of settlements had "no legal validity" and constituted a "flagrant violation under international law" (United Nations Security Council, 2016).[18] This period also coincided with Israeli efforts to strengthen enforcement against settler crime, including the creation of a dedicated Nationalistic Crime Unit (U.S. Department of State, 2023).[19] Consistent with these tighter constraints on forbearance, OCHA documents a steady decline in settler violence between 2013 and 2016, followed by a renewed increase in 2017 (OCHA, 2017).

Trump's election marked a departure from this trajectory. During the campaign, he had signaled strong support for Israel and openness to settlement expansion, breaking with longstanding bipartisan restraint. Four days after his inauguration, Israel's Defense Ministry announced plans to advance approximately 2,500 housing units in West Bank settlements (Kershner, 2017). In February 2017 the Knesset enacted the Regularization Law, which let the state take possession and use rights over privately owned Palestinian land and allocate them to settlements, an appropriation the owners had no right to refuse; in 2020 the High Court of Justice invalidated it (Supreme Court of Israel, sitting as the

[16]Figure E.32 in the Appendix shows that polling stations within 2 km of an outpost consistently record higher vote shares for right-wing and far-right parties than those farther away, with support near outposts remaining above 80%.

[17]Ben-Shahar et al. (2019)

[18]The last adopted Security Council resolution with comparably explicit settlement language was Resolution 465 in 1980 (United Nations Security Council, 1980a). Earlier settlement resolutions, 446 and 452 in 1979 (United Nations Security Council, 1979b), had passed with U.S. abstentions. Between 1980 and 2016, comparable settlement-focused drafts were blocked by U.S. vetoes, including S/15895 (1983), S/1997/199 and S/1997/241 (1997), and S/2011/24 (2011) (United Nations Security Council, 1983, 1997a,b, 2011).

[19]The State Department report notes that the unit was tasked with preventing and investigating ideologically motivated offenses in the West Bank, while also reporting that arrests in such cases rarely led to indictments or convictions (U.S. Department of State, 2023).

Figure 2: Number of Daily Violent Events in the West Bank

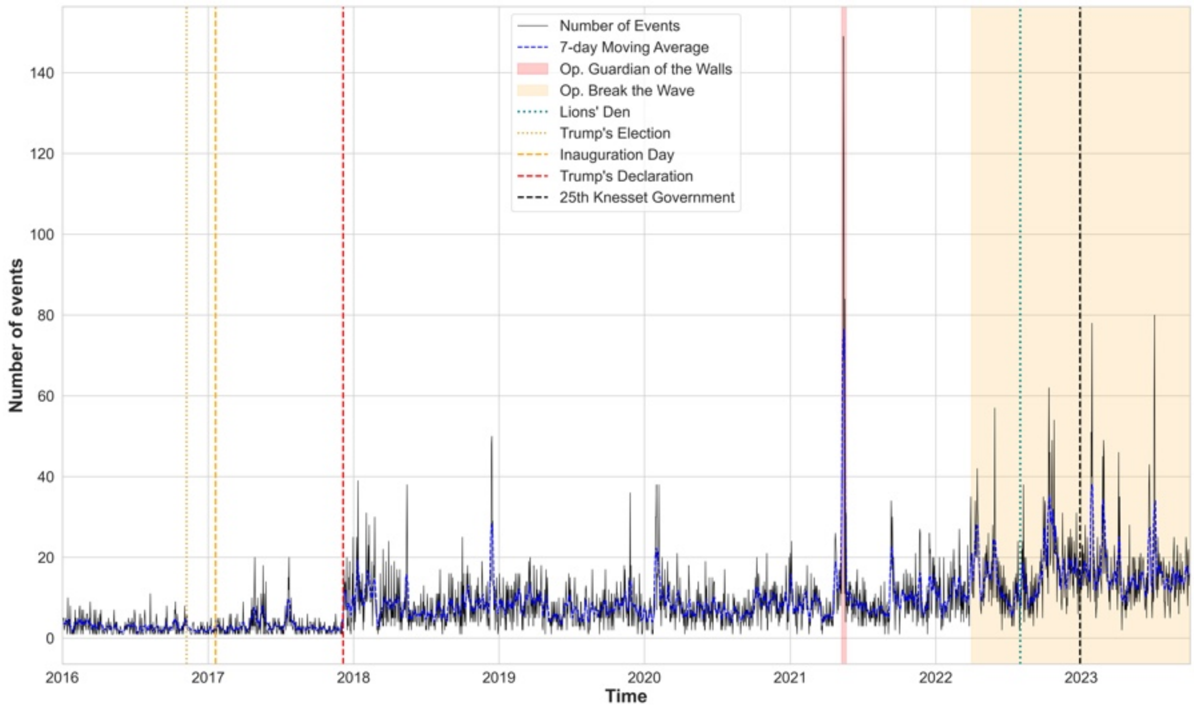

Notes: Time series of daily violent events in the West Bank, retrieved from ACLED. The dashed vertical lines indicate key dates in the political shock sequence: Trump's election (Nov 2016), inauguration (Jan 2017), and the recognition of Jerusalem (Dec 2017). Shaded areas depict important events following the Jerusalem Declaration, such as Operation Guardian of the Walls and Operation Break the Wave, as well as the birth of the Palestinian militia Lion's Den. The dashed blue line is a 7 day moving average. The series extends to September 2023.

High Court of Justice, 2020; Sharvit Baruch, 2020).[20] The shift became operational in March 2017: the cabinet approved the establishment of Amichai as permanent housing for the evacuees from the Amona outpost[21], a decision widely described at the time as approval of the first wholly new government-authorized settlement in roughly two decades (Ahren and TOI Staff, 2017; Haaretz, 2017). I read this sequence as signaling to radical settlers that unauthorized construction ends in compensation, not loss. The same day, the government issued tenders for additional construction and classified some

[20]Owners retained underlying title and were compensated with 125% of use value or alternative land. Chief Justice Hayut wrote that the law *"knowingly and unequally infringes upon the property rights of Palestinian residents of the area alone"* (Supreme Court of Israel, sitting as the High Court of Justice, 2020).

[21]The Supreme Court ordered full evacuation of the outpost in December 2014. The government sought delays, and the evacuation was carried out only in February 2017 (Reuters Staff, 2017c; Times of Israel Staff, 2016; Reuters Staff, 2017a,b).

900 dunams[22] around existing outposts as "state land" under the Israeli-administered land regime (Haaretz, 2017). Figures E.34a and E.34b document a broader increase in state transfers to settlements and construction tenders beginning in 2017.

The most explicit diplomatic signal came on December 6, 2017, when Trump formally recognized Jerusalem as Israel's capital, a move that had been consistently deferred by every preceding U.S. president.[23] Jerusalem lies at the heart of the conflict's most intractable claims: for Israel, it is the biblical heart of the Jewish people and the site of their ancient Temples; for Palestinians, it is the home of the Al-Aqsa Mosque and the intended capital of their future state (European Parliament, 2012).[24] The declaration was particularly salient for radical settlers, who are disproportionately drawn from messianic currents of Religious Zionism within which sovereignty over Jerusalem carries redemptive significance well beyond ordinary diplomacy (Shalom Hartman Institute, 2022; Hershkowitz, 2026).[25] It was therefore perceived as a validation of their maximalist territorial claims, a step toward Jewish sovereignty over the entirety of *Eretz Yisrael*.[26]

The declaration became behaviorally salient in the weeks that followed. It triggered widespread Palestinian mobilization and clashes with Israeli forces, while also reinforcing the perception among radical settlers that territorial assertiveness would face weaker external constraint. In this context, the killing of Rabbi Raziel Shevach by a Palestinian gunman near the unauthorized outpost of Havat Gilad in January 2018 became a focal event for settler violence and demands for consolidation (TOI Staff, 2018). Within days, settler leaders and right-wing lawmakers called for legalization; Netanyahu instructed the Defense Ministry to connect the outpost to the electricity grid, and less than a month later the cabinet unanimously approved the initiation of a process to grant it government recognition and planning authorization (Magid, 2018b,a). The response made the new

[22] Approximately 90 hectares (222 acres). One dunam equals 1,000 square meters.

[23] The proclamation did not determine Jerusalem's boundaries or recognize Israeli sovereignty over the entire city; it expressly left boundaries and other final-status questions to negotiations (Trump, 2017).

[24] East Jerusalem is the portion of the city captured and occupied by Israel during the 1967 Six-Day War. Under international law, it is considered occupied territory (United Nations Security Council, 1980b, 2016).

[25] For some of the most radical activists this symbolism extends to aspirations for the restoration of the Temple, though that stronger position should not be attributed to the settler movement as a whole (Don-Yehiya, 2014; Nicolle-Hasid, 2019).

[26] Hebrew for "Land of Israel", referring to the biblical promised land (Havelock, 2011). In modern political use, particularly by nationalists, it often denotes a territory that includes the West Bank (Jewish Virtual Library, 1977).

permissiveness concrete: violence around an unauthorized outpost was followed by visible efforts to normalize and entrench the outpost itself.

Together, these events mark a sequence of increasing political permissiveness: Trump's election shifted expectations, early 2017 policy moves made the shift concrete, and the Jerusalem Declaration provided its most salient signal. Figure 2 shows modest peaks after Trump's inauguration and the sharpest, most persistent increase after the Jerusalem Declaration and Havat Gilad. The increase never fully reverts, with a consistently higher level of violence through 2023 than in the pre-2017 period.

4. Data

This section describes the data sources used in this study: daily geo-referenced violent events from the ACLED (2024b) project, and comprehensive spatial data from Israeli NGOs and international bodies (Peace Now, 2025; B'Tselem, 2024), complemented by satellite imagery to date outpost emergence (European Union, Copernicus Land Monitoring Service, 2025; Maxar Technologies, 2023).

Political Violence Data ACLED (2024b) maintains daily, geo-referenced records of political violence events, demonstrations, and other politically relevant developments across the West Bank (ACLED, 2024a). The database systematically compiles information from diverse local, national, and international news sources, capturing detailed information on location, timing, and event characteristics, along with a short textual description of each event.[27]

The data starts from January 1, 2016 and is analyzed here through September 2023. For the remainder of the paper, a "violent event" is defined broadly to include not only acts against individuals but also those directed at property, such as looting, property destruction, and so forth. To obtain additional information on the nature of each violent event, I feed the textual description to ChatGPT 5-mini. The model is prompted to classify the main perpetrators of the event, the main targets, and the number of casualties involved. Appendix G describes the procedure and displays validation with a random sample of human-coded events. Figure G.40 shows a mild increase in settler violence

[27] ACLED employs a rigorous data collection methodology, including a tailor-made sourcing process for individual regions and countries. In recent years, several studies have relied on this data source (Kafando and Sakurai, 2024; Rohner et al., 2013; Bertoni et al., 2019; Berman and Couttenier, 2015).

starting 2017, followed by another sharp increase the next year and enduring over time.[28]

Geographic Data I rely on detailed spatial data from two key Israeli civil society organizations. Peace Now, through its Settlement Watch portal, monitors and campaigns against settlement construction. Similarly, B'Tselem, the Israeli Information Center for Human Rights in the Occupied Territories, maintains an updated database on settlements and outposts.[29] I merge these two sources to obtain an exhaustive list of settlements and outposts, alongside Palestinian towns and villages, with information on location, and year of establishment. I also retrieve geographic covariates from various sources:[30] such as the road network, Jewish, Christian, and Muslim holy sites and terrain elevation. Figure A.2 shows the distribution of settlements, outposts, Palestinian towns and villages, and the Oslo Areas partitions across the West Bank and other relevant information such as military bases and built-up areas. Finally, since the year of establishment of outposts is often imprecisely recorded, I use satellite imagery to date their emergence, combining high-resolution imagery from Maxar Technologies (2023) to locate the structures characteristic of new outposts with the Sentinel-2 Level 2A time series of the European Space Agency's Copernicus program (European Union, Copernicus Land Monitoring Service, 2025) to identify their first appearance.[31] Importantly, since the high-resolution imagery was retrieved as of 2023, the outposts I map are those still in place at that date: structures established and subsequently dismantled are not captured.

Knesset Speeches I also consider the corpus of parliamentary speeches from the Israeli Knesset compiled by Goldin et al. (2024), which covers plenary debates over several decades and includes the full text of speeches together with metadata on speakers, parties, and dates. I first apply a coarse text classification procedure to isolate speeches concerning the occupied territories, settlements, and issues related to the Israeli-Palestine conflict. I then use this filtered subset to provide descriptive evidence on the political debate surrounding Israeli-Palestinian violence 8. Figure A.1 in the Appendix shows the

[28] Figure G.41 in the Appendix shows the full classification for both perpetrators and targets.

[29] Data from B'Tselem was also used in Durante and Zhuravskaya (2018) to gather information on IDF and Palestinian militia attacks.

[30] Palestinian Central Bureau of Statistics (2025), United Nations Office for the Coordination of Humanitarian Affairs (OCHA) (2017), OpenStreetMap Contributors (2017), European Space Agency and Airbus Defence and Space (2021), and NASA Land Processes Distributed Active Archive Center (LP DAAC) (2016)

[31] Figure E.33 in the Appendix provides an example.

number of speeches per year, as well as the distribution of speakers by party.

5. Methodology

Empirical Framework The model implies that an aggregate political shock should not affect all places equally. Its effects should be strongest where radical actors are already positioned to convert violence into material gains. In the West Bank, unauthorized outposts provide this empirical margin. They identify the radical outpost frontier, where territorial encroachment is actively pursued. The empirical design therefore asks whether violence increases more after the Trump-era shift in areas that were more exposed, before the shock, to this radical outpost frontier.

Figure 3 translates this logic into the empirical design. The Trump-era political shift S_t affects forbearance f^*_{it}, understood as the expected permissiveness of the enforcement environment faced by radical actors. Higher f^*_{it} can affect violence Y_{it} directly, by lowering expected punishment or obstruction, and indirectly through unauthorized outpost presence O_{it}, e.g. by making territorial encroachment easier to sustain. These pathways are complementary: weaker constraints on forbearance can both activate violent behavior directly and facilitate the expansion or persistence of unauthorized outposts, which may in turn generate more violence. Forbearance is not directly observed, so I treat f^*_{it} as a latent mechanism and return to it in Section 8.

The main empirical challenge is that outposts are not randomly located. Local geography, access, land-use patterns, and proximity to existing settler infrastructure affect both the feasibility of outpost expansion and baseline conflict risk, generating a backdoor path from E_i—local opportunity for encroachment and "productivity" of violence in the notation of the model—to both O_{it} and Y_{it}. I therefore construct a pre-shock outpost-suitability measure to proxy for E_i from pre-2016 spatial patterns, described in the next subsection, and compare locations with different ex ante exposure to the radical outpost frontier, conditional on fixed effects and controls.

The design therefore identifies the reduced-form effect of the Trump-era political shift S_t on violence Y_{it} across locations with different pre-shock exposure. It does not separately identify violence around pre-existing outposts from violence generated by subsequent outpost expansion; Section 8 provides further evidence on the interaction between geography, outpost location and violence.

Outpost Suitability To operationalize E_i, I model where unauthorized outposts

Figure 3: Causal DAG

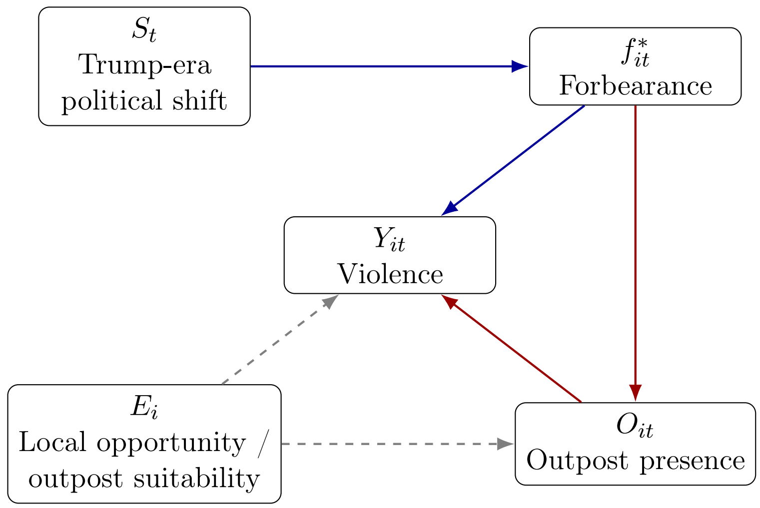

Notes: Blue arrows indicate the forbearance/activation channel. Red arrows indicate the outpost expansion channel. Gray dashed arrows indicate the confounding path through pre-existing local opportunity E_i, proxied by outpost suitability. The empirical strategy uses pre-determined suitability and cell fixed effects to isolate differential exposure to the Trump-era political shift.

were likely to expand before Trump's election. I begin by discretizing the West Bank into a hexagonal grid and restricting attention to locations that are plausibly exposed to outpost expansion, namely cells with at least 5% of their area in Oslo Area C. I then estimate a PPML model of unauthorized outpost expansion over annual periods from 1990 through October 2016. The dependent variable is the number of new outposts appearing in cell i during year t. The specification combines static geographic and institutional covariates with dynamic frontier variables that capture the evolution of the existing outpost network:

$$\mathbb{E}\left[O_{it} \mid X_i, D_{it-1}, N_{it-1}\right] = \exp\left(f(t) + X_i'\beta + g(D_{it-1}) + h(N_{it-1})\right), \tag{1}$$

where O_{it} is the number of new unauthorized outposts in cell i during year t, $f(t)$ is a flexible spline in calendar year, X_i includes pre-determined cell characteristics, D_{it-1} captures distance to the nearest existing outpost, and N_{it-1} summarizes local outpost density and neighborhood exposure.[32]

[32] Specifically, N_{it-1} includes (i) a measure of local outpost density around cell i, and (ii) a spatial diffusion term based on queen-contiguity weights, computed as the share of adjacent cells already hosting at least one outpost in period $t-1$. These variables capture both the local concentration of the outpost network and its expansion across contiguous space.

The static component X_i includes institutional, accessibility, settlement-proximity, and terrain characteristics measured prior to the shock.[33]

The fitted model yields E_i, the predicted pre-shock intensity of outpost expansion in each location. The measure predicts post-election outpost formation well (AUC $\approx$ 0.79); Appendix Table B.1 and Figure A.3 report model fit and the resulting suitability surface.

Because outpost activity often extends beyond the cell in which an outpost is located, the raw suitability score does not fully capture local exposure to the frontier. I therefore construct a binary treatment measure that incorporates this broader spatial footprint. I first identify fine-grid cells in the top decile of the pre-shock suitability distribution and draw a 2 km buffer around them. A regression cell is then classified as treated if at least 50% of its area falls within this buffered high-suitability region. Treatment is thus determined entirely by pre-shock geography and the predicted spatial reach of outpost expansion, rather than by realized post-shock outpost locations. Appendix Figure A.4 shows the construction and resulting treatment assignment.[34]

Estimation I estimate the effect of the Trump-era political shift using an event-study design that compares the evolution of violence in cells with high versus low exposure to radical settler activity, taking Trump's November 2016 election as the onset of the shift. The dynamic coefficients allow the response to build up through subsequent milestones, including the inauguration and the December 2017 Jerusalem Declaration.

Outcomes are measured monthly at the hex-cell level, as both event counts and indicators for any event. The analysis focuses primarily on settler violence against Palestinians, the outcome most directly linked to the theoretical mechanism, and reports Palestinian violence against settlers as a benchmark. I also report results for civilian targeting and other perpetrator–target pairs as secondary outcomes to document the broader conflict dynamics during this period.[35]

Identification relies on no anticipation and parallel trends. No anticipation is plausible

[33] Specifically: the share of cell area in Area C and in natural reserves, a military-zone indicator, distances to settlements, Palestinian villages, the Green Line, Jewish holy sites and roads, counts of nearby settlements, the share of the spatial unit under settlement municipality administration, elevation, elevation dispersion, slope and terrain ruggedness. The Green Line refers to the demarcation lines established in the 1949 Armistice Agreements between Israel and its neighboring Arab states (Egypt, Jordan, Lebanon, and Syria) following the 1948 Arab-Israeli War.

[34] The results are robust to alternative specifications, see 9.

[35] Perpetrator–target outcomes are based on the classification described in Section 4.

given that Trump's victory was widely unexpected. Treated and control cells differ on observables (Table B.2), as expected given that treatment reflects structural exposure to the outpost frontier; I therefore assess parallel trends through the pre-treatment event-study coefficients and a joint Wald test, which does not reject the null that they are jointly zero. Section 9 additionally reports a matched specification restricting the comparison to observationally similar cells.

The baseline specification is:

$$Y_{it} = \alpha_i + \lambda_t + \sum_{\tau \neq -1} \beta_\tau \left(T_i \cdot D_{t,\tau}\right) + \mathbf{X}_{it}'\gamma + \varepsilon_{it}, \tag{2}$$

where Y_{it} is violence in cell i and month t, T_i is a binary indicator for high pre-shock outpost suitability, and $D_{t,\tau}$ indexes event time relative to Trump's election in November 2016. The vector $\mathbf{X}_{it}$ includes pre-determined spatial characteristics interacted with the post-shock period, and calendar controls for Ramadan, the olive harvest, and Jewish holidays interacted with local proximity measures.[36] Standard errors are clustered at the hex-cell level, with an alternative specification also using Conley standard errors using a 5 km cutoff. The main sample runs from January 2016 to March 2020, before the onset of COVID-19.[37]

6. Results

6.1. Main Results

Settler Violence at the Outpost Frontier I begin by estimating equation 2 with monthly counts of settler violence against Palestinians as the outcome, using Palestinian violence against settlers as a benchmark.

Figure 4 reports the results. The left panel shows no immediate jump after the election: the coefficients rise gradually during 2017 and break sharply upward in January 2018. The timing follows the Jerusalem Declaration, though the one-month lag suggests

[36]Specifically, the controls include $Post_t$ interacted with Oslo Area share and local Palestinian village counts in the cell and its first two neighboring rings; Ramadan and olive harvest indicators interacted with proximity to Palestinian communities; and Jewish holiday indicators interacted with proximity to Israeli settlements.

[37]In other specification I will also consider a longer horizon to evaluate the dynamics of violence until September 2023.

Figure 4: Event-Study Estimates: Settler–Palestinian Violence

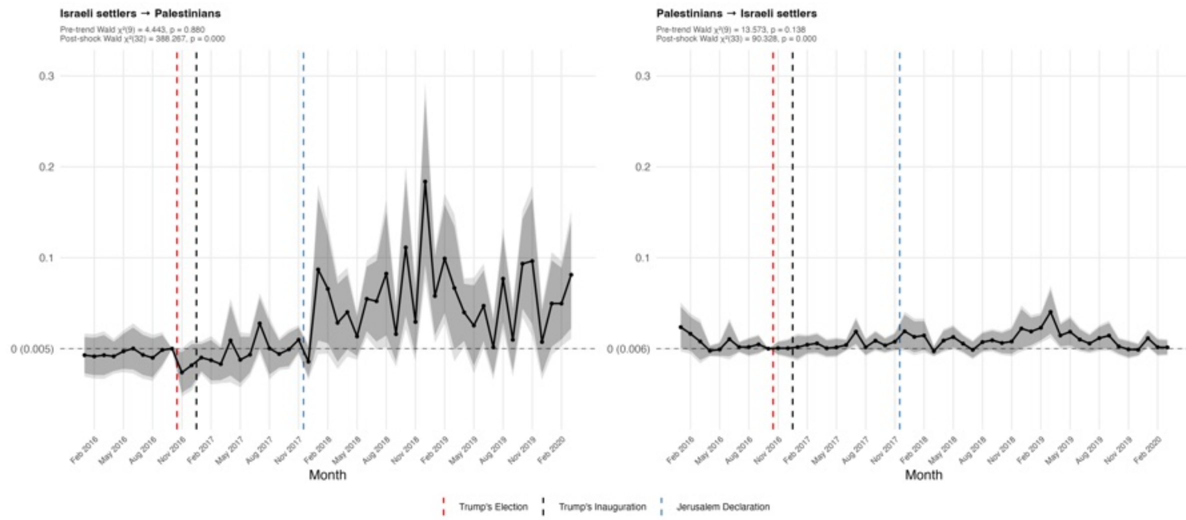

Notes: The figure reports event-study coefficients from the baseline TWFE specification using monthly event counts. The omitted period is the month immediately before Trump's election. All specifications include hex-cell fixed effects, month-year fixed effects, targeted controls, and Conley standard errors. Darker (lighter) shaded areas denote 95% (90%) confidence intervals. Vertical lines mark Trump's election, Trump's inauguration, and the Jerusalem Declaration.

the declaration weakened the constraints on forbearance while the Havat Gilad killing may have served as the trigger. The coefficients remain elevated through the end of the sample. Table B.3 reports the corresponding TWFE estimates.

The right panel shows a different pattern. Palestinian violence against settlers is smaller in magnitude and does not display the same persistent increase, inconsistent with symmetric conflict dynamics or a mechanical settler response to rising Palestinian attacks. Figure A.5 in the Appendix confirms the pattern using linear-probability incidence outcomes.

Broader Conflict As secondary outcomes, I estimate equation 2 for IDF–Palestinian confrontations and civilian-targeting events to document the broader conflict environment at the outpost frontier.[38] IDF–Palestinian confrontations display a pattern closer to symmetric violence (Figures A.6 and A.7).

The post-period effect on IDF-perpetrated events is significant for raw counts but not for incidence; pre-period coefficients are individually insignificant but noisier in the count specification. This is consistent with the fact that military operations reflect a different behavioral margin—institutional deployments driven by intelligence and directives—

[38] Civilian targeting is defined by ACLED as events involving bodily harm to one or more individuals.

rather than individual responses to perceived impunity. Palestinian violence against the IDF shows no gradual movement between the election and the declaration, rising only sharply afterward. Civilian-targeting outcomes track the settler-violence results—flat pre-trends, a gradual increase after the election, and a sharp break starting January 2018 (Figures A.8a and A.8b; Table B.5).

Long-Term Dynamics I also estimate equation 2 on the extended sample through September 2023 (Figure 5). The pattern should be read descriptively rather than as evidence that Trump's election mechanically caused each later episode; what the extended sample documents is whether the initial shift persisted, reversed, or was compounded by subsequent events.

Settler violence against Palestinians remains consistently above the pre-2017 baseline across the entire extended period. It does not revert after Biden's election or during the Bennett–Lapid government,[39] suggesting that the initial shift moved the conflict environment to a persistently higher level rather than producing a temporary spike. A further increase occurs around Operation Guardian of the Walls in 2021.[40] The strongest escalation occurs from 2022 onward, coinciding with Operation Break the Wave,[41] the emergence of the Lions' Den, and the formation of the 25th Knesset government at the end of December 2022, when politicians aligned with the settler movement acquired ministerial authority over policy areas relevant to police priorities and West Bank civilian administration (Chacar, 2022; Williams, 2022). Each of these episodes compounded a conflict that had already shifted to a higher baseline after 2016.

Palestinian violence against settlers follows a different trajectory. It remains muted for most of the period and rises only from 2022 onward with the reactivation of Palestinian armed groups, e.g. Lions' Den (ACLED, 2023). This lag is difficult to reconcile with a simple retaliation account and reinforces the reading of the earlier results: settler

[39] The Bennett–Lapid government was more moderate than the Netanyahu-led coalition that followed, but Bennett himself came from the national-religious right and had long taken hawkish positions on settlements and settler violence (TOI Staff, 2021). The interlude did not represent a clear ideological reversal on the settlement question.

[40] The May 2021 escalation was triggered by rising tensions in East Jerusalem, particularly over the scheduled forced evictions of Palestinian families in Sheikh Jarrah and clashes at the Al-Aqsa Mosque compound during Ramadan (United Nations Office for the Coordination of Humanitarian Affairs, 2021).

[41] Beginning on 31 March 2022, the Israeli military launched Operation Break the Wave, an ongoing counterinsurgency campaign characterized by near-daily raids in Jenin, Nablus, and Tulkarm (Israel Defense Forces, 2023). During this period, a new generation of decentralized Palestinian armed groups also emerged, such as the Lions' Den in Nablus, alongside the intensification of activity by long-standing paramilitary groups such as the Al-Aqsa Martyrs' Brigade (ACLED, 2023, 2024b).

Figure 5: Event-Study Estimates: Settler–Palestinian Violence

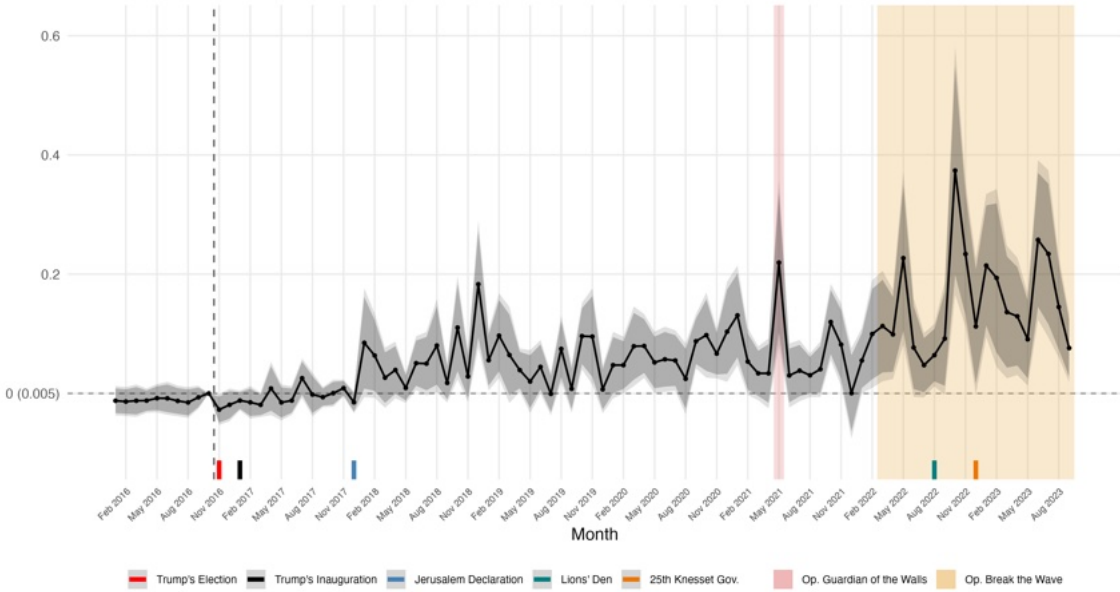

(a) Israeli Settlers → Palestinians

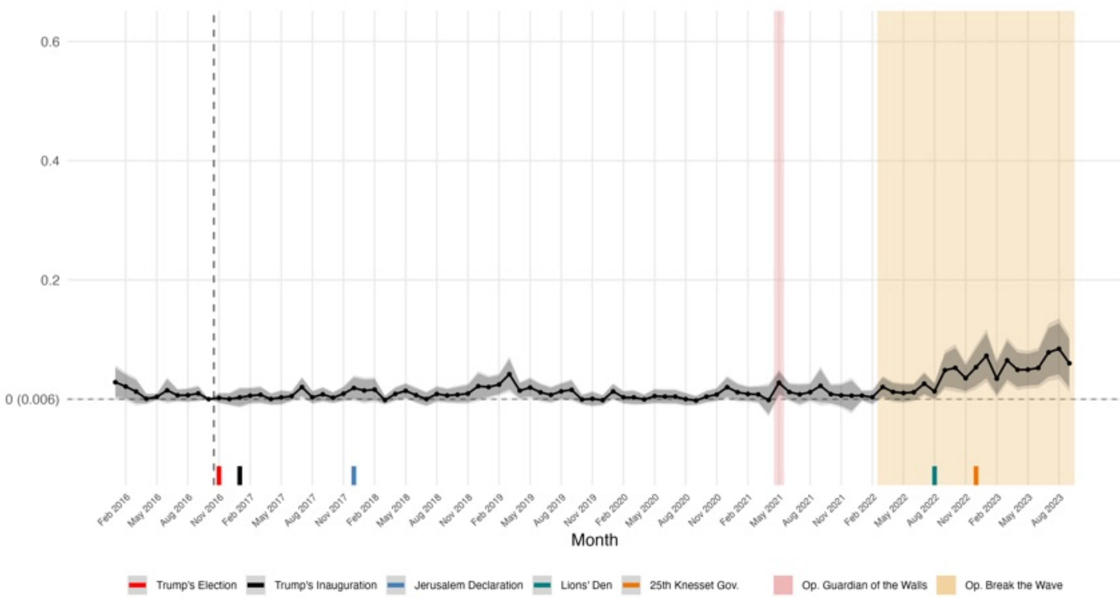

(b) Palestinians → Israeli Settlers

Notes: The figure reports event-study coefficients from the TWFE specification with monthly event counts. Bottom markers signal Trump's election, Trump's inauguration, and the Jerusalem Declaration as well as the emergence of the Palestinian militia Lion's Den and the start of the 25th Knesset government in 2022. Shaded areas depict Operation Guardian of the Walls and Operation Break the Wave. Both plots share the same y-axis scale. All specifications include hex-cell fixed effects, month-year fixed effects, controls, and Conley standard errors. Darker (lighter) shaded areas denote 95% (90%) confidence intervals.

violence drove the initial escalation, with a broader and more symmetric conflict dynamic emerging only later. The absence of reversal across different governments and political periods is consistent with the post-2016 shift having moved the conflict environment into a more permissive equilibrium, one that was reinforced by the rightward trajectory of Israeli politics rather than reversed by it—the persistence-and-feedback pattern the dynamic extension of the model formalizes (Appendix F.7).[42]

6.2. Local Triggers and Violent Escalation

Settler Fatalities & the Political Discourse A possible concern is that the January 2018 break reflects retaliation for the killing of Rabbi Raziel Shevach near Havat Gilad rather than the political shift. To assess this, I re-center the event study around fatal attacks against settlers, using settler violence against Palestinians as the outcome.[43]

Figure 6: Settler Violence after Fatal Attacks on Settlers

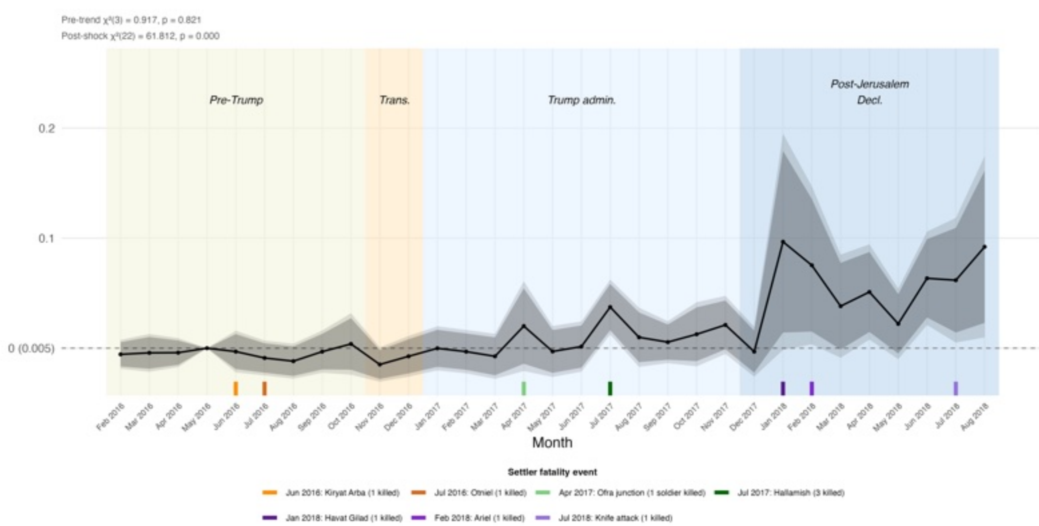

Notes: The figure reports event-study coefficients for settler violence against Palestinians from the TWFE specification with monthly event counts, re-centered around the first fatal attack against settlers in the sample. The omitted month is May 2016. Shaded background areas indicate political periods, and colored ticks mark fatal attacks against settlers. All specifications include hex-cell fixed effects, month-year fixed effects, controls, and Conley standard errors. Darker and lighter shaded confidence bands denote 95% and 90% confidence intervals, respectively.

[42] The U.S. position shifted only belatedly: the Biden administration restored the pre-Trump view that West Bank settlements are inconsistent with international law only in February 2024, after the escalation that followed October 7, 2023 (Bertrand and Hansler, 2024).

[43] The sample starts in February 2016 so that the first recorded settler fatality (January 2016) has a valid pre-event window.

Figure 6 shows that fatal attacks are not, by themselves, associated with sustained increases in settler violence. Before Trump's election, the coefficients remain close to zero; afterward, the response to the two attacks in 2017 is short-lived, while a sustained increase emerges only after the Jerusalem Declaration. Local triggers appear to have become more consequential once political constraints weakened. Appendix Figure A.9 confirms the pattern using linear-probability incidence outcomes.

Timing of the Shock: Structural Break Estimation The event-study evidence suggests that violence rises in stages, but several political and security shocks overlap during the sample period. I therefore estimate unknown structural breaks in the raw monthly treated–control gap in violence, to identify when that gap shifts discretely and whether further breaks emerge during the later escalation (Andrews, 1993; Bai, 1997; Bai and Perron, 1998, 2003).

Figure 7 reports the results. Panels 7a and 7b use settler violence against Palestinians and Palestinian violence against settlers as the outcome, respectively. In Panel 7a, the first estimated break occurs in April 2017,[44] with a 95% confidence interval from March 2017 to May 2017 (sup-Wald = 77.5; 5 percent critical value = 11.01). The raw treated–control gap therefore shifts upward already between Trump's inauguration and the Jerusalem Declaration: a first, mild level increase consistent with the election and the early 2017 policy moves having begun to activate the frontier before the Declaration's most salient signal. A second, substantially larger break follows in January 2018, with a 95% confidence interval from October 2017 to April 2018 (sup-Wald = 88.0; 5 percent critical value = 10.19), immediately after the Jerusalem Declaration and around the Havat Gilad killing. The sequence, a mild shift in spring 2017 followed by a sharp escalation after the Declaration, mirrors the staged structure of the political shock itself: the election and inauguration produced a first discrete but modest response, and the Declaration triggered the main escalation. Conversely, Panel 7b shows that Palestinian violence against settlers displays no break in either 2017 or 2018, with its first estimated break occurring only in 2022, consistent with the event-study evidence that Palestinian violence against settlers rises only in the later phase of the conflict.

This exercise also sheds light on the longer-run dynamics of violence. Panel a identifies a further break in settler violence in March 2022, with a 95% confidence interval

[44] As described in Section 3, this is precisely the moment in which settlers from the recently evacuated Amona outpost get compensated with the planned construction of the Amichai settlement.

Figure 7: Structural Break Estimation: Settler–Palestinian Violence

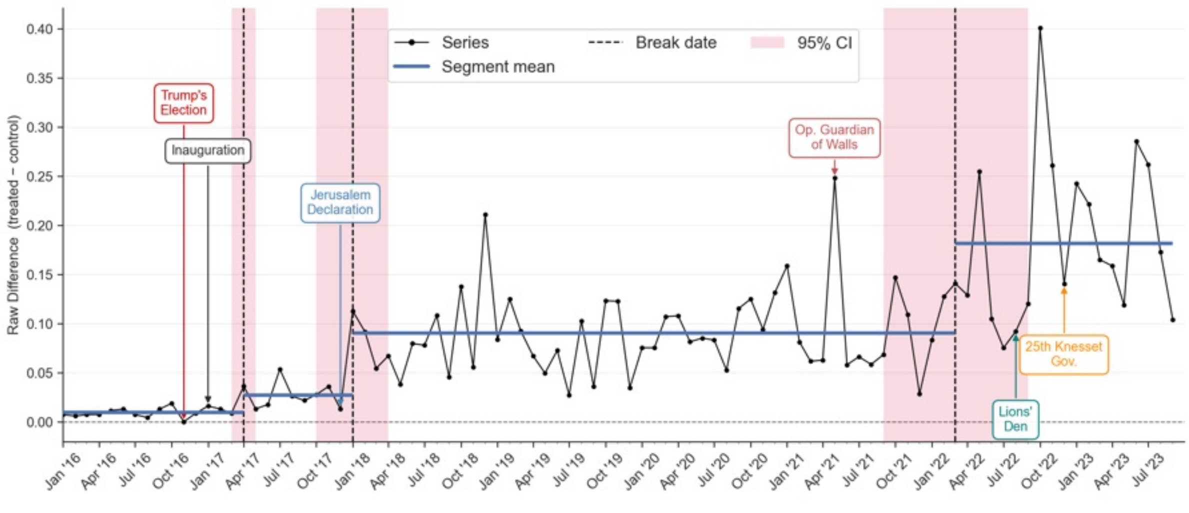

(a) Israeli Settlers → Palestinians

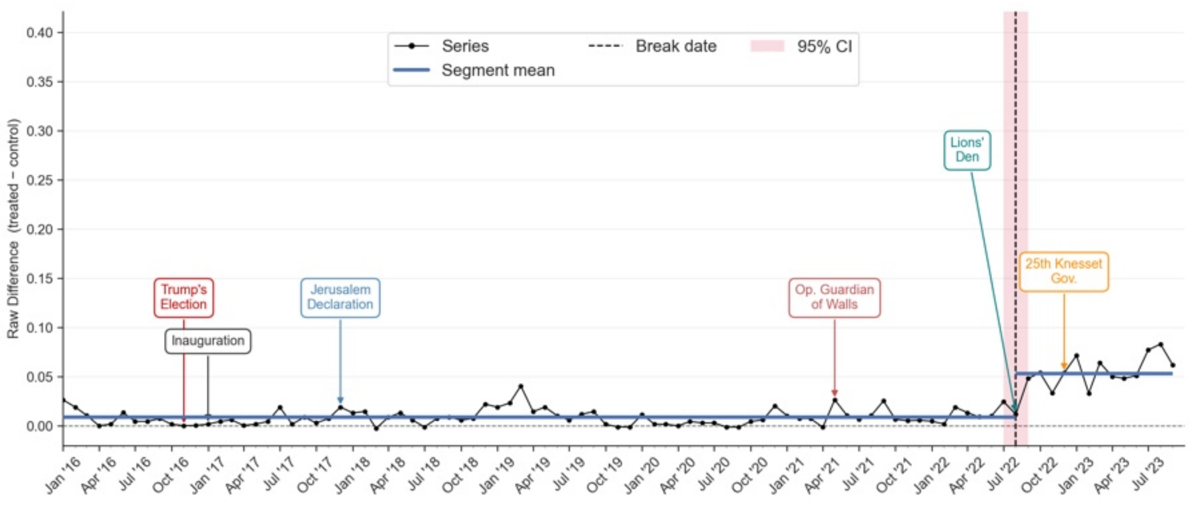

(b) Palestinians → Israeli Settlers

Notes: The figure reports agnostic structural-break estimates for the raw monthly difference in violence between treated and control cells. The black line plots the monthly treated–control difference. Blue horizontal lines show estimated segment means. Dashed vertical lines mark estimated break dates, and shaded regions report 95% confidence intervals for the break dates. Panel A uses settler violence against Palestinians as the outcome; Panel B uses Palestinian violence against Israeli settlers. Event labels mark major political and conflict episodes. Break tests use HAC/Newey–West long-run variance estimates over the monthly difference series.

from September 2021 to September 2022 (sup-Wald = 32.9; 5 percent critical value = 8.66). The timing coincides with a sharp deterioration in the Israeli security environment: the March 2022 attacks in Beersheba, Hadera, and Bnei Brak, and the beginning of Operation Break the Wave (Israel Defense Forces, 2023). Palestinian violence shifts later: Panel b estimates a break in August 2022 (95% confidence interval from July to September 2022; sup-Wald = 142.2; 5 percent critical value = 8.69), aligning with the emergence of Lions' Den in Nablus and the reorganization of armed Palestinian activity in the northern West Bank (ACLED, 2023). Taken together, the exercise corroborates the reading of the Trump election and the Jerusalem Declaration as successive realizations of the same political shock—an early mild activation followed by a sustained escalation—while providing suggestive evidence of a second regime change in 2022, when the conflict evolved into a broader escalation.

7. The Geography of Activation

7.1. Settlement Proximity or Radical Expansion?

A natural concern is that the results capture proximity to Israeli settlers rather than exposure to radical expansion. If the effect were driven by contact or friction between Israelis and Palestinians, similar increases should appear near established settlements outside the outpost frontier. To test this, I draw a 2 km buffer around each established settlement and partition buffered cells into two mutually exclusive groups. *Non-frontier settlement-adjacent* cells ($N_i = 1$) lie within the buffer but outside the high outpost-suitability zone: near established settlements, but away from the radical frontier. *Frontier settlement-adjacent* cells ($R_i = 1$) lie within both the buffer and a high-suitability area,[45] where local opportunity E_i is higher. Both groups are estimated against a common control group of cells that are neither settlement-adjacent nor in a high-suitability area (Appendix Figure A.11).

I estimate the following two-arm event-study specification:

$$Y_{it} = \alpha_i + \lambda_t + \sum_{\tau \neq -1} \beta_{N,\tau} \left(N_i \times D_{t,\tau} \right) + \sum_{\tau \neq -1} \beta_{R,\tau} \left(R_i \times D_{t,\tau} \right) + u_{it}, \tag{3}$$

[45] High refers to the top decile of outpost suitability used to define treatment areas in Section 5.

where α_i are hex-cell fixed effects, λ_t are period fixed effects, and $D_{t,\tau}$ is the relative-time indicator, equal to one when month t is τ months relative to November 2016 and zero otherwise. Both arms are estimated relative to the same control group. Standard errors are Conley-corrected with a 5 km cutoff, and I include the same controls as in equation 2.

Figure 8: Settlement Proximity vs. Radical Frontier: Event-Study Estimates

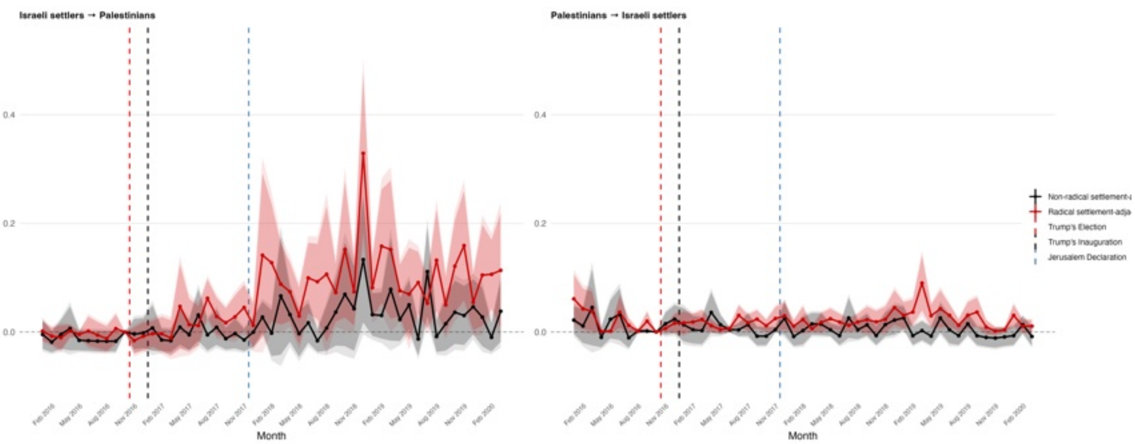

Notes: The figure reports event-study coefficients for Israeli settler violence against Palestinians from the TWFE specification with monthly event counts (equation (3)), monthly hex-cell panel, Nov 2015 – Mar 2020. Black line: non-frontier settlement-adjacent arm ($N_i = 1$, within 2 km of an established settlement, outside high outpost-suitability zone). Red line: frontier settlement-adjacent arm ($R_i = 1$, within 2 km of a settlement and in high outpost-suitability zone). Both arms estimated vs. the same pure-control group (not settlement-adjacent, not treated). Shaded bands: 95% (light) and 90% (dark) confidence intervals. Conley spatial standard errors, 5 km cutoff. Vertical lines: Trump's election (dashed red), inauguration (dashed black), Jerusalem Declaration (dashed blue).

Figure 8 presents the results. The frontier arm ($\beta_{R,\tau}$, red) presents a similar pattern as the results in Figure 4, with a mild increase starting in 2017 and a sharp rise in violence starting 2018. The non-frontier arm ($\beta_{N,\tau}$, black) moves somewhat but remains consistently smaller and statistically insignificant. The pattern is consistent with the territorial encroachment mechanism: violence is not a generic by-product of Israeli–Palestinian proximity but arises at the active expansion margin, where a shift in political constraints produces the largest behavioral response. Appendix Figure A.12 confirms the pattern using linear-probability incidence outcomes.

7.2. Opportunity or Presence?

A potential concern is that the baseline suitability measure partly reflects the pre-existing outpost network, so that high-suitability locations are simply places where radical settlers were already present before the shock; a nationwide change affecting radical settlers could then generate the observed spatial pattern even if territorial opportunity itself played no role. I separate the two explanations by distinguishing *structural opportunity* from *pre-shock radical presence*. If violence rose simply because radical settlers were already nearby, controlling flexibly for the location of existing outposts should absorb the effect; if it instead continues to rise where further outpost expansion was geographically favorable, this points to the opportunity margin emphasized by Prediction 2.

To isolate this margin, I construct an alternative suitability measure, $\hat{E}_i^{NO}$, that removes the contribution of the existing outpost network. Using the fitted outpost-expansion model of Section 5, I set the network covariates—distance to prior outposts, $D_{i,t-1}$, and local outpost density, $N_{i,t-1}$—to common reference values throughout the West Bank. The remaining variation therefore comes from terrain, institutional geography, accessibility, and settlement structure rather than from where outposts were already located.[46] I define T_i^{NO} using the top decile of this no-network suitability measure.

I then estimate an event study that allows pre-shock outpost presence to have its own flexible time path:

$$Y_{it} = \alpha_i + \gamma_t + \sum_{\tau \neq -1} \beta_\tau \left(T_i^{NO} \times D_{t,\tau}\right) + \sum_{\tau \neq -1} \boldsymbol{\theta}'_\tau \left(HC_i \times D_{t,\tau}\right) + X'_{it}\delta + \varepsilon_{it}, \qquad (4)$$

where $D_{t,\tau}$ indexes months relative to November 2016 and HC_i captures pre-shock outpost presence and proximity.[47]

The coefficient β_τ is the object of interest. It measures whether violence evolved differently in high-opportunity locations after accounting for the fact that some cells were already closer to, or contained more, outposts before the shock. A positive post-shock β_τ therefore indicates that violence increased disproportionately where further territorial encroachment was structurally easier, rather than merely where radical settlers were already present. The coefficients on HC_i capture the separate association with pre-

[46]Figure A.13 compares the resulting treatment map with the baseline allocation.

[47]Specifically,

$$HC_i = \left(\mathbf{1}[O_i = 1], \mathbf{1}[O_i \geq 2], d_i\right)',$$

where O_i is the number of pre-November-2016 outposts within 2 km and d_i is distance to the nearest pre-shock outpost. Cells with no outpost within 2 km form the omitted presence category. Presence enters through mutually exclusive bins because an incidence–count specification becomes nearly collinear when interacted month by month. Appendix Table B.6 reports the corresponding static difference-in-differences estimates.

existing presence; because presence and distance have partly distinct spatial support, I interpret these as conditional gradients rather than causal effects of locating an outpost.

Figure 9: Territorial Opportunity vs. Radical Presence: Event-Study Estimates

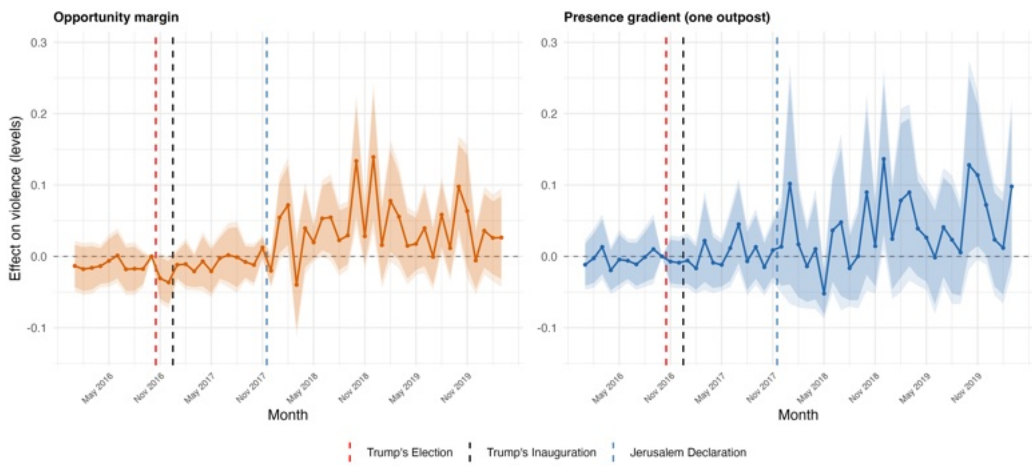

Notes: Event-study estimates for settler violence against Palestinians. The left panel reports the opportunity coefficients β_τ from equation (4). The right panel reports the conditional gradient associated with exactly one pre-2016 outpost within 2 km, relative to the omitted zero-outpost category. Opportunity, pre-shock presence, and distance to the nearest outpost are interacted with the same relative-time indicators, so both panels come from one specification. The omitted period is the month before Trump's election. All regressions include hex-cell and month-year fixed effects, targeted controls, and Conley standard errors with a 5 km cutoff. Darker and lighter bands denote 95% and 90% confidence intervals. Vertical lines mark Trump's election, inauguration, and the Jerusalem Declaration.

Figure 9 shows a clear difference between the two margins. The opportunity coefficients are flat before the shock, rise after the Jerusalem Declaration, and remain elevated thereafter. By contrast, the pre-existing-outpost gradient remains close to zero through 2017 and increases only later, with substantially wider confidence intervals. Therefore, existing presence also predicts some subsequent violence, but it does not account for the opportunity effect.

The contrast is particularly informative for Palestinian violence against settlers. There, the opportunity coefficient is essentially zero, while pre-existing outpost presence is predictive. This is what one would expect when violence depends mainly on the availability of nearby physical targets. Settler violence follows a different pattern: it rises where further territorial encroachment is feasible even after conditioning on where radical settlers were already located.

Taken together, these results favor an opportunity interpretation of the main effect. The post-shock increase in settler violence was not confined to the existing outpost network; it was strongest where the frontier could expand further. This is the spatial prediction of the model: when expected restraint weakens, violence responds most where it can generate larger territorial gains. Section 8 examines why actors could expect those gains to persist.

8. Additional Evidence on the DAG

The previous section established where post-shock violence concentrated. Two questions follow: did territorial encroachment itself shift toward that margin? And why could settlers expect those gains to stand? The first question concerns the expansion channel in Figure 3, $S_t \to f^*_{it} \to O_{it}$; the second concerns forbearance itself, the latent link both channels share. This section takes each in turn.

Trump-Era Outpost Expansion If weaker constraints on forbearance made territorial encroachment easier to sustain, new outposts should increasingly appear where expansion was structurally most feasible. I test this using the satellite-based outpost dates described in Section 4.

Because new outposts are rare, I work with a coarser 5 km cell-by-year panel. The key predictor is the geography-only suitability measure $\hat{E}_i^{NO}$, which holds the outpost-network covariates fixed so that variation across cells comes only from geography. To keep the prediction genuinely out of sample, I estimate this measure on outposts established through 2011 and study new outpost formation from 2012 onward.[48]

The test is whether the relationship between geographic opportunity and new outpost formation becomes stronger after the political shock. I estimate

$$Y_{it} = \alpha_i + \lambda_t + \sum_{\tau \neq 2016} \beta_\tau \left(E_i^{rank} \cdot D_{t,\tau} \right) + Post_t \cdot \Gamma' N_i^0 + \eta_{it}, \tag{5}$$

where Y_{it} equals one if a new outpost appears in cell i during year t, and E_i^{rank} is the percentile rank of $\hat{E}_i^{NO}$.[49] The coefficients β_τ therefore show how strongly new outpost formation is associated with geographic opportunity in each year relative to 2016, moving from the bottom to the top of the opportunity distribution.

[48] Appendix Figure A.14 maps the resulting opportunity gradient across 5 km hex cells in the West Bank.

[49] $\hat{E}^{NO}$ is identified only up to scale and is severely right-skewed, so the rank transformation makes the measure scale-free and spreads identifying variation evenly across $[0, 1]$.

The specification also controls for the inherited outpost network at the start of 2017, N_i^0, interacted with the post-shock period. This ensures that the opportunity gradient is not simply picking up expansion around locations where outposts were already concentrated.[50] Cell and year fixed effects absorb time-invariant differences across locations and aggregate changes in outpost formation. All cells are retained after an outpost appears; standard errors are Conley with a 15 km cutoff.

Figure 10 shows a clear change after the shock. Before 2017, geographic opportunity does not predict where new outposts appear: high- and low-suitability cells were equally likely to see a new outpost, and the pre-period coefficients are jointly indistinguishable from zero. The gradient remains close to zero in 2017, but becomes positive from 2018 onward and stays elevated through the rest of the sample, reaching its largest value in 2023. The timing closely mirrors the violence results: the spatial shift in outpost expansion begins after the Jerusalem Declaration rather than immediately after Trump's election.

Table B.8 reports the corresponding static estimates. Moving from the bottom to the top of the opportunity distribution increases the annual probability of a new outpost by 6.8 percentage points after 2017. Controlling for the inherited network leaves the estimate essentially unchanged, at 8.0 percentage points, and the count specification produces a similar result. The key point is that post-shock expansion was not confined to places where outposts already existed: new outposts increasingly appeared in locations that were geographically suitable for further expansion but had previously remained empty. Moreover, since the data record only outposts still present in the 2023 inventory, these estimates capture durable expansion rather than every short-lived attempt at establishment.

The Domestic Accountability Environment In the model, forbearance is cheap when both the external and the domestic constraints on tolerating aligned violence are weak. The previous exhibits speak to the external side; Knesset speeches around fatality events characterize the domestic one. The benchmark is simple: if domestic demand for enforcement does not depend on perpetrator identity, parliamentary responses should not

[50] N_i^0 is a January-2017 snapshot of the local network: in-cell outpost stock (bins 0/1/2+), external outposts within 5 km, and distance to the nearest external outpost (bins). Because it is time-invariant and predates the shock, its levels are absorbed by α_i and only the *Post* interactions enter, so the control neither changes at the treatment boundary nor uses post-2017 outposts. The reduced-form specification without these controls is reported in Appendix Figure A.15.

Figure 10: New Outpost Formation and Geographic Opportunity

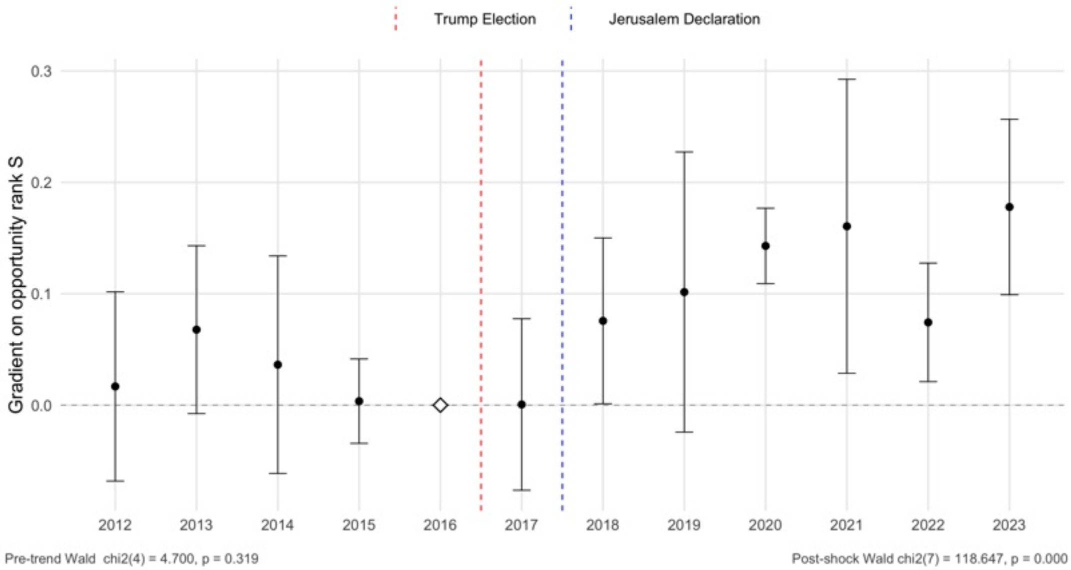

Notes: Event-study estimates of equation (5) on a 5 km cell × year panel, 2012–2023, conditional on the inherited-network block N_i^0. Cell and year fixed effects; omitted year 2016; Conley standard errors with a 15 km cutoff. Vertical lines mark Trump's election and the Jerusalem Declaration. Joint Wald tests for pre- and post-shock coefficients appear at the bottom of the panel. Coefficients identify where new outposts appear, not the total effect of the shock on expansion.

systematically differ depending on who committed the killing. If Right-bloc politicians demand punishment when Palestinians kill settlers but not when settlers kill Palestinians, this indicates weaker political pressure to enforce against aligned actors. I therefore test whether parliamentary responses to fatalities depend on perpetrator identity, and whether this asymmetry is concentrated in blocs politically aligned with the settler movement.

For each fatality in which a settler kills a Palestinian or a Palestinian kills a settler, I collect topic-relevant Knesset speeches[51] in the following 15 days and classify whether they discuss the event, condemn the perpetrator, demand enforcement, redirect attention to violence by the other side, or defend the perpetrator side. The first three measure incident-specific accountability; the latter two capture the broader rhetorical environment after a fatality. The annotation procedure, the exact definition of each measure, and the validation exercise are reported in Appendix H.

[51] I use gpt-4o-mini to assess whether a speech discusses physical violence between Israelis and Palestinians.

I aggregate to the event × bloc level and estimate:

$$\begin{aligned} Y_{eg} = \alpha_e &+ \delta_R Right_g + \delta_A Arab_g \\ &+ \beta_R \left(Right_g \times SettlerPerp_e \right) + \beta_A \left(Arab_g \times SettlerPerp_e \right) + \nu_{eg}, \end{aligned} \tag{6}$$

where Y_{eg} is the share of topic-relevant speeches with a given rhetorical feature in event e and bloc g, and $SettlerPerp_e$ equals one when the perpetrator is a settler. Event fixed effects compare political blocs responding to the same fatality, absorbing differences in salience, timing, and severity. The omitted bloc is Center-left, so δ_R and δ_A give the Right–Center-left and Arab–Center-left gaps when the perpetrator is Palestinian, and β_R and β_A test whether those gaps change when the perpetrator is a settler instead. Standard errors are clustered by fatality event. Panel B of the table reports the implied bloc gaps at settler-perpetrator events ($\delta_R+\beta_R$ and $\delta_A+\beta_A$), and even-numbered columns allow the bloc differences to vary across Knesset terms.

Table 1 shows a clear asymmetry. When the perpetrator is Palestinian, Right-bloc speeches are substantially more likely than Center-left speeches to condemn the perpetrator and demand enforcement. When the perpetrator is a settler, these gaps shrink sharply or reverse, while Right-bloc speeches become more likely to redirect attention toward Palestinian violence or use defensive frames. The same pattern survives bloc-by-Knesset-term controls and non-overlapping event samples.

Parliamentary speech does not measure enforcement itself; it captures the political demand surrounding it. Because the analysis pools fatality events across 2016–2023, it identifies a persistent asymmetry rather than a post-Trump change. Right-bloc politicians demand punishment much more readily when the perpetrator is Palestinian than when the perpetrator is a settler, and this pattern is not driven by a single Knesset term.[52] The evidence therefore points to persistently weak domestic pressure to punish settler violence. This matters for the Trump-era shock: because domestic pressure was already weak, external political pressure was an important additional constraint on forbearance.

[52]Throughout the sample period (2016–2023), Right-bloc parties have been part of every governing coalition, giving this rhetorical asymmetry direct relevance for the political constraints facing security and law-enforcement agencies.

Table 1: Fatalities and Knesset Speeches

	Focal/Same-Pair		Condemnation		Enforcement		Opp. Side Attention		Perp.-Side Def.	
	(1)	(2)	(3)	(4)	(5)	(6)	(7)	(8)	(9)	(10)
Panel A: Main effects and interactions										
Right	0.110**		0.109***		0.036**		−0.118***		−0.001	
	(0.044)		(0.030)		(0.017)		(0.044)		(0.002)	
Arab	−0.123***		−0.063***		−0.031***		0.368***		0.058*	
	(0.026)		(0.016)		(0.010)		(0.083)		(0.033)	
Right × Settler perp.	−0.197***	−0.209***	−0.197***	−0.202***	−0.051**	−0.056***	0.315***	0.305***	0.063***	0.078***
	(0.063)	(0.066)	(0.056)	(0.056)	(0.021)	(0.021)	(0.073)	(0.069)	(0.023)	(0.024)
Arab × Settler perp.	0.198***	0.220***	0.088	0.113**	0.053**	0.055**	−0.733***	−0.742***	−0.112***	−0.112***
	(0.072)	(0.066)	(0.055)	(0.047)	(0.022)	(0.025)	(0.097)	(0.094)	(0.040)	(0.037)
Panel B: Implied bloc gaps at settler-perpetrator events										
Right gap	−0.087*	−0.091*	−0.088*	−0.093*	−0.015	−0.014	0.198***	0.206***	0.062***	0.063***
(Implied gap, settler perp.)	(0.045)	(0.052)	(0.047)	(0.051)	(0.013)	(0.013)	(0.059)	(0.051)	(0.023)	(0.019)
Arab gap	0.075	0.071	0.025	0.020	0.022	0.023	−0.365***	−0.357***	−0.054**	−0.053**
(Implied gap, settler perp.)	(0.067)	(0.068)	(0.052)	(0.052)	(0.020)	(0.020)	(0.051)	(0.046)	(0.022)	(0.021)
Observations	169	169	169	169	169	169	169	169	169	169
Events	58	58	58	58	58	58	58	58	58	58
R^2	0.633	0.668	0.517	0.594	0.454	0.527	0.785	0.820	0.560	0.599
Event FE	✓	✓	✓	✓	✓	✓	✓	✓	✓	✓
Knesset × Bloc		✓		✓		✓		✓		✓

Notes: The unit of observation is an event × bloc-group cell. Outcomes are shares of topic-relevant speeches in the 15-day post-event window; coefficients are proportions, so 0.10 corresponds to 10 percentage points. The omitted bloc is Center-left. *Right* includes Right, Far Right, Religious Zionist, and Orthodox blocs; *Arab* includes Arab party lists. Odd columns report the baseline specification with event fixed effects. Even columns add bloc-by-Knesset-term controls, allowing baseline gaps to vary across parliamentary terms. *Settler perp.* equals one when the perpetrator is a settler (i.e. a Palestinian was killed by a settler) and zero when the perpetrator is Palestinian (i.e. a settler was killed by a Palestinian). Panel B reports the implied bloc gaps at settler-perpetrator events; in even columns these are averaged over settler-perpetrator events using the event's Knesset-specific baseline gap. Standard errors are clustered by fatality event; Panel B standard errors use the delta method. $^{*}p < 0.10$, $^{**}p < 0.05$, $^{***}p < 0.01$.

Enforcement After the Shock Section 3.2 documents that during the Obama years this external constraint had real content: settlement expansion drew consistent U.S. pressure, enforcement against settler crime was institutionalized in a dedicated unit, and settler violence declined through 2016. With domestic pressure to punish settler violence already weak, the model implies that weakening this external constraint should also be visible in enforcement behavior. Because non-enforcement is difficult to observe directly, I use ACLED-recorded IDF–settler confrontations relative to settler-perpetrated violence as a narrow proxy for one visible component of coercive enforcement (Figure A.16). Settler violence rises sharply after 2018 and again in 2021–2022, while IDF–settler confrontations remain rare and do not scale proportionally.[53] After 2018, observable confrontations remain below roughly three percent of settler-perpetrated events. This ratio is not a direct measure of enforcement, but it shows that settler violence expanded without a proportional increase in recorded IDF–settler confrontations, a pattern consistent

[53]The elevated ratio in 2017 reflects the court-ordered evacuation of Amona rather than a general enforcement increase as described in Section 3.

with increased forbearance.

Responsibility for enforcement is divided across military, civilian-police, and prosecutorial institutions, with documented coordination and investigative failures (Shalom Hartman Institute, 2022). In Yesh Din's monitored sample as of August 2015, 940 of 1,026 concluded investigation files concerning alleged offenses by Israeli civilians against Palestinians or their property (91.6%) were closed without indictment, while 75 (7.3%) resulted in an indictment (Yesh Din, 2015).[54]

9. Robustness Checks

Reverse Causality I test whether lagged violence predicts subsequent outpost formation by estimating:

$$\begin{aligned}\text{OutpostHazard}_{it} = \alpha_i + \theta_t + \sum_{k=1}^{12} \mu_k \, \text{ViolenceAgainstIsraelis}_{i,t-k} \\ + \sum_{k=1}^{12} \delta_k \, \text{ViolenceAgainstPalestinians}_{i,t-k} + \mathbf{X}'_{it}\gamma + \epsilon_{it},\end{aligned} \tag{7}$$

where $\text{OutpostHazard}_{it}$ indicates the appearance of a new outpost in cell i during month t, with cell and month fixed effects and the same controls as the baseline. Figure C.18 shows that the lag coefficients are individually small and insignificant, as well as jointly insignificant.

Havat Gilad Killing The sharp increase in settler violence coincides with the killing of Rabbi Raziel Shevach near Havat Gilad. I re-estimate the main specification excluding the area surrounding Havat Gilad, Nablus and Yitzhar.[55] The January 2018 jump is expectedly reduced, but the post-treatment coefficients remain positive and significant (Appendix Figure C.19).

Matching on Geography The suitability measure may capture generic conflict geography rather than exposure to the radical frontier. I re-estimate the main specification on

[54]For the later period, Graham-Harrison (2026) reports that since 2020 1,100 Palestinians have been killed by Israeli soldiers or settlers with no Israeli citizen charged, that former Prime Minister Ehud Olmert called for International Criminal Court intervention against state-backed settler violence, and that a public letter signed by former senior Israeli security officials described near-daily attacks on Palestinians as "Jewish terrorism."

[55]This area is one of the best-documented hubs of radical settler activity in the northern West Bank.

a matched sample that substantially improves covariate balance (Table D.10). The estimates are somewhat attenuated but the pattern is unchanged (Table D.11; Figure C.20).

Alternative Suitability Thresholds I vary the percentile cutoff defining high-suitability areas (95th, 97.5th, and 99th). The post-shock increase is consistently positive and significant across all thresholds (Figures C.21 and C.22).

Alternative Buffer Sizes I vary the buffer radius from 1 to 4 km in 0.5 km steps. The estimates are stable, with expected attenuation at larger buffers as the suitability signal dilutes spatially (Figures C.23 and C.24).

Donut Design To address potential spillovers from treated to adjacent control cells, I exclude control cells directly bordering the treated area. The estimates are broadly similar to the baseline (Figure C.26; map in Figure C.25).

Spatial Placebo I exclude treated cells and reassign treatment to the adjacent ring. The placebo coefficients are small and insignificant, confirming that the effects are localized to high-suitability cells (Figure C.28; map in Figure C.27).

Geographic Leave-Out To check that the results are not driven by a few influential locations, I iteratively drop each treated cell and its adjacent treated neighbors (clusters of up to five cells)[56] and re-estimate the static TWFE. The distribution of leave-out estimates is tight around the baseline, confirming that no single geographic pocket drives the results (Figures C.29 and C.30).

10. Conclusion

This paper asks why governments sometimes fail to stop violence they have the capacity to stop. The answer developed here is that non-enforcement can itself be politically useful: when violent actors pursue goals political authorities partly share, governments need not organize, direct, or bargain with them—it may be enough to punish them less.

The West Bank provides evidence consistent with this argument. After the Trump-era shift in U.S. policy, settler violence against Palestinians rises sharply along the radical outpost frontier, with the main escalation following the December 2017 Jerusalem Declaration and no reversal through 2023. Where it rises is especially revealing: not simply

[56]More specifically: $\max(5, \text{number of adjacent treated cells})$.

near Israeli settlements or where radical settlers were already present, but where further territorial expansion was feasible. Palestinian violence against settlers, by contrast, follows existing settler presence rather than territorial opportunity, and new unauthorized outposts later concentrate in the same high-opportunity areas. The pattern is therefore not just one of more violence, but of violence moving toward places where it could change what radical settlers call *facts on the ground*.

The paper cannot observe forbearance directly, nor can the reduced-form design separate enforcement from every other effect of the political shift. But the surrounding evidence points the same way. Right-wing Knesset blocs demand punishment far more consistently when Palestinians kill settlers than when settlers kill Palestinians, and recorded IDF–settler confrontations, a narrow proxy for coercive enforcement, remain rare as settler violence expands. With domestic pressure already weak, U.S. diplomatic pressure was an important remaining constraint, and the Trump-era shift weakened it.

The broader contribution is to show how little organization may be required for governments to benefit from non-state violence. Where existing accounts rely on delegation or exchange, here private actors act on their own, yet their actions advance goals political authorities share: by deciding how costly those actions will be, the state can restrain them or let them spread without ever issuing an order. The mechanism should matter wherever domestic accountability is weak and private violence can produce durable political gains, and it may become self-reinforcing—by 2023, politicians aligned with the settler movement held ministerial authority over policy areas relevant to policing, planning, land administration, and enforcement (Chacar, 2022; Williams, 2022). At that point the problem is no longer simply that the state looks away, but that the boundary between those who commit violence and those responsible for restraining it begins to narrow.

References

Acemoglu, D., Egorov, G., and Sonin, K. (2015). Political economy in a changing world. *Journal of Political Economy*, 123(5):1038–1086.

Acemoglu, D., Santos, R. J., and Robinson, J. A. (2013). The monopoly of violence: Evidence from colombia. *Journal of the European Economic Association*, 11(S1):5–44.

ACLED (2023). Resurgence of armed groups in the west bank and their connections to gaza. https://acleddata.com/report/resurgence-armed-groups-west-bank-and-their-connections-gaza. Accessed: 2025-02-07.

ACLED (2024a). Acled codebook. Technical report, Armed Conflict Location & Event Data Project (ACLED). Accessed on July 11, 2025.

ACLED (2024b). Acled dataset. Accessed on 2024-04-17.

Adnan, W. (2015). Who gets to cross the border? the impact of mobility restrictions on labor flows in the west bank. *Labour Economics*, 34:86–99.

Ahren, R. and TOI Staff (2017). Israel okays first new settlement in decades to replace evacuated Amona. *The Times of Israel*. Accessed: 2026-07-15.

Albornoz, F., Bradley, J., and Sonderegger, S. (2022). Updating the social norm: the case of hate crime after the brexit referendum. Working Paper 203, Red Nacional de Investigadores en Economía (RedNIE).

Alvarez-Benjumea, A. and Valentim, V. (2024). The enforcement of political norms. *British Journal of Political Science*, 54:1043–1066.

Andrews, D. W. K. (1993). Tests for parameter instability and structural change with unknown change point. *Econometrica*, 61(4):821–856.

Bai, J. (1997). Estimation of a change point in multiple regression models. *The Review of Economics and Statistics*, 79(4):551–563.

Bai, J. and Perron, P. (1998). Estimating and testing linear models with multiple structural changes. *Econometrica*, 66(1):47–78.

Bai, J. and Perron, P. (2003). Computation and analysis of multiple structural change models. *Journal of Applied Econometrics*, 18(1):1–22.

Ben-Shahar, D., Gabriel, S., and Golan, R. (2019). Ideology, religion, and cheap housing: Israeli settlement of the west bank. Working paper, UCLA Ziman Center for Real Estate. Version: December 18, 2019.

Berman, N. and Couttenier, M. (2015). External shocks, internal shots: the geography of civil conflicts. *Review of Economics and Statistics*, 97(4):758–776.

Bertoni, E., Di Maio, M., Molini, V., and Nistico, R. (2019). Education is forbidden: The effect of the boko haram conflict on education in north-east nigeria. *Journal of Development Economics*, 141:102249.

Bertrand, N. and Hansler, J. (2024). Blinken says israeli settlements in west bank are inconsistent with international law. *CNN*.

Bisin, A., Schiavone, M., Traverso, F. E., and Verdier, T. (2026). The political economy of autocratic transitions: The role of delegation of violence. Working paper.

B'Tselem (2021). State business: Israel's misappropriation of land in the west bank through settler violence. Report, B'Tselem - The Israeli Information Center for Human Rights in the Occupied Territories. Accessed: 2025-06-17.

B'Tselem (2021). This is ours and this too: Israel's settlement policy in the west bank.

B'Tselem (2024). B'tselem statistics. Map data. Accessed on 2024-04-17.

B'Tselem (2025). Interactive map of the west bank. Online Interactive Map. Accessed: 2025-04-17.

Bursztyn, L., Egorov, G., and Fiorin, S. (2020). From extreme to mainstream: The erosion of social norms. *American Economic Review*, 110(11):3522–3548.

Caetano, M. A. L. (2021). Political activity in social media induces forest fires in the brazilian amazon. *Technological Forecasting and Social Change*, 167:120676.

Calì, M. and Miaari, S. H. (2018). The labor market impact of mobility restrictions: Evidence from the west bank. *Labour Economics*, 51:136–151.

Carey, S. C., Mitchell, N. J., and Lowe, W. (2013). States, the security sector, and the monopoly of violence: A new database on pro-government militias. *Journal of Peace Research*, 50(2):249–258.

Chacar, H. (2022). Israeli far-right's ben-gvir to be national security minister under coalition deal. *Reuters*.

Chen, J. and Roth, J. (2024). Logs with zeros? some problems and solutions. *The Quarterly Journal of Economics*, 139(2):891–936.

Don-Yehiya, E. (2014). Messianism and politics: The ideological transformation of religious zionism. *Israel Studies*, 19(2):239–263.

Dube, O. and Naidu, S. (2015). Bases, bullets, and ballots: The effect of u.s. military aid on political conflict in colombia. *The Journal of Politics*, 77(1):249–267.

Durante, R. and Zhuravskaya, E. (2018). Attack when the world is not watching? us news and the israeli-palestinian conflict. *Journal of Political Economy*, 126(3):1085–1133.

European Parliament (2012). Jerusalem: The Heart of the Israeli-Palestinian Conflict. Technical report, Directorate-General for External Policies of the Union. Briefing Note.

European Space Agency and Airbus Defence and Space (2021). Copernicus digital elevation model (dem) glo-30, cloud-optimized geotiff (cog). 30-meter resolution global DEM derived from TanDEM-X. Product: `Copernicus_DSM_COG_10`. Accessed: 2024.

European Union, Copernicus Land Monitoring Service (2025). Copernicus sentinel-2 level-2a data. Accessed via openEO Platform API (e.g., openeo.cloud or specific backend). European Union's Copernicus Land Monitoring Service information.

Fearon, J. D. and Laitin, D. D. (2003). Ethnicity, insurgency, and civil war. *American Political Science Review*, 97(1):75–90.

Giani, M. and Méon, P.-G. (2021). Global racist contagion following donald trump's election. *British Journal of Political Science*, 51(4):1332–1343. Documents international spillover effects of Trump's election on racist behavior and hate crimes globally.

Goldin, G., Howell, N., Ordan, N., Rabinovich, E., and Wintner, S. (2024). The knesset corpus: An annotated corpus of hebrew parliamentary proceedings.

Goldin, G., Howell, N., Ordan, N., Rabinovich, E., and Wintner, S. (2025). The knesset corpus: an annotated corpus of hebrew parliamentary proceedings: G. goldin et al. *Language Resources and Evaluation*, pages 1–32.

Government of Israel and Palestine Liberation Organization (1993). Declaration of principles on interim self-government arrangements. Signed at Washington, D.C., 13 September 1993.

Government of Israel and Palestine Liberation Organization (1995). Israeli-palestinian interim agreement on the west bank and the gaza strip. Signed at Washington, D.C., 28 September 1995.

Graham-Harrison, E. (2026). No israel prosecutions for killing palestinian civilians in occupied west bank since start of decade. *The Guardian*. Accessed: 2026-03-27.

Haaretz (2017). Israel approves first new West Bank settlement in over 20 years for Amona evacuees. *Haaretz*. Accessed: 2026-07-15.

Havelock, R. (2011). *River Jordan: The Mythology of a Dividing Line*. University of Chicago Press, Chicago.

Heilman, U. (2015). Naftali bennett: Time to annex parts of west bank. *Jewish Telegraphic Agency*. Accessed August 27, 2026.

Herbst, J. (2000). *States and Power in Africa: Comparative Lessons in Authority and Control*. Princeton University Press, Princeton, NJ.

Hershkowitz, I. (2026). From fringe to core: The temple mount in religious zionism's evolving identity. *Modern Judaism—A Journal of Jewish Ideas and Experience*, 46(1):1–19.

Hirsch-Hoefler, S. and Mudde, C. (2020). *The Israeli Settler Movement: Assessing and Explaining Social Movement Success*. Cambridge University Press, Cambridge.

Holland, A. C. (2016). Forbearance. *American Political Science Review*, 110(2):232–246.

Human Rights Watch (2019). Violent cow protection in india: Vigilante groups attack minorities. Technical report, Human Rights Watch. Accessed: 2026-05-19.

International Committee of the Red Cross (1949). Geneva convention relative to the protection of civilian persons in time of war (fourth geneva convention). Adopted in Geneva. Official text available from the International Committee of the Red Cross (ICRC) or United Nations Treaty Series (UNTS Vol. 75, No. 973). Commonly known as the Fourth Geneva Convention.

International Committee of the Red Cross (2024). What does the law say about the responsibilities of the occupying power in the occupied palestinian territory?

International Court of Justice (2024). Legal consequences arising from the policies and practices of israel in the occupied palestinian territory, including east jerusalem. Advisory Opinion of 19 July 2024, General List No. 186.

Israel Defense Forces (2023). One year since operation break the wave. https://www.idf.il/en/articles/2023/one-year-since-operation-break-the-wave/. Accessed: 2025-02-07.

Israel Hayom (2017). Netanyahu to cabinet: We will build in jerusalem without restriction. *Israel Hayom*. Accessed August 27, 2026.

Jaeger, D. A., Klor, E. F., Miaari, S. H., and Paserman, M. D. (2012). The struggle for palestinian hearts and minds: Violence and public opinion in the second intifada. *Journal of Public Economics*, 96(3-4):354–368.

Jentzsch, C., Kalyvas, S. N., and Schubiger, L. I. (2015). Militias in civil wars. *Journal of Conflict Resolution*, 59(5):755–769.

Jewish Virtual Library (1977). Original party platform of the likud party. Accessed: 2026-03-30.

Kafando, W. A. and Sakurai, T. (2024). Armed conflicts and household food insecurity: Effects and mechanisms. *Agricultural Economics*, 55(2):313–328.

Kershner, I. (2017). Israel approves 2,500 new settlement homes in west bank. *The New York Times*. Accessed: 2026-03-26.

Knesset Election Results Data (2025). Online Data Portal. Accessed: 2025-04-17. Provides access to datasets on Knesset election results. Specific dataset version/election year used should ideally be cited.

Koplewitz, T. (2025). Settler violence: Turning the west bank into a tinderbox. The Washington Institute for Near East Policy, Accessed: 2026-03-30.

Kurtzer, D. C. (2016). Sleight of hand: Israel, settlements, and unauthorized outposts. Policy Focus 24, Middle East Institute.

Lessing, B. (2015). Logics of violence in criminal war. *Journal of Conflict Resolution*, 59(8):1486–1516.

Lessing, B. (2018). *Making Peace in Drug Wars: Crackdowns and Cartels in Latin America*. Cambridge University Press, Cambridge.

Magid, J. (2018a). Cabinet votes to advance legalization of slain rabbi's west bank outpost. *The Times of Israel*.

Magid, J. (2018b). Pm orders illegal outpost hooked up to power grid after terror attack. *The Times of Israel*.

Maskara, S. (2021). Cow protection legislation and vigilante violence in india. Armed Conflict Location & Event Data Project. Accessed: 2026-05-19.

Maxar Technologies (2023). Maxar satellite imagery of the West Bank. https://www.arcgis.com/home/item.html?id=10df2279f9684e4a9f6a7f08febac2a9. Imagery acquired October 21, 2023. Accessed July 11, 2025.

Migdal, J. S. (1988). *Strong Societies and Weak States: State-Society Relations and State Capabilities in the Third World*. Princeton University Press, Princeton, NJ.

Milgrom, P. and Shannon, C. (1994). Monotone comparative statics. *Econometrica*, 62(1):157–180.

Ministry of Foreign Affairs, State of Israel (2015). Israeli settlements and international law.

Müller, K. and Schwarz, C. (2023). From hashtag to hate crime: Twitter and antiminority sentiment. *American Economic Journal: Applied Economics*, 15(3):270–312.

NASA Land Processes Distributed Active Archive Center (LP DAAC) (2016). MOD13Q1: MODIS/terra vegetation indices 16-day L3 global 250 m SIN grid, version

6.1. Tile h21v05, year 2016 (summer composite). Retrieved from AWS Open Data: https://registry.opendata.aws/modis-astraea/. Accessed: 2024.

Nellis, G., Weaver, M., and Rosenzweig, S. C. (2016). Do parties matter for ethnic violence? evidence from india. *Quarterly Journal of Political Science*, 11(3):249–277.

Nicolle-Hasid, P. (2019). Beyond and despite the state: Young religious settlers' vision of messianic redemption. *Quest: Issues in Contemporary Jewish History*, 16:116–143.

Nunes, F. S. M., Soares-Filho, B. S., Oliveira, A. R., Veloso, L. V. S., Schmitt, J., Van der Hoff, R., Assis, D. C., Costa, R. P., Börner, J., Ribeiro, S. M. C., Rajão, R. G. L., de Oliveira, U., and Costa, M. A. (2024). Lessons from the historical dynamics of environmental law enforcement in the brazilian amazon. *Scientific Reports*, 14:1828.

OCHA (2017). Increase in settler violence during the first half of 2017. Report, OCHA oPt. Part of The Monthly Humanitarian Bulletin, May 2018. Accessed: 2025-04-17.

Office of the United Nations High Commissioner for Human Rights (2023). The human rights situation in the occupied west bank including east jerusalem. Flash Report.

OpenStreetMap Contributors (2017). Openstreetmap: Religious and archaeological sites in the west bank (historical snapshot, 31 december 2017). Retrieved via Overpass API (https://overpass-api.de) with time-travel query dated 2017-12-31. Bounding box: West Bank (31.3°N–32.6°N, 34.8°E–35.6°E).

Palestinian Central Bureau of Statistics (2025). Estimated population in the palestine mid-year by governorate, 1997-2026. Accessed: 2024-07-16.

Pappe, I. (2017). *The Biggest Prison on Earth: A History of the Occupied Territories*. Oneworld Publications, London.

Peace Now (2017a). Unraveling the mechanism behind illegal outposts. Report, Peace Now. Report authors: Ofran, Hagit and Shem-Tov, Aharon.

Peace Now (2017b). Unraveling the mechanism behind illegal outposts - full report. Full report, Peace Now.

Peace Now (2024). Settlement watch data and reports. Settlement Watch. Accessed on 2024-04-17.

Peace Now (2025). Settlement watch data and reports. Online Data Portal / Project Website. Provides ongoing data and reports on Israeli settlements and outposts. Accessed: 2025-04-17.

Reuters Staff (2017a). Israel legalizes settler homes on private palestinian land. *Reuters*.

Reuters Staff (2017b). Israel removes settlers from homes on private palestinian land. *Reuters*.

Reuters Staff (2017c). Israel wraps up illegal outpost evacuation, promises new settlement. *Reuters*.

Rohner, D., Thoenig, M., and Zilibotti, F. (2013). Seeds of distrust: Conflict in uganda. *Journal of Economic Growth*, 18(3):217–252.

Shalom Hartman Institute (2022). The hilltop youth and jewish terrorism. Accessed: 2026-03-30.

Sharvit Baruch, P. (2020). The settlement law. Institute for National Security Studies (INSS), Accessed: 2026-03-30.

Staniland, P. (2012). States, insurgents, and wartime political orders. *Perspectives on politics*, 10(2):243–264.

Staniland, P. (2015). Militias, ideology, and the state. *Journal of Conflict Resolution*, 59(5):770–793.

Supreme Court of Israel, sitting as the High Court of Justice (2005). Mara'abe v. Prime Minister of Israel. HCJ 7957/04, judgment of 15 September 2005.

Supreme Court of Israel, sitting as the High Court of Justice (2011). Al-Nabut et al. v. Minister of Defense et al. HCJ 8887/06, judgment of 2 August 2011. Migron case.

Supreme Court of Israel, sitting as the High Court of Justice (2014). Hamad et al. v. Minister of Defense et al. HCJ 9949/08, judgment of 25 December 2014. Amona case.

Supreme Court of Israel, sitting as the High Court of Justice (2020). Silwad Municipality et al. v. Knesset et al. HCJ 1308/17 and HCJ 2055/17, judgment of 9 June 2020. Settlement Regularization Law case.

Times of Israel Staff (2016). State asks high court to delay amona outpost demolition. *The Times of Israel*.

TOI Staff (2018). Terror victim raziel shevach remembered as unique, kindhearted man. *The Times of Israel*. Updated January 9, 2018, 11:51 p.m.; accessed 21 May 2026.

TOI Staff (2021). Bennett scolds police minister for discussing settler violence with us official. *The Times of Israel*.

Trump, D. J. (2017). Presidential proclamation recognizing jerusalem as the capital of the state of israel and relocating the united states embassy to israel to jerusalem. Proclamation 9683, 82 Fed. Reg. 58331.

United Nations Office for the Coordination of Humanitarian Affairs (2021). Escalation of hostilities and unrest in the opt: Flash appeal. https://www.unocha.org/publications/report/occupied-palestinian-territory/

escalation-hostilities-and-unrest-opt-flash-appeal-27-may-2021. Accessed: 2025-02-07.

United Nations Office for the Coordination of Humanitarian Affairs (OCHA) (2017). Common operational datasets: Administrative boundaries and road network for the occupied palestinian territory. Administrative boundaries: https://data.humdata.org/dataset/2caf8373-816f-458c-9913-71bddb9cab7c; Road network (OCHA/JRC): https://data.humdata.org/dataset/916c7ce0-1c2b-47fb-b134-b7c93ddf89a4. Accessed: 2024.

United Nations Security Council (1979a). Resolution 446 (1979). UN Document S/RES/446.

United Nations Security Council (1979b). Resolution 452 (1979). UN document S/RES/452(1979). Adopted by the Security Council on 20 July 1979.

United Nations Security Council (1980a). Resolution 465 (1980). UN document S/RES/465(1980). Adopted by the Security Council on 1 March 1980.

United Nations Security Council (1980b). Resolution 478 (1980). UN Document S/RES/478.

United Nations Security Council (1981). Resolution 497 (1981). UN Document S/RES/497. On the Israeli decision to apply its law, jurisdiction and administration in the occupied Syrian Golan Heights.

United Nations Security Council (1983). Draft Resolution S/15895. UN document S/15895. Draft resolution concerning Israeli settlement policies in the occupied Arab territories; not adopted owing to the negative vote of a permanent member.

United Nations Security Council (1997a). Draft Resolution S/1997/199. UN document S/1997/199. Draft resolution concerning Israeli settlement activities in East Jerusalem; not adopted owing to the negative vote of a permanent member.

United Nations Security Council (1997b). Draft Resolution S/1997/241. UN document S/1997/241. Draft resolution concerning the Jabal Abu Ghneim settlement in East Jerusalem; not adopted owing to the negative vote of a permanent member.

United Nations Security Council (2011). Draft Resolution S/2011/24. UN document S/2011/24. Draft resolution on cessation of Israeli settlement activities in the Occupied Palestinian Territory, including East Jerusalem; not adopted owing to the negative vote of a permanent member.

United Nations Security Council (2016). Resolution 2334 (2016). UN Document S/RES/2334.

U.S. Department of State (2023). West Bank and Gaza. https://2021-2025.state.gov/report/custom/adc605fb0b/. International Religious Freedom report, accessed May 19, 2026.

Weymouth, L. (2013). Lally weymouth interviews israeli politician naftali bennett. *The Washington Post*. Accessed August 27, 2026.

Wilkinson, S. I. (2004). *Votes and Violence: Electoral Competition and Ethnic Riots in India*. Cambridge University Press, Cambridge.

Williams, D. (2022). Israel's netanyahu returns with hard-right cabinet set to expand settlements. *Reuters*.

Yanagizawa-Drott, D. (2014). Propaganda and conflict: Evidence from the rwandan genocide. *The Quarterly Journal of Economics*, 129(4):1947–1994.

Yesh Din (2015). Data sheet october 2015: Law enforcement on israeli citizens who harm palestinians and their property in the west bank.

Ynetnews (2015). Deputy foreign minister hotovely tells world: Don't be afraid of me. *Ynetnews*. Accessed August 27, 2026.

A. Figures

Figure A.1: Knesset Speech Data

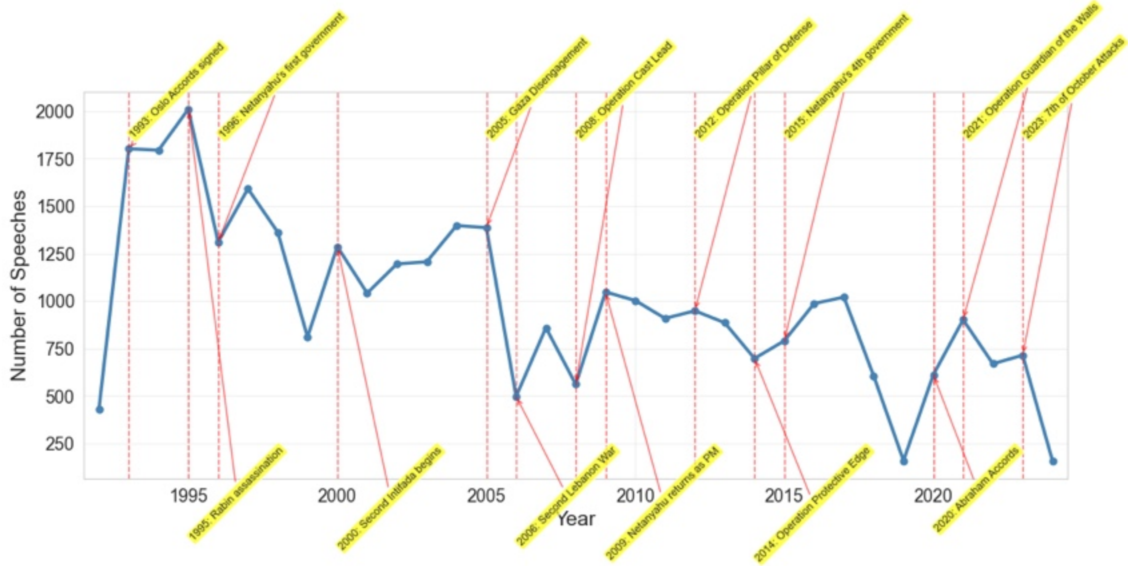

(a) Number of speeches by year

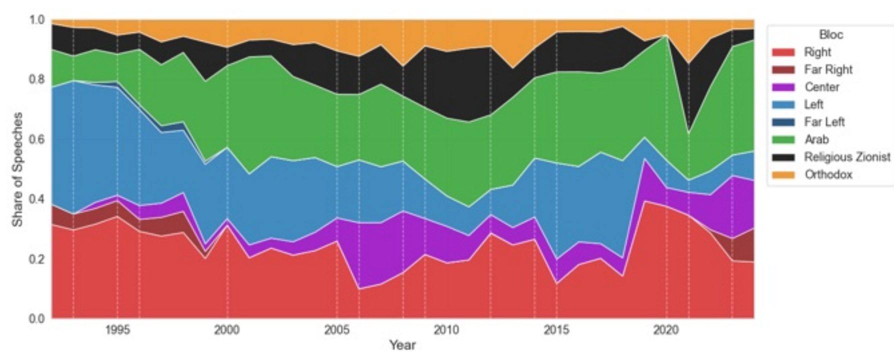

(b) Share of speeches by bloc

Notes: Time series of Knesset speeches on topics related to occupied territories. Panel (a) shows the total number of speeches per year along with important events in the Israeli-Palestinian conflict, while Panel (b) shows the share of speeches by political bloc. The data has been retrieved from Goldin et al. (2024) and classified using ChatGPT 4o-mini as explained in Section 4. Party classification into different faction follows Goldin et al. (2025) and is reported in Appendix Table H.13.

Figure A.2: Map of the West Bank

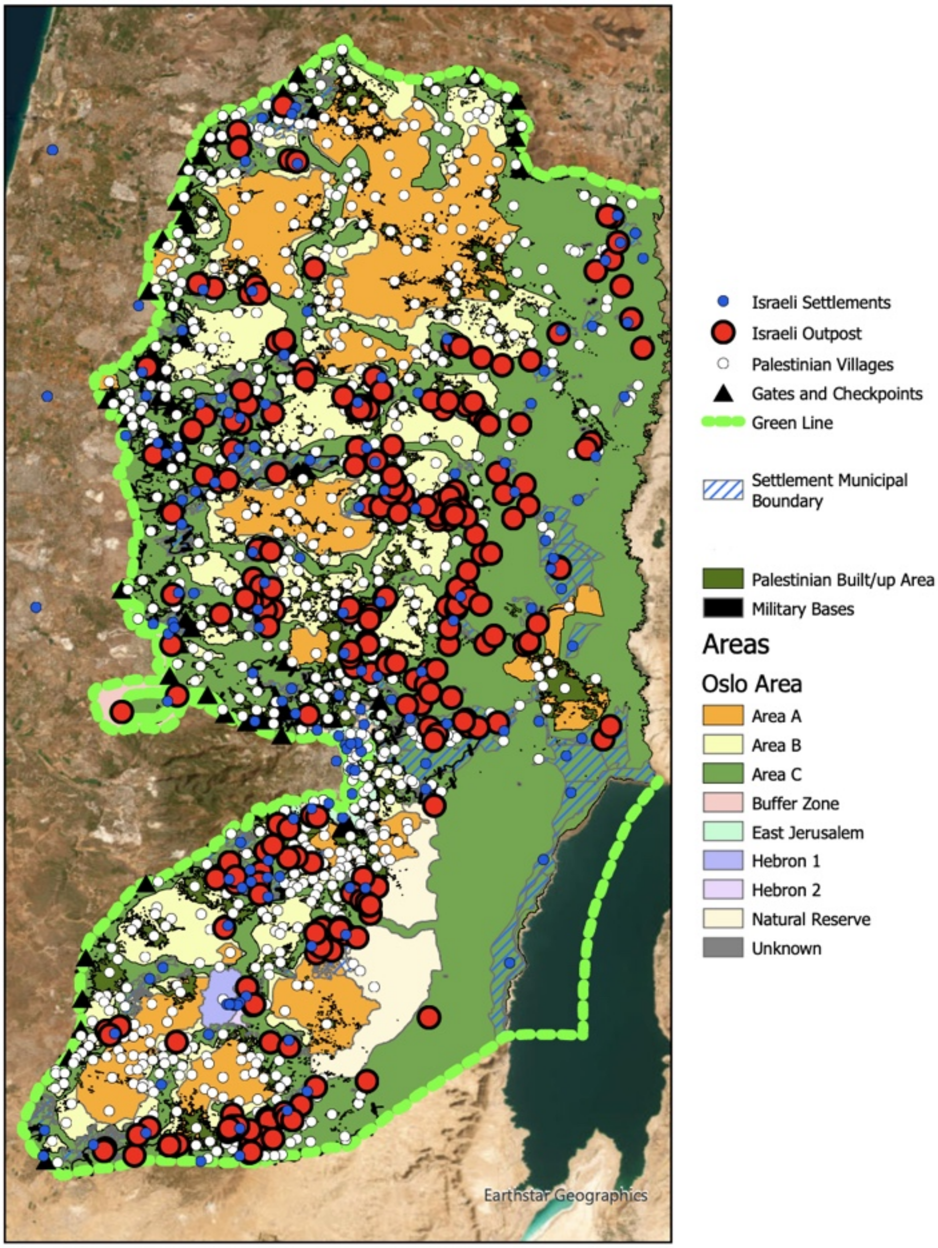

Notes: Map of the West Bank. Point geometries include Palestinian towns and villages (white dots), Israeli settlements (blue dots), Israeli outposts (red dots). Polygon geometries include Oslo Areas partitions, settlement municipality areas, Palestinian built-up areas and military bases. Source: B'Tselem (2025) and Peace Now (2024).

Figure A.3: Outpost Suitability Map

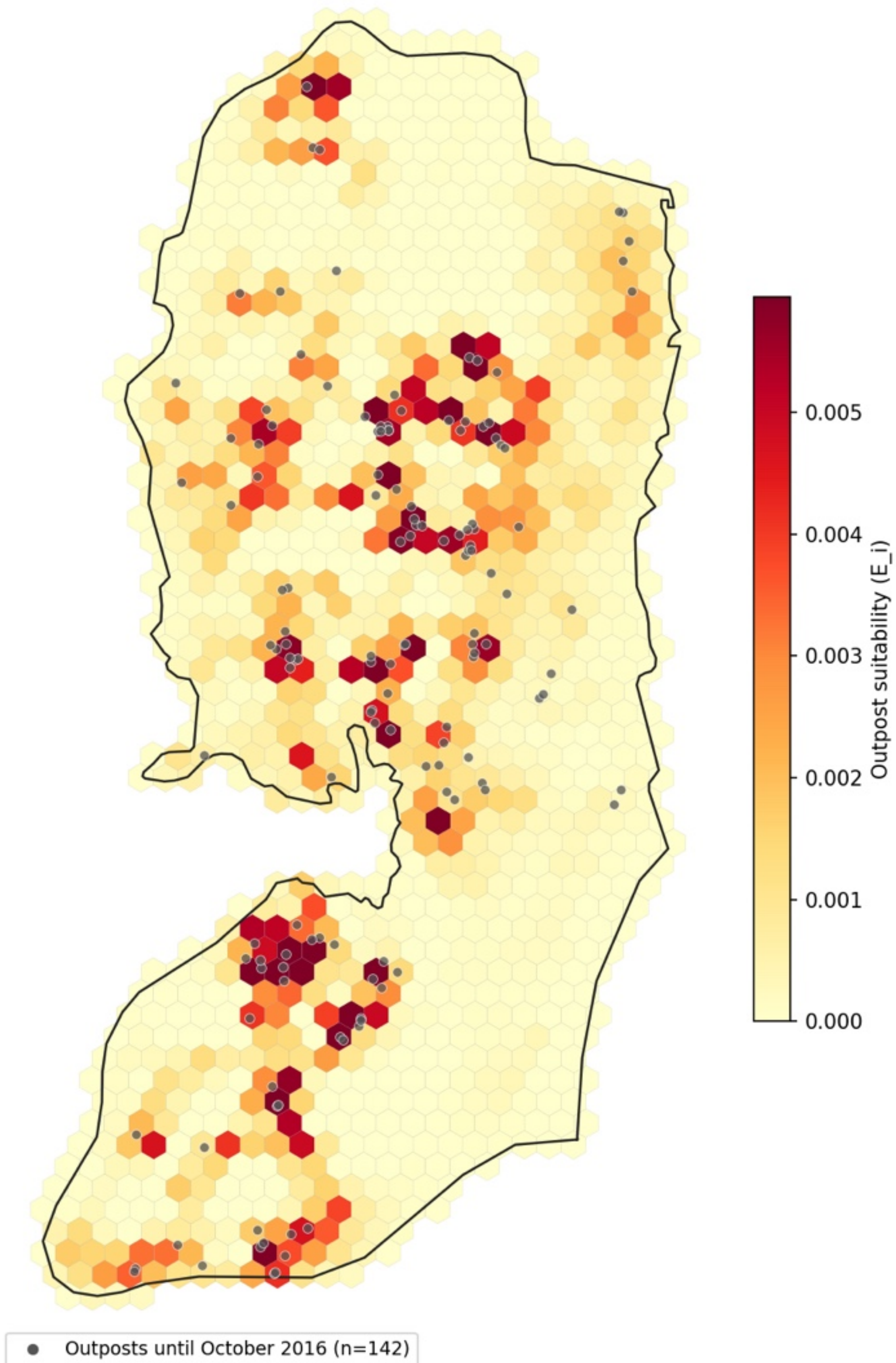

Notes: Predicted outpost suitability E_i for each hex cell, estimated from the PPML model on 1990–2016 outpost expansion data. Darker cells indicate higher predicted suitability.

Figure A.4: Treatment Construction Maps

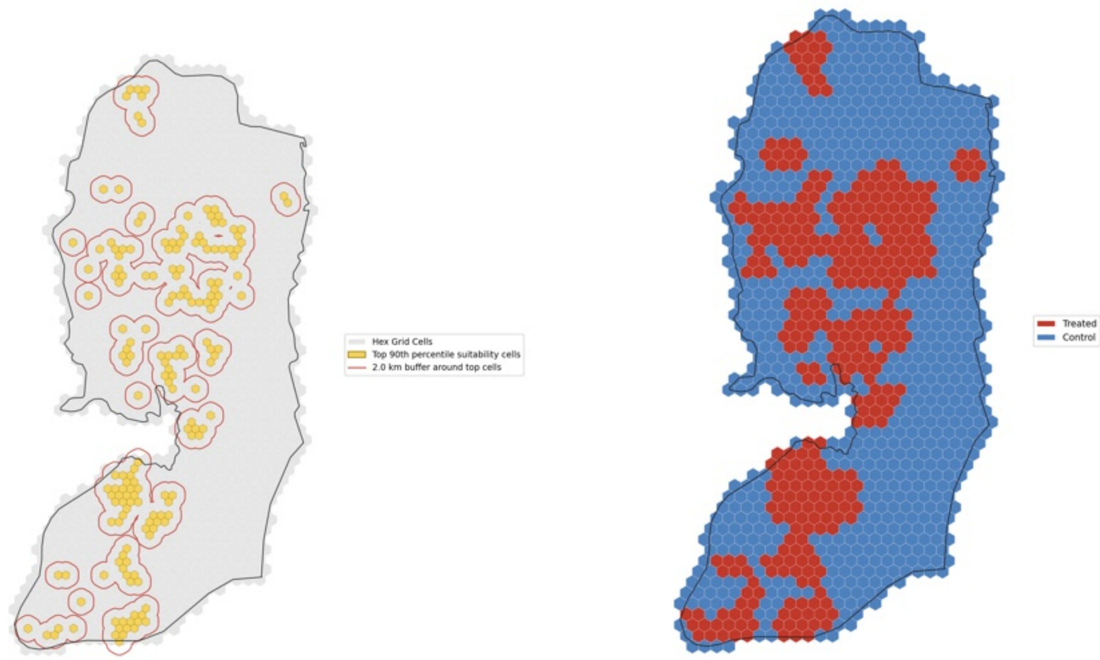

(a) Top 10% Suitability + 2 km Buffer

(b) Treated and Control Cells

Notes: Panel (a) shows the top-decile suitability cells and the 2 km buffer used to construct the treatment area. Panel (b) shows the resulting treated (red) and control (blue) grid cells.

Figure A.5: Event-Study Estimates: Settler–Palestinian Violence

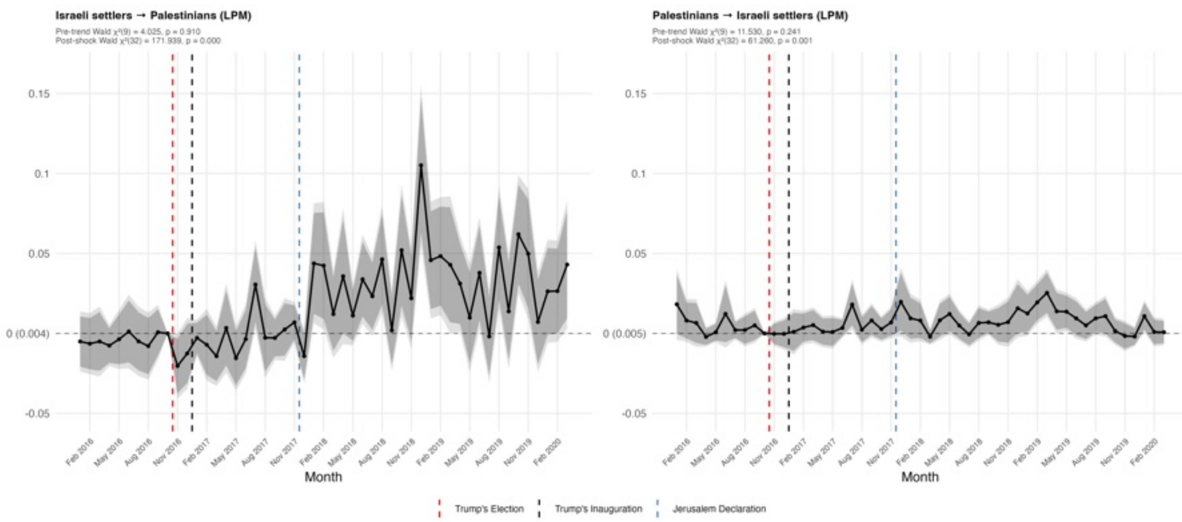

Notes: The figure reports event-study coefficients from the baseline LPM specification using the monthly event incidence. The omitted period is the month immediately before Trump's election. All specifications include hex-cell fixed effects, month-year fixed effects, controls, and Conley standard errors. Darker (lighter) shaded areas denote 95% (90%) confidence intervals. Vertical lines mark Trump's election, Trump's inauguration, and the Jerusalem Declaration.

Figure A.6: Event-Study Estimates: IDF–Palestinian Violence

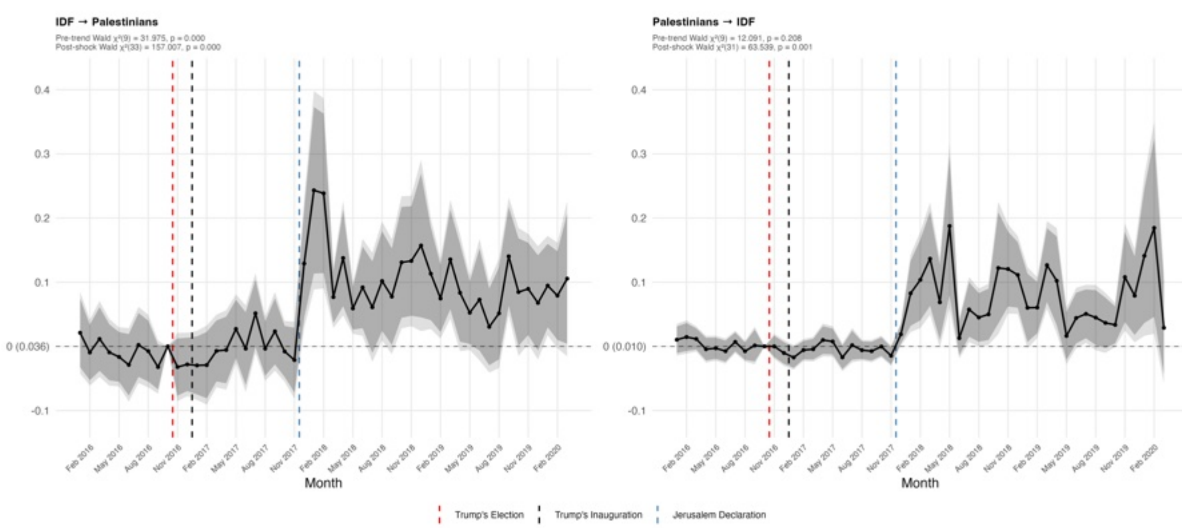

Notes: The figure reports event-study coefficients from the baseline TWFE specification using the monthly event counts. The omitted period is the month immediately before Trump's election. All specifications include hex-cell fixed effects, month-year fixed effects, controls, and Conley standard errors. Darker (lighter) shaded areas denote 95% (90%) confidence intervals. Vertical lines mark Trump's election, Trump's inauguration, and the Jerusalem Declaration.

Figure A.7: Event-Study Estimates: IDF–Palestinian Violence

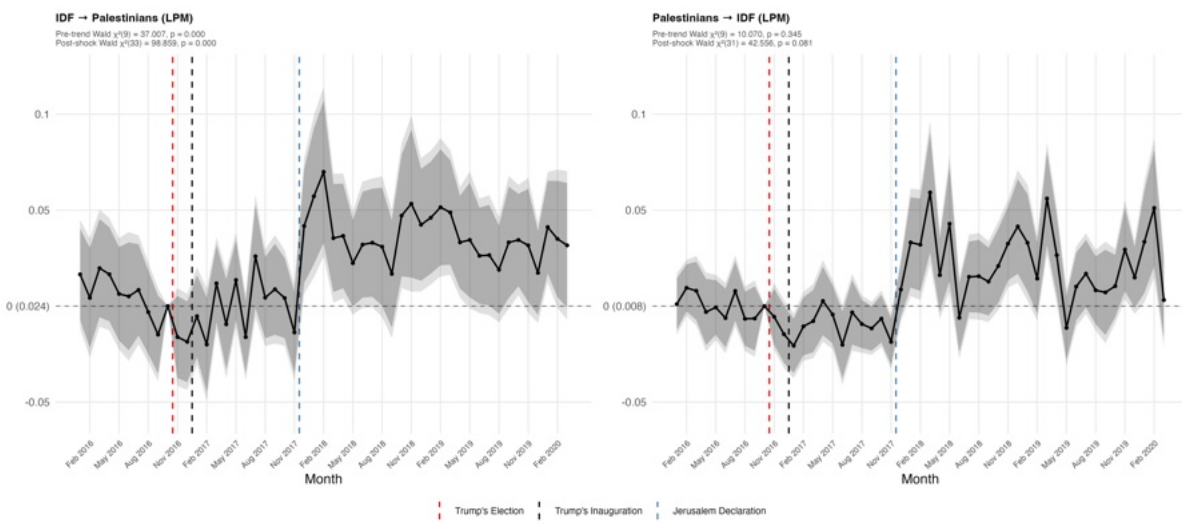

Notes: The figure reports event-study coefficients from the baseline LPM specification using the monthly event incidence. The omitted period is the month immediately before Trump's election. All specifications include hex-cell fixed effects, month-year fixed effects, controls, and Conley standard errors. Darker (lighter) shaded areas denote 95% (90%) confidence intervals. Vertical lines mark Trump's election, Trump's inauguration, and the Jerusalem Declaration.

Figure A.8: Event-Study Estimates: Civilian Targeting

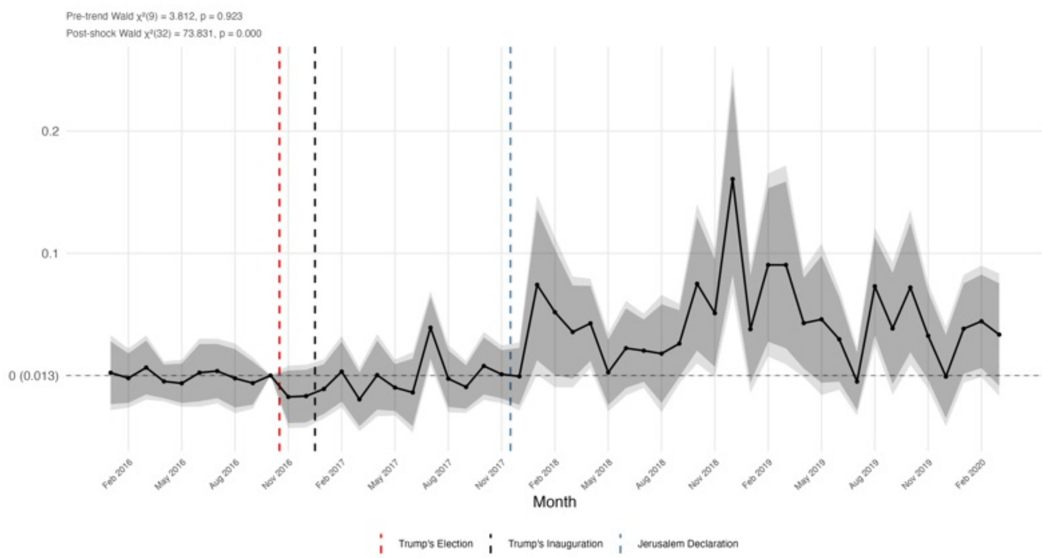

(a) Civilian Targeting: Event counts

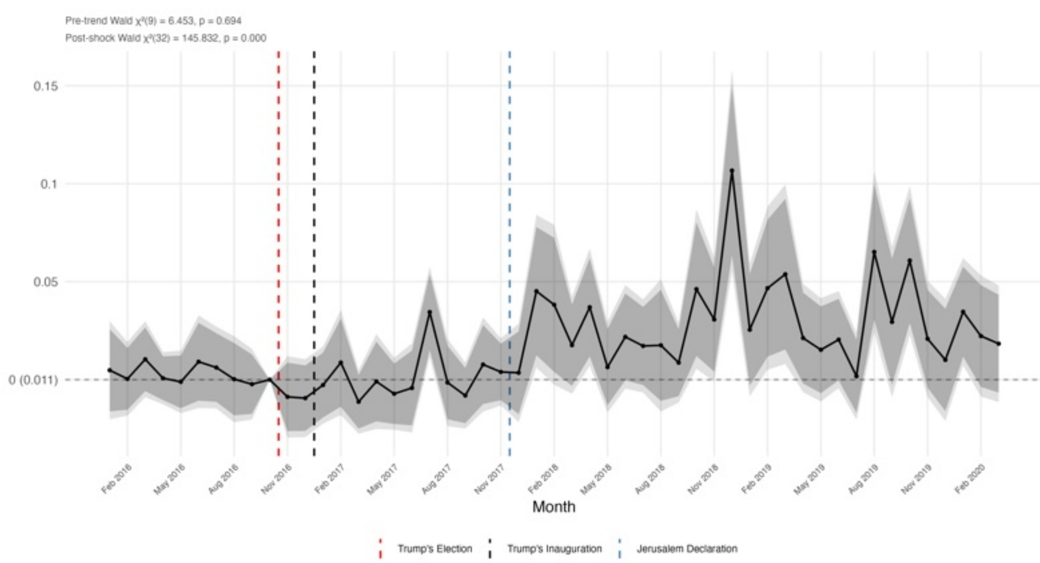

(b) Civilian Targeting: LPM

Notes: The figure reports event-study coefficients from the baseline TWFE specification using monthly event counts and LPM specification. The omitted period is the month immediately before Trump's election. All specifications include hex-cell fixed effects, month-year fixed effects, controls, and Conley standard errors. Darker (lighter) shaded areas denote 95% (90%) confidence intervals. Vertical lines mark Trump's election, Trump's inauguration, and the Jerusalem Declaration.

Figure A.9: Settler Violence after Fatal Attacks on Settlers (LPM)

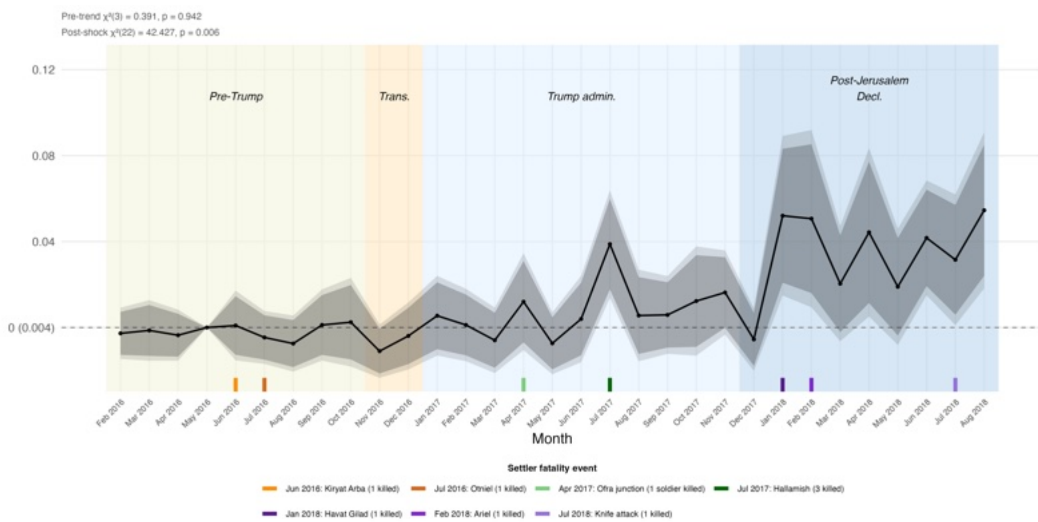

Notes: The figure reports event-study coefficients for settler violence against Palestinians from the LPM specification, using an incidence outcome equal to one if at least one settler-on-Palestinian event occurs in a hex cell-month, re-centered around the first fatal attack against settlers in the sample. This is the linear-probability counterpart to the event-count specification reported in Figure 6. The omitted month is May 2016. Shaded background areas indicate political periods, and colored ticks mark fatal attacks against settlers. All specifications include hex-cell fixed effects, month-year fixed effects, controls, and Conley standard errors. Darker and lighter shaded confidence bands denote 95% and 90% confidence intervals, respectively.

Figure A.10: Event-Study Estimates: Settler–Palestinian Violence

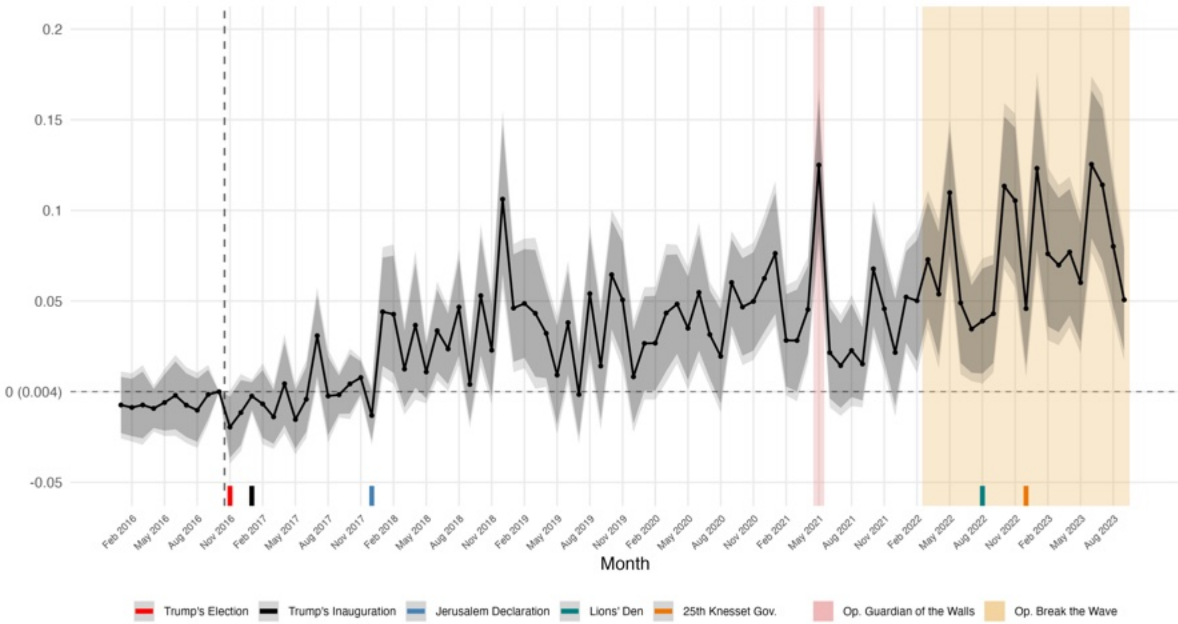

(a) Israeli Settlers → Palestinians

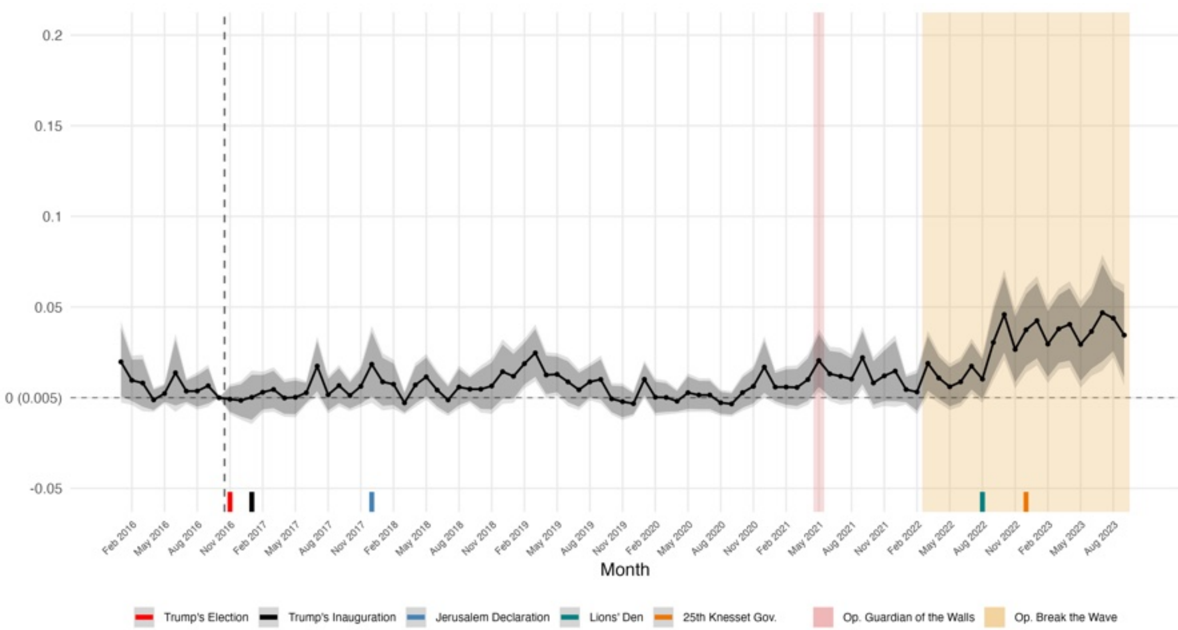

(b) Palestinians → Israeli Settlers

Notes: The figure reports event-study coefficients from the baseline LPM specification using monthly event incidence. Bottom markers signal Trump's election, Trump's inauguration, and the Jerusalem Declaration as well as the emergence of the Palestinian militia Lion's Den and the start of the 25th Knesset government in 2022. Shaded areas depict Operation Guardian of the Walls and Operation Break the Wave. Both plots share the same y-axis scale. All specifications include hex-cell fixed effects, month-year fixed effects, controls, and Conley standard errors. Darker (lighter) shaded areas denote 95% (90%) confidence intervals.

Figure A.11: Settlement Proximity vs. Radical Frontier: Groups across the West Bank

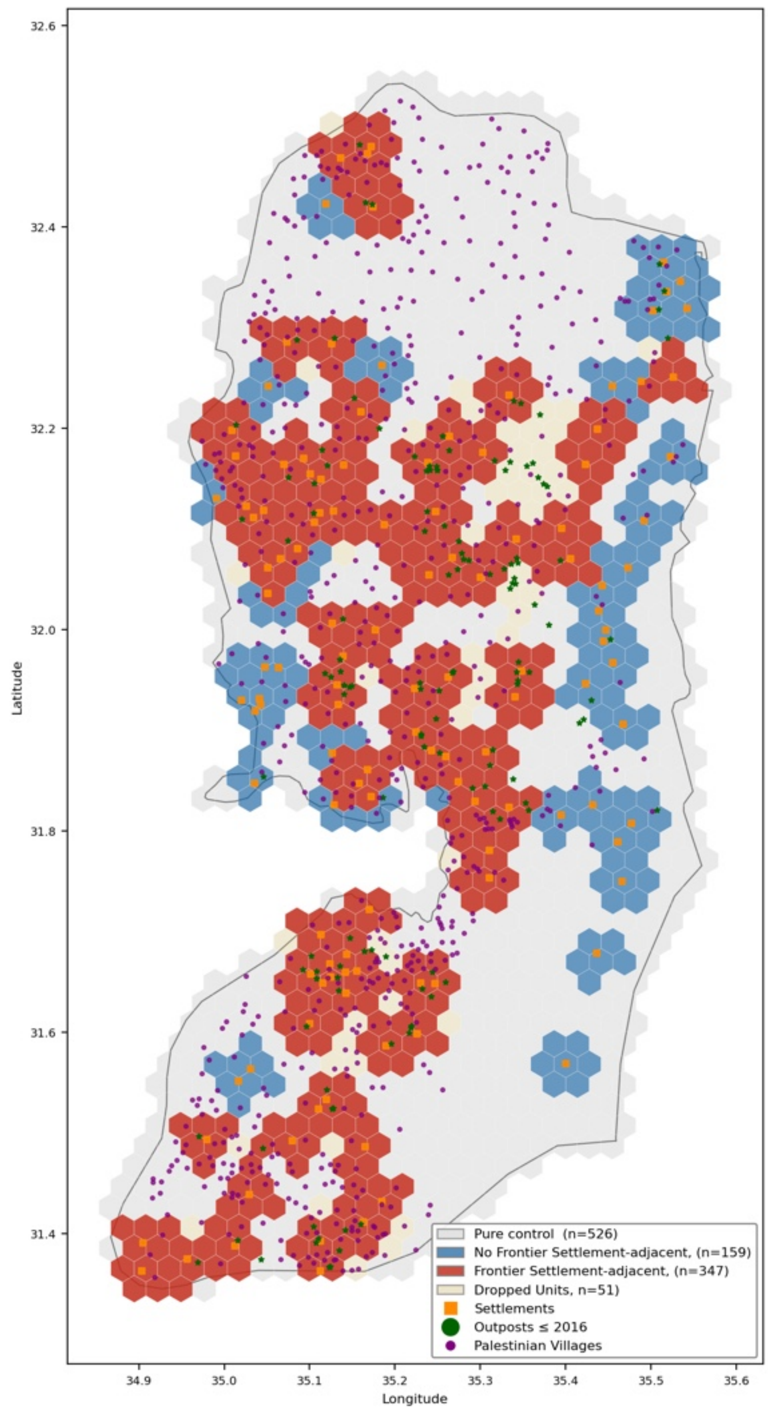

Notes: Spatial distribution of the three sample groups used in the two-arm event study of Section 7. Grey cells: pure controls (not settlement-adjacent, not in high outpost-suitability zone). Black cells: non-frontier settlement-adjacent ($N_i = 1$, within 2 km of a settlement, outside high-suitability zone). Red cells: frontier settlement-adjacent ($R_i = 1$, within 2 km of a settlement and in high-suitability zone). Orange squares: established settlement centroids. Green stars: outposts established by 2016.

Figure A.12: Settlement Proximity vs. Radical Frontier: Event-Study Estimates (LPM)

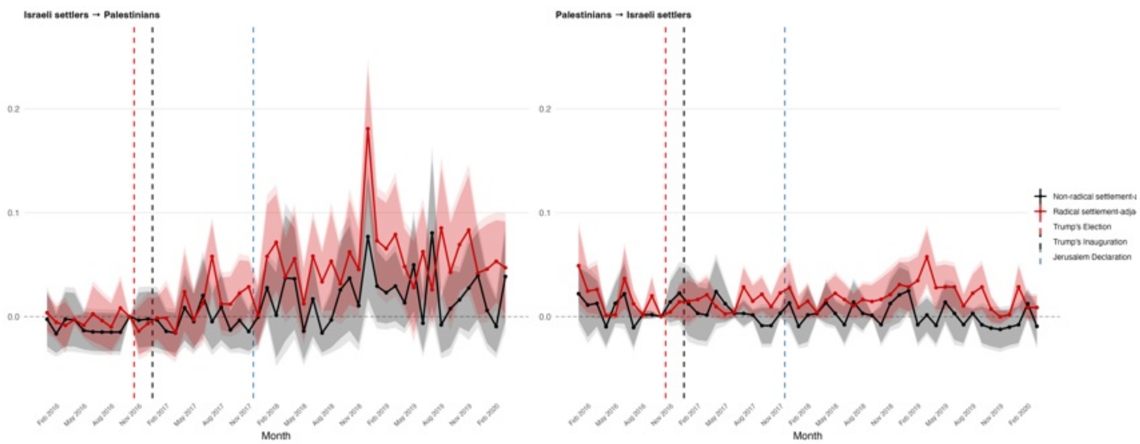

Notes: The figure reports event-study coefficients for Israeli settler violence against Palestinians from the LPM specification with monthly incidence. This is the linear-probability counterpart to the event-count specification reported in Figure 8. Two-arm event study (equation (3)), monthly hex-cell panel, Nov 2015 – Mar 2020. Black line: non-frontier settlement-adjacent arm ($N_i = 1$, within 2 km of an established settlement, outside high outpost-suitability zone). Red line: frontier settlement-adjacent arm ($R_i = 1$, within 2 km of a settlement and in high outpost-suitability zone). Both arms estimated vs. the same pure-control group (not settlement-adjacent, not treated). Shaded bands: 95% (light) and 90% (dark) confidence intervals. Conley spatial standard errors, 5 km cutoff. Vertical lines: Trump's election (dashed red), inauguration (dashed black), Jerusalem Declaration (dashed blue).

Figure A.13: Treatment Construction Map: Baseline vs. No-outpost Design($\hat{E}^{NO}$)

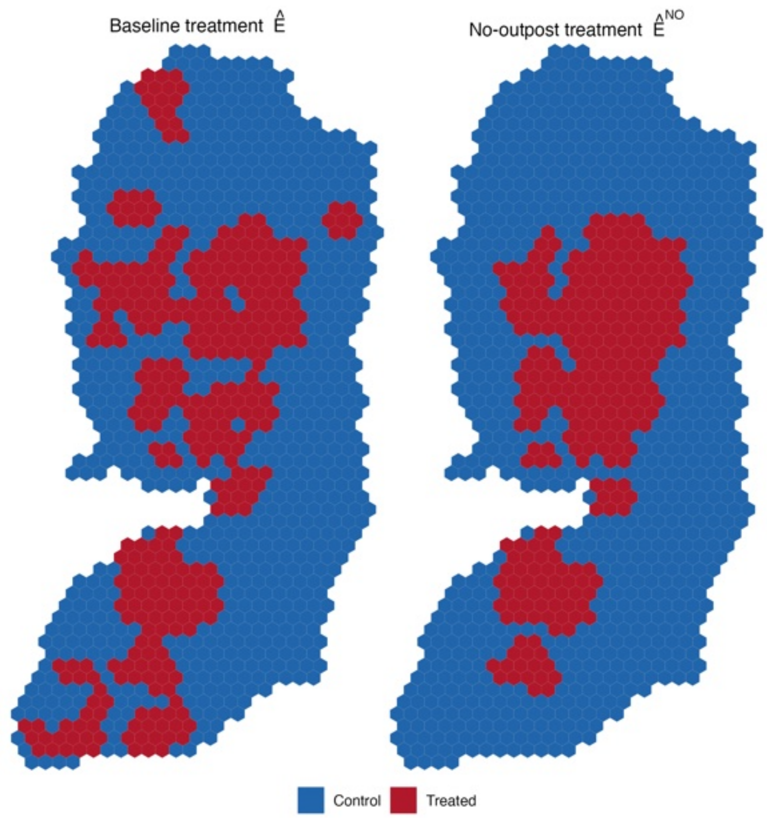

Notes: Treatment map comparing the baseline design (left) with the no-outpost-network design ($\hat{E}^{NO}$).

Figure A.14: Geographic Opportunity Gradient Across the West Bank

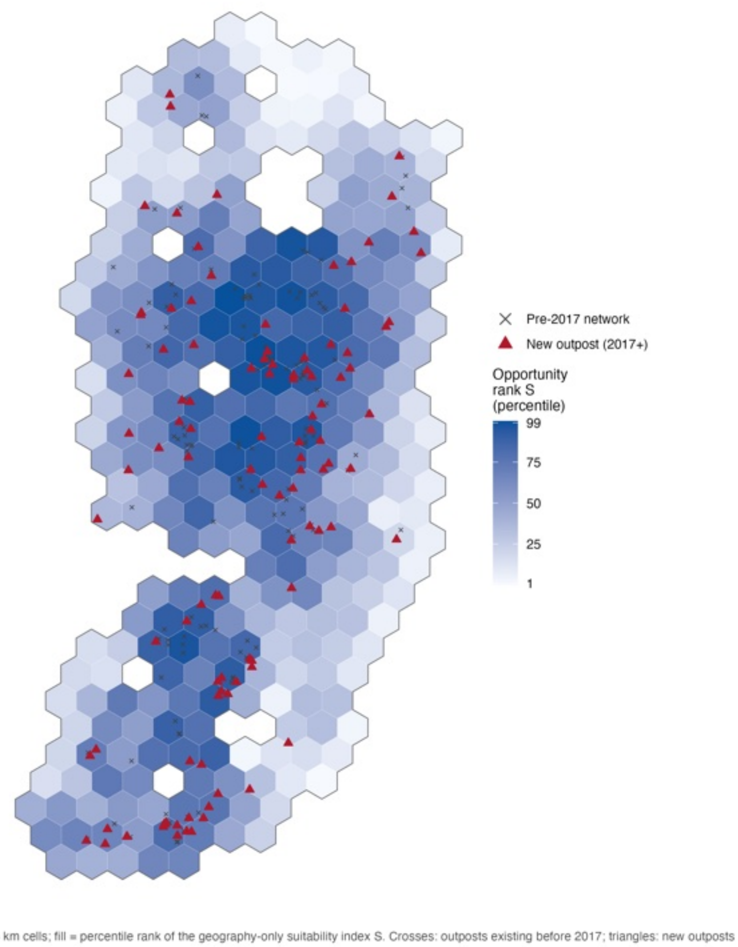

Notes: Map of the estimated geographic-opportunity gradient $\hat{E}_i^{NO}$ across 5 km grid hex cells in the West Bank. Darker shading indicates higher opportunity for new outpost formation.

Figure A.15: Event Study: New Outpost Formation and Geographic Opportunity (Reduced Form)

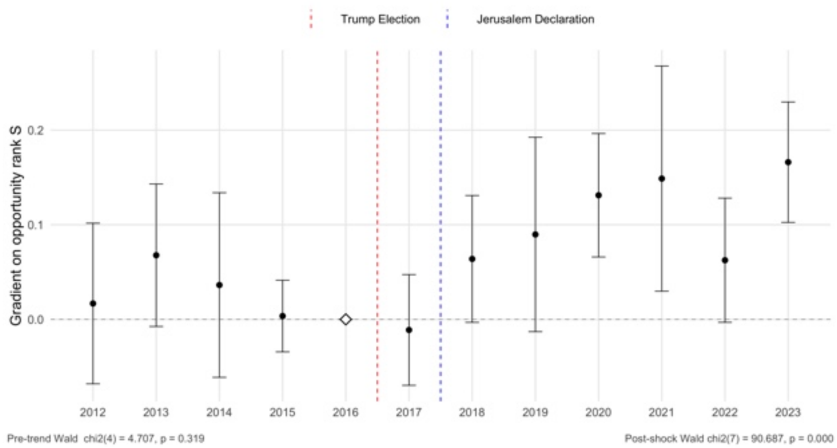

Notes: Reduced-form counterpart to Figure 10, omitting the inherited-network block N_i^0. Event-study estimates of equation (5) on a 5 km cell × year panel, 2012–2023. Cell and year fixed effects; omitted year 2016; Conley standard errors with a 15 km cutoff. Vertical lines mark Trump's election and the Jerusalem Declaration. Joint Wald tests for pre- and post-shock coefficients appear at the bottom of the panel.

Figure A.16: Institutional Forbearance: Settler Violence and Recorded IDF–Settler Confrontations

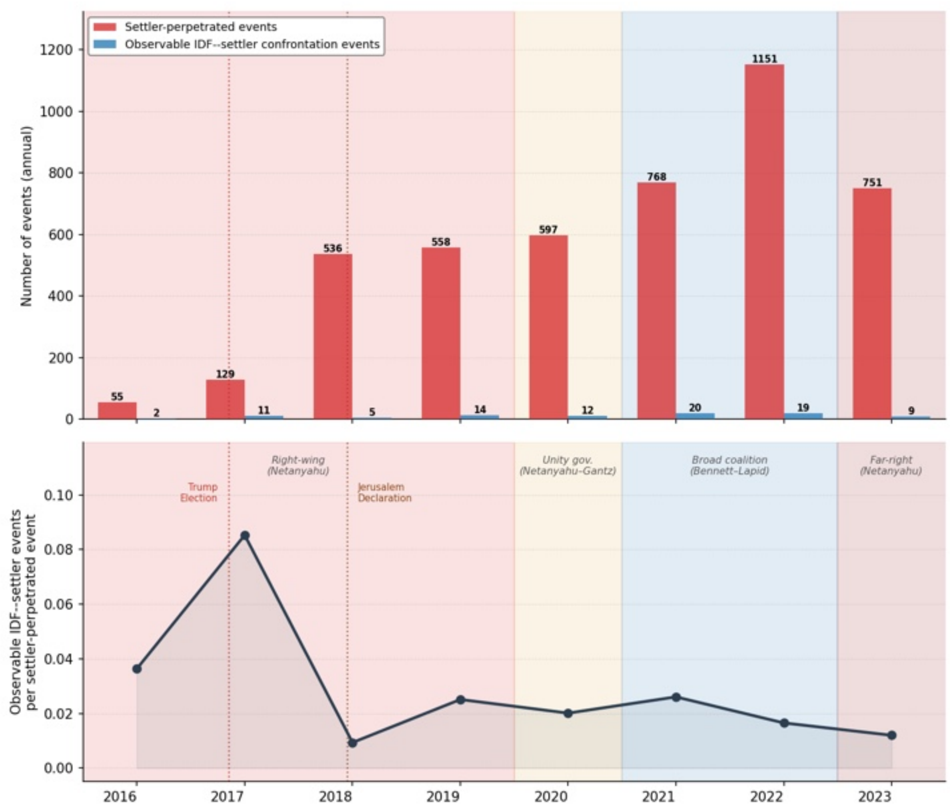

Notes: Top panel: Settler perpetrated events (red bar), confrontation between Israeli authorities and settlers (blue bar). Bottom panel: share of confrontation events over total settler-perpetrated events. The shaded areas track the difference governing coalitions from 2016 to 2023. The red-dashed line represents Trump's election.

B. Tables

Table B.1: Validation of the Outpost Suitability Index (PPML)

Panel A: PPML Model Fit		
Estimation observations	47,088	
Total new outposts	136	
Log-likelihood	-711.76	
AIC	1487.51	
Panel B: Predictive Performance (Post-Election Outposts)		
	PPML	Naive intensity
AUC-ROC (2017 outposts)	0.803	0.799
AUC-ROC (2018 outposts)	0.786	0.636
AUC-ROC (all post-election outposts)	0.793	0.692
Panel C: Institutional Geography by Suitability Quartile		
Area C share (lowest quartile)	53.1%	
Area C share (second quartile)	71.6%	
Area C share (third quartile)	79.3%	
Area C share (highest quartile)	89.4%	

Notes: The suitability index E_i is constructed from a PPML model of unauthorized outpost-expansion intensity estimated on pre-election data (1990 through October 2016). The dependent variable is the number of new outposts appearing in cell i during year t. Unlike a first-emergence hazard model, this specification does not remove cells from the risk set once an outpost appears, capturing the local intensity of the radical outpost frontier. After estimation, the outpost network is frozen at its pre-election configuration and E_i is defined as the fitted terminal pre-shock intensity. Panel A reports in-sample model fit statistics. Panel B evaluates out-of-sample predictive performance for outposts established after the election using the area under the ROC curve (AUC) and the share of new outposts located in the top decile of predicted suitability cells. The naive intensity benchmark is the raw count of pre-election outposts per cell, included to assess the value added by the model's geographic and frontier covariates over simple historical clustering. Panel C reports the average share of hex-cell area located in Oslo Area C across quartiles of the suitability index.

Table B.2: Pre-treatment Balance: Treated vs. Control Hex Cells

	Control Mean	Treated Mean	Difference (Trt − Ctrl)	SMD	p-value
Panel A: Hex-cell geography (pre-period mean)					
Elevation (mean, m)	208.249	554.645	346.396***	1.137	0.000
Slope (mean, deg)	9.913	11.603	1.690***	0.397	0.000
Terrain ruggedness	13.473	15.368	1.895***	0.323	0.000
Distance to road (km)	2.772	1.329	-1.443***	-0.712	0.000
Distance to village (km)	3.309	1.323	-1.986***	-0.622	0.000
Municipal area share	0.009	0.069	0.060***	0.822	0.000
Panel B: Pre-treatment violence (mean per cell)					
All Violent Events *(mean)*	0.0317	0.1006	0.0689***	0.266	0.000
Israeli settlers → Palestinian *(mean)*	0.0018	0.0106	0.0088***	0.308	0.000
Palestinian → Israeli settlers *(mean)*	0.0034	0.0108	0.0074**	0.161	0.013
Panel C: Pre-trend Wald tests					
All Violent Events			$\chi^2(11) = 16.789$		0.114
Israeli settlers → Palestinian			$\chi^2(11) = 8.146$		0.700
Palestinian → Israeli settlers			$\chi^2(11) = 10.802$		0.460
Hex cells (control / treated)	736	347			

Notes: Pre-treatment sample Panel A: pre-period cell means. Panel B: pre-treatment outcome averages. Panel C: Wald joint test that all pre-treatment event-study leads ($k < -1$) are zero, from a TWFE regression with hex-cell and time FE, SEs clustered by hex cell, no covariates. SMD = standardized mean difference. p-values in Panels A–B from Welch t-tests. $^{*}p < 0.10$, $^{**}p < 0.05$, $^{***}p < 0.01$.

Table B.3: TWFE: Treatment Effect on Settler–Palestinian Violence

	Israeli settlers → Palestinians			Palestinians → Israeli settlers		
	(1)	(2)	(3)	(4)	(5)	(6)
Panel A: Event counts						
$E_i \times$ Post	0.053018***	0.047910***	0.047910***	-0.000268	-0.000638	-0.000638
	(0.010377)	(0.010320)	(0.014625)	(0.002782)	(0.002934)	(0.003108)
Pre-treat. mean $\bar{Y}$	0.0047	0.0047	0.0047	0.0061	0.0061	0.0061
Panel B: Event counts $\log(Y+1)$						
$E_i \times$ Post	0.029640***	0.026674***	0.026674***	-0.000125	-0.000370	-0.000370
	(0.004965)	(0.004852)	(0.007284)	(0.001642)	(0.001715)	(0.001866)
Pre-treat. mean $\bar{Y}$	0.0032	0.0032	0.0032	0.0039	0.0039	0.0039
Panel C: Incidence (LPM)						
$E_i \times$ Post	0.033046***	0.029675***	0.029675***	0.000070	-0.000256	-0.000256
	(0.004868)	(0.004749)	(0.007255)	(0.001947)	(0.002002)	(0.002284)
Pre-treat. mean $\bar{Y}$	0.0043	0.0043	0.0043	0.0050	0.0050	0.0050
Hex FE	✓	✓	✓	✓	✓	✓
Period FE	✓	✓	✓	✓	✓	✓
Targeted controls		✓	✓		✓	✓
Std. errors	Clustered (hex)	Clustered (hex)	Conley (5 km)	Clustered (hex)	Clustered (hex)	Conley (5 km)
N	55,233	55,233	55,233	55,233	55,233	55,233

Notes: monthly hex-cell panel, Jan 2016–Mar 2020. Panel A: raw event counts per hex-month. Panel B: $\log(1+Y)$ transformation of the same counts. Panel C: linear probability model (LPM) incidence outcomes. Consistent with Chen and Roth (2024), Panel A and Panel C are more useful to understand ATEs in percentage terms. $E_i = 1$ if at least 50% of cell area intersects the 2 km buffer around the top-decile suitability cells. Post $= \mathbf{1}[t \geq$ Nov 2016]. Specifications (2) and (3) include Oslo-area × Post and seasonal-proximity interactions. All models include hex and period fixed effects. Spec. (3): Conley spatial SEs (5 km cutoff). $^{*}p < 0.1$, $^{**}p < 0.05$, $^{***}p < 0.01$.

Table B.4: TWFE: Treatment Effect on IDF–Palestinian Violence

	IDF → Palestinians			Palestinians → IDF		
	(1)	(2)	(3)	(4)	(5)	(6)
Panel A: Event counts						
$E_i \times$ Post	0.076339***	0.078179***	0.078179***	0.050692***	0.048646***	0.048646***
	(0.020313)	(0.021677)	(0.026069)	(0.015085)	(0.015061)	(0.017253)
Pre-treat. mean $\bar{Y}$	0.0362	0.0362	0.0362	0.0101	0.0101	0.0101
Panel B: Event counts $\log(Y+1)$						
$E_i \times$ Post	0.030039***	0.029982***	0.029982***	0.021807***	0.020519***	0.020519***
	(0.007446)	(0.007727)	(0.009932)	(0.006031)	(0.006170)	(0.007501)
Pre-treat. mean $\bar{Y}$	0.0210	0.0210	0.0210	0.0064	0.0064	0.0064
Panel C: Incidence (LPM)						
$E_i \times$ Post	0.022124***	0.021180***	0.021180***	0.017387***	0.015921***	0.015921**
	(0.006013)	(0.006083)	(0.007918)	(0.005075)	(0.005351)	(0.006554)
Pre-treat. mean $\bar{Y}$	0.0244	0.0244	0.0244	0.0084	0.0084	0.0084
Hex FE	✓	✓	✓	✓	✓	✓
Period FE	✓	✓	✓	✓	✓	✓
Targeted controls		✓	✓		✓	✓
Std. errors	Clustered (hex)	Clustered (hex)	Conley (5 km)	Clustered (hex)	Clustered (hex)	Conley (5 km)
N	55,233	55,233	55,233	55,233	55,233	55,233

Notes: monthly hex-cell panel, Jan 2016–Mar 2020. Panel A: raw event counts per hex-month. Panel B: $\log(1+Y)$ transformation of the same counts. Panel C: linear probability model (LPM) incidence outcomes. Consistent with Chen and Roth (2024), Panel A and Panel C are more useful to understand ATEs in percentage terms. $E_i = 1$ if at least 50% of cell area intersects the 2 km buffer around the top-decile suitability cells. Post $= \mathbf{1}[t \geq$ Nov 2016]. Specifications (2) and (3) include Oslo-area × Post and seasonal-proximity interactions. All models include hex and period fixed effects. Spec. (3): Conley spatial SEs (5 km cutoff). $^{*}p < 0.1$, $^{**}p < 0.05$, $^{***}p < 0.01$.

Table B.5: TWFE: Treatment Effect on Civilian Targeting

	(1)	(2)	(3)
Panel A: Event counts			
$E_i \times$ Post	0.036055***	0.033328***	0.033328***
	(0.009346)	(0.009820)	(0.011388)
Pre-treat. mean $\bar{Y}$	0.0128	0.0128	0.0128
Panel B: Event counts $\log(Y+1)$			
$E_i \times$ Post	0.019400***	0.017566***	0.017566***
	(0.004212)	(0.004258)	(0.005611)
Pre-treat. mean $\bar{Y}$	0.0084	0.0084	0.0084
Panel C: Incidence (LPM)			
$E_i \times$ Post	0.020947***	0.018627***	0.018627***
	(0.004270)	(0.004189)	(0.006057)
Pre-treat. mean $\bar{Y}$	0.0113	0.0113	0.0113
Hex FE	✓	✓	✓
Period FE	✓	✓	✓
Targeted controls		✓	✓
Std. errors	Clustered (hex)	Clustered (hex)	Conley (5 km)
N	55,233	55,233	55,233

Notes: monthly hex-cell panel, Jan 2016–Mar 2020. Panel A: raw event counts per hex-month. Panel B: $\log(1+Y)$ transformation of the same counts. Panel C: linear probability model (LPM) incidence outcomes. Consistent with Chen and Roth (2024), Panel A and Panel C are more useful to understand ATEs in percentage terms. $E_i = 1$ if at least 50% of cell area intersects the 2 km buffer around the top-decile suitability cells. Post $= \mathbf{1}[t \geq \text{Nov 2016}]$. Specifications (2) and (3) include Oslo-area $\times$ Post and seasonal-proximity interactions. All models include hex and period fixed effects. Spec. (3): Conley spatial SEs (5 km cutoff). $^{*}p < 0.1$, $^{**}p < 0.05$, $^{***}p < 0.01$.

Table B.6: Territorial opportunity and radical presence: settler violence after the shock

	(1)	(2)	(3)	(4)
	Settlers → Palestinian			Placebo
Suitability measure	Top-dec. $\hat{E}^{NO}$	Top-dec. $\hat{E}$ (full)	$\hat{E}^{NO}$ (rank)	Top-dec. $\hat{E}^{NO}$
Opportunity margin				
Suitability × Post	0.0356**	0.0258**	0.0435**	0.0003
	(0.0148)	(0.0115)	(0.0170)	(0.0040)
Pre-2016 radical presence (mutually exclusive bins)				
$\mathbf{1}[O_i{=}1]\times$ Post	0.0321*	0.0314	0.0323*	0.0073**
	(0.0190)	(0.0194)	(0.0191)	(0.0034)
$\mathbf{1}[O_i{\geq}2]\times$ Post	0.0734*	0.0780*	0.0808*	−0.0026
	(0.0429)	(0.0440)	(0.0446)	(0.0059)
Dist. to nearest outpost × Post	−0.0005	−0.0005	−0.0003	0.0002
	(0.0006)	(0.0006)	(0.0007)	(0.0002)
Joint Wald, presence block	p=0.001	p=0.006	p=0.051	p=0.074
Hex FE	✓	✓	✓	✓
Month-year FE	✓	✓	✓	✓
Targeted controls	✓	✓	✓	✓
Observations	55,233	55,233	55,233	55,233

Notes: Monthly hex-cell panel, 2016m1–2020m3. Conley (1999) standard errors (5 km Bartlett kernel) in parentheses. All columns include hex and month-year fixed effects and the baseline targeted controls (Oslo area shares × *Post*; Ramadan and olive-harvest × near-village; Jewish-holiday × near-settlement). Dependent variable: monthly settler-on-Palestinian event counts in columns (1)–(3) and Palestinian-on-settler counts in column (4). The opportunity regressor is a top-decile indicator of the no-outpost suitability index $\hat{E}^{NO}$ (cols. 1, 4), a top-decile indicator of the full suitability index $\hat{E}$ (col. 2), or the percentile rank of $\hat{E}^{NO}$ (col. 3), each interacted with *Post* (from 2016m11). O_i is the count of pre-November-2016 outposts within 2 km of the cell; presence enters as mutually exclusive bins $\mathbf{1}[O_i{=}1]$ and $\mathbf{1}[O_i{\geq}2]$ ($O_i{=}0$ omitted), so each bin coefficient is that cell type's post-period shift relative to zero-outpost cells. Because zero-outpost cells necessarily lie more than 2 km from the nearest outpost, bin coefficients are conditional presence gradients, not causal effects of outpost placement. $^{*}p < 0.1$, $^{**}p < 0.05$, $^{***}p < 0.01$.

Table B.7: Opportunity coefficient across presence parameterizations

Presence parameterization	Top-decile $\hat{E}^{NO} \times$ Post
Indicator only	0.0398***
	(0.0152)
Linear count	0.0325**
	(0.0142)
Log count	0.0342**
	(0.0144)
Indicator + linear	0.0324**
	(0.0142)
Bins (0 / 1 / 2+)	0.0356**
	(0.0148)
Observations	55,233

Notes: Each row re-estimates the static horse race (settler-on-Palestinian counts) varying only the functional form of the pre-2016 outpost count O_i in the presence block. Every specification includes the opportunity regressor (the top-decile no-outpost index $\hat{E}^{NO}$), distance to the nearest outpost × *Post*, hex and month-year fixed effects, and the baseline targeted controls. Only the coefficient on $\hat{E}^{NO}$ × *Post* is reported. Bins use dummies for O_i=1 and $O_i \geq 2$ (O_i=0 omitted). Conley (1999) standard errors (5 km Bartlett kernel). $^{*}p < 0.1$, $^{**}p < 0.05$, $^{***}p < 0.01$.

Table B.8: New-outpost formation and geographic opportunity, before vs after Trump

	Any new outpost		Number
	Reduced form	Conditional (main)	Conditional (count)
Opportunity rank × Post	0.0681**	0.0799***	0.0869**
	(0.0278)	(0.0287)	(0.0343)
Post period	2017–2023	2017–2023	2017–2023
Inherited network × Post		✓	✓
Cell FE, Year FE	✓	✓	✓
Observations	3,552	3,552	3,552

Notes: Coarse 5 km cell × year panel, 2012–2023, all cells retained after occupation; *Post* turns on in 2017. *Opportunity rank* is the percentile rank of the geography-only suitability index $\hat{E}^{NO}$ trained on outposts through 2011 (out-of-sample for 2012+). The inherited-network control is a single January-2017 snapshot — in-cell outpost stock (bins 0/1/2+), *external* outpost count within 5 km (log(1+·)), and distance to the nearest *external* outpost (bins) — interacted with *Post* (levels absorbed by cell FE). Conley (1999) 15 km (uniform kernel) SEs. $^{*}p < 0.1$, $^{**}p < 0.05$, $^{***}p < 0.01$.

Table B.9: Fatalities and Knesset Speeches — Non-Overlapping Events

	Focal/Same-Pair		Condemnation		Enforcement		Opp. Side Attention		Perp.-Side Def.	
	(1)	(2)	(3)	(4)	(5)	(6)	(7)	(8)	(9)	(10)
Panel A: Non-overlapping events (>15-day gap, 34 events)										
Right	0.100**		0.097***		0.023		−0.117**		−0.002	
	(0.047)		(0.034)		(0.020)		(0.052)		(0.003)	
Arab	−0.115***		−0.052***		−0.029**		0.357***		0.077	
	(0.035)		(0.019)		(0.013)		(0.095)		(0.051)	
Right × Settler perp.	−0.175***	−0.216***	−0.184***	−0.225***	−0.047	−0.059*	0.294**	0.276**	0.065*	0.095**
	(0.057)	(0.061)	(0.056)	(0.072)	(0.033)	(0.034)	(0.113)	(0.112)	(0.035)	(0.044)
Arab × Settler perp.	0.229**	0.240**	0.111**	0.127*	0.033	0.027	−0.739***	−0.731***	−0.130*	−0.129**
	(0.095)	(0.106)	(0.054)	(0.068)	(0.037)	(0.043)	(0.125)	(0.123)	(0.064)	(0.063)
Right gap, settler perp.	−0.074**	−0.078***	−0.087*	−0.087**	−0.024	−0.023	0.177*	0.207**	0.062*	0.068**
	(0.033)	(0.028)	(0.045)	(0.041)	(0.026)	(0.020)	(0.100)	(0.085)	(0.034)	(0.029)
Arab gap, settler perp.	0.114	0.110	0.059	0.059	0.004	0.005	−0.381***	−0.352***	−0.052	−0.047
	(0.088)	(0.087)	(0.051)	(0.049)	(0.035)	(0.031)	(0.081)	(0.069)	(0.040)	(0.041)
Observations	97	97	97	97	97	97	97	97	97	97
Events	34	34	34	34	34	34	34	34	34	34
R^2	0.704	0.732	0.597	0.666	0.409	0.540	0.764	0.815	0.539	0.583
Event FE	✓	✓	✓	✓	✓	✓	✓	✓	✓	✓
Knesset × Bloc		✓		✓		✓		✓		✓
Panel B: Non-overlapping events (>30-day gap, 30 events)										
Right	0.126**		0.105**		0.051**		−0.121*		−0.003	
	(0.054)		(0.045)		(0.025)		(0.068)		(0.005)	
Arab	−0.117***		−0.065***		−0.021*		0.328**		0.083	
	(0.040)		(0.023)		(0.012)		(0.122)		(0.063)	
Right × Settler perp.	−0.188***	−0.244***	−0.184***	−0.233**	−0.073*	−0.070*	0.313**	0.318**	0.069*	0.096*
	(0.063)	(0.080)	(0.064)	(0.095)	(0.036)	(0.037)	(0.123)	(0.126)	(0.035)	(0.049)
Arab × Settler perp.	0.242**	0.247**	0.115**	0.133*	0.032	0.031	−0.698***	−0.663***	−0.133*	−0.133*
	(0.099)	(0.114)	(0.056)	(0.072)	(0.038)	(0.042)	(0.147)	(0.165)	(0.075)	(0.067)
Right gap, settler perp.	−0.062*	−0.069**	−0.079*	−0.080*	−0.022	−0.021	0.192*	0.224**	0.065*	0.070**
	(0.033)	(0.030)	(0.045)	(0.043)	(0.026)	(0.023)	(0.103)	(0.091)	(0.035)	(0.029)
Arab gap, settler perp.	0.125	0.118	0.050	0.050	0.010	0.011	−0.370***	−0.337***	−0.050	−0.045
	(0.090)	(0.091)	(0.051)	(0.049)	(0.036)	(0.035)	(0.083)	(0.078)	(0.040)	(0.040)
Observations	85	85	85	85	85	85	85	85	85	85
Events	30	30	30	30	30	30	30	30	30	30
R^2	0.710	0.741	0.588	0.655	0.437	0.533	0.748	0.808	0.541	0.583
Event FE	✓	✓	✓	✓	✓	✓	✓	✓	✓	✓
Knesset × Bloc		✓		✓		✓		✓		✓

Notes: Same specification as Table 1, estimated on non-overlapping event samples. Events are sorted chronologically; an event is retained only if it occurs more than N days after the last retained event (Panel A: $N = 15$; Panel B: $N = 30$). Within each panel, odd columns report the baseline specification with event fixed effects; even columns add bloc-by-Knesset-term controls. The omitted category is Center-left. *Right* includes Right, Far Right, Religious Zionist, and Orthodox blocs; *Arab* includes Arab party lists. *Settler perp.* equals one when the perpetrator is a settler and zero when the perpetrator is Palestinian. Implied gaps report the total bloc differential at settler-perpetrator events; in even columns these are averaged over Knesset terms weighted by the share of settler-perpetrator events in each term. Standard errors (in parentheses) are clustered by fatality event; implied-gap standard errors use the delta method. $^{*}p < 0.10$, $^{**}p < 0.05$, $^{***}p < 0.01$.

C. Robustness Checks: Figures

Figure C.17: Opportunity Effect in Cells with No Pre-Shock Outpost Within 2 km

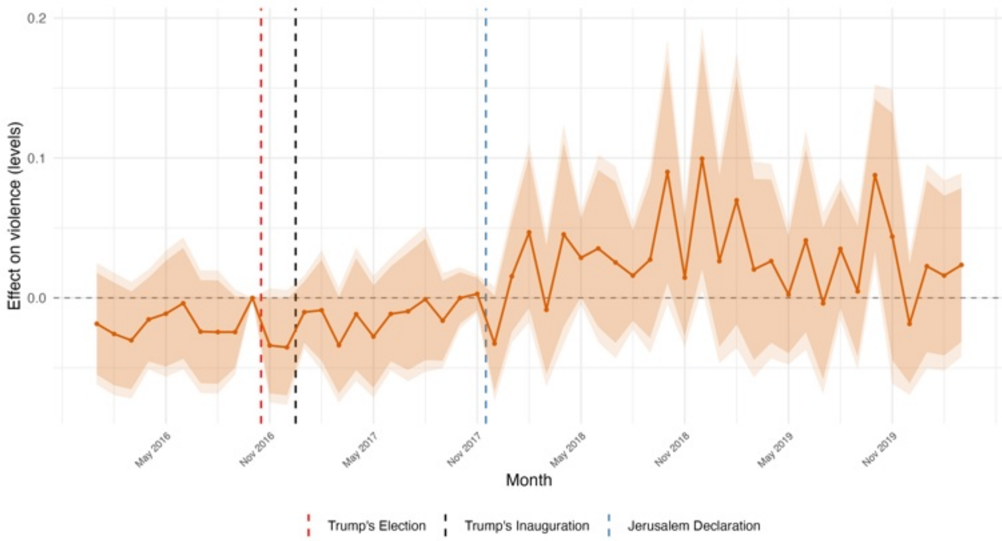

Notes: Event-study estimates of the no-outpost-network opportunity effect (T_i^{NO}) restricted to cells with no pre-November-2016 outpost within 2 km ($O_i = 0$), so identification comes from the band just beyond the existing outpost frontier. Outcome: settler violence against Palestinians. Dashed vertical lines mark Trump's election, inauguration, and the Jerusalem Declaration. Shaded bands show 90% and 95% confidence intervals based on Conley standard errors (5 km cutoff).

Figure C.18: Robustness: Reverse Causality

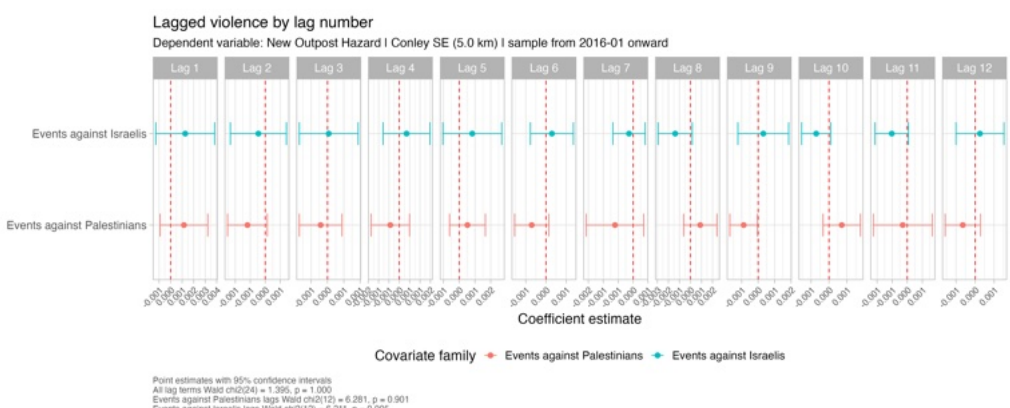

Notes: Coefficients from regressions of new outpost formation on lagged violence measures, estimated separately for treated and control cells. No lagged coefficient is statistically significant. Annotated on the bottom right of the figure the Wald tests for the joint significance of the coefficients.

Figure C.19: Robustness: Excluding Havat Gilad Area

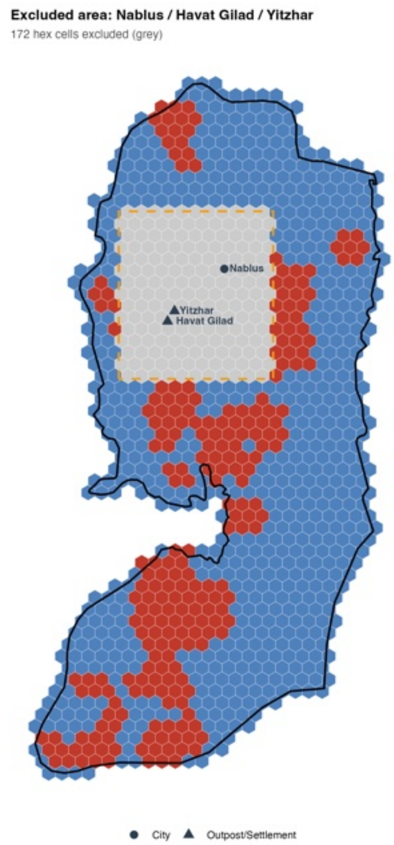

(a) Excluded area

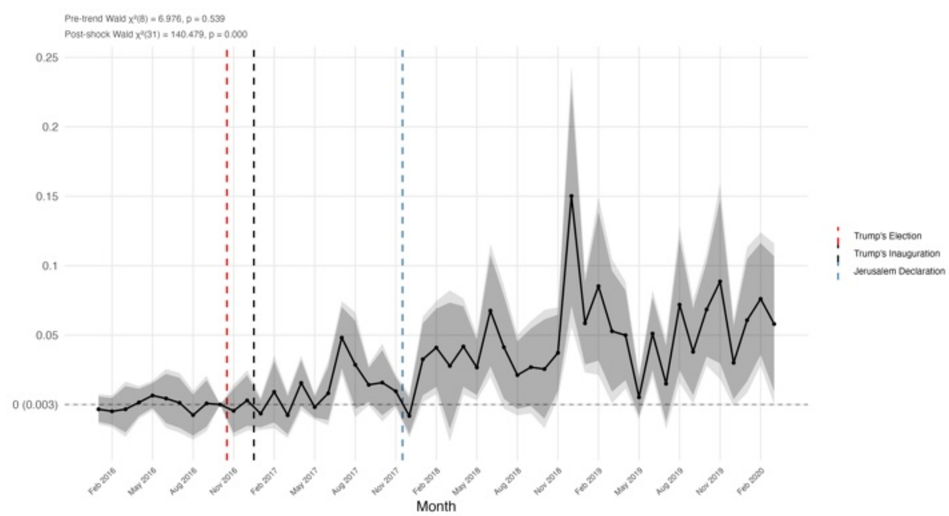

(b) Event study: settler violence → Palestinians

Notes: Panel (a) shows the hex cells excluded from the estimation sample (grey). The excluded area is defined by a bounding box centered on Nablus, Havat Gilad, and Yitzhar with a 0.1-degree padding. Panel (b) reports event-study estimates for Israeli settler violence against Palestinians on the restricted sample. Dashed vertical lines mark Trump's election, inauguration, and the Jerusalem Declaration. Shaded bands show 90% and 95% confidence intervals based on Conley standard errors (5 km cutoff).

Figure C.20: Robustness: Geographic Robustness, Civilian Violence Pair

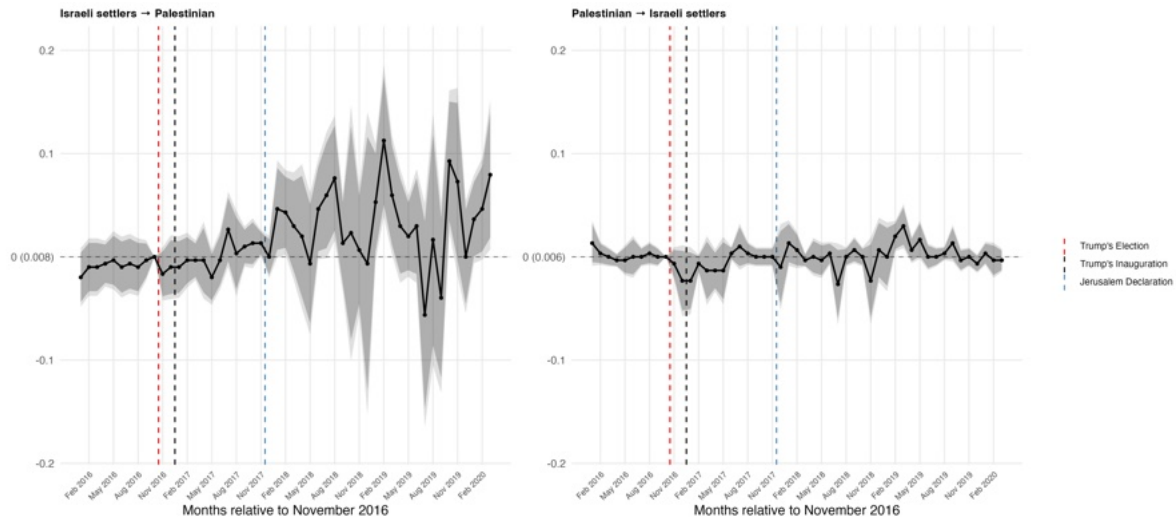

(a) Event counts

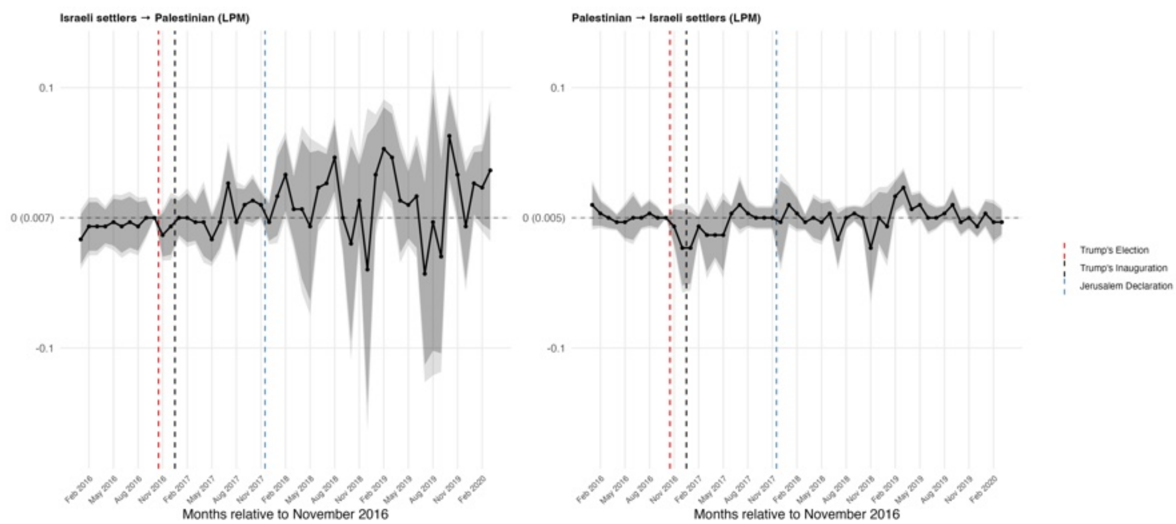

(b) Incidence (LPM)

Notes: Geographic robustness checks for civilian violence pair outcomes. Dashed vertical lines mark Trump's election, inauguration, and the Jerusalem Declaration. Shaded bands show 90% and 95% confidence intervals based on Conley standard errors (5 km cutoff).

Figure C.21: Robustness: Suitability Threshold, Civilian Violence Pair

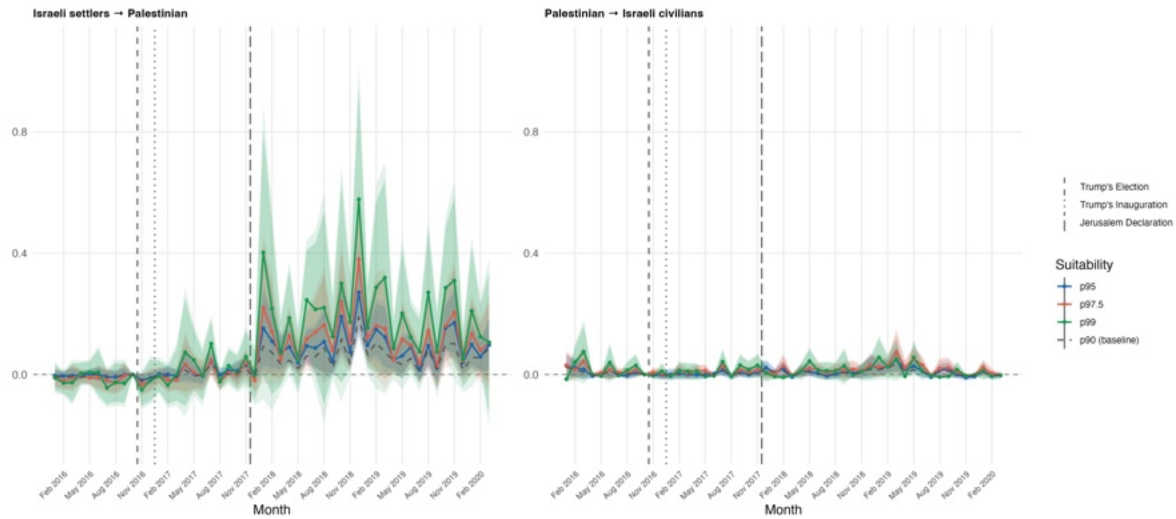

(a) Event counts

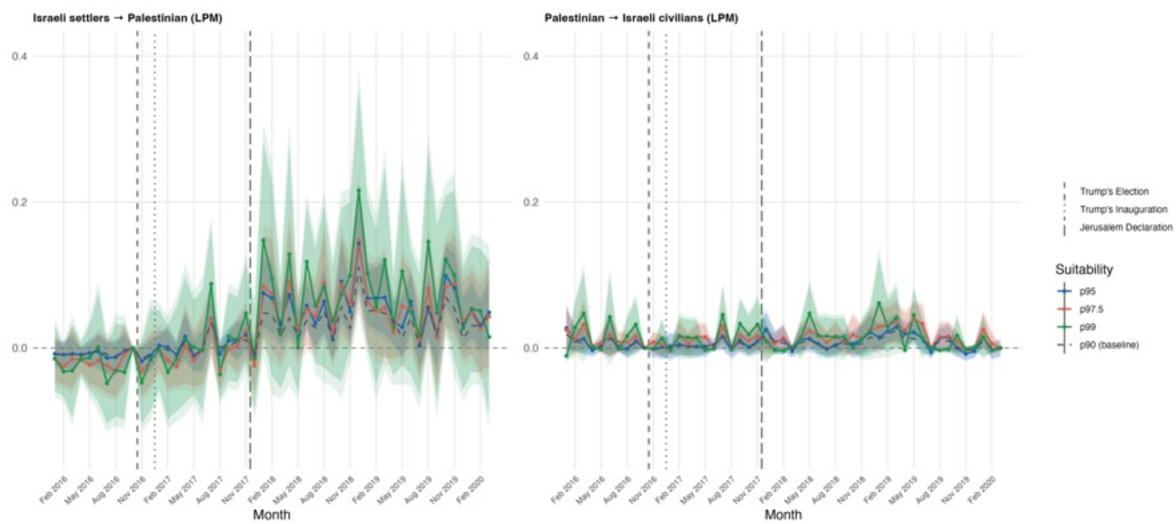

(b) Incidence (LPM)

Notes: Robustness checks with alternative suitability thresholds for civilian violence pair outcomes. The baseline threshold is depicted in red; all other thresholds are in blue.

Figure C.22: Robustness: Suitability Threshold, Settler–Palestinian Violence

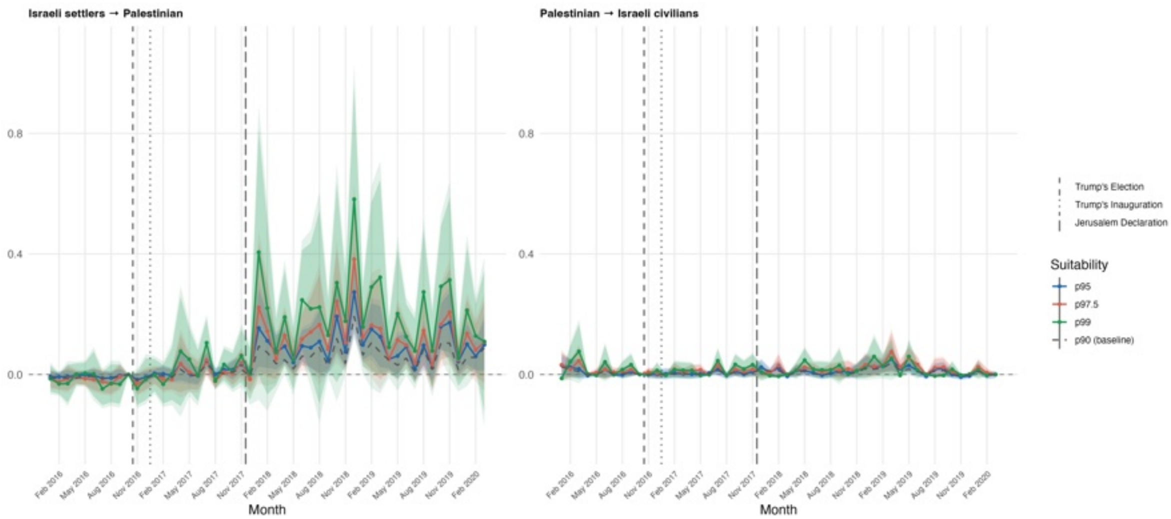

(a) Event counts

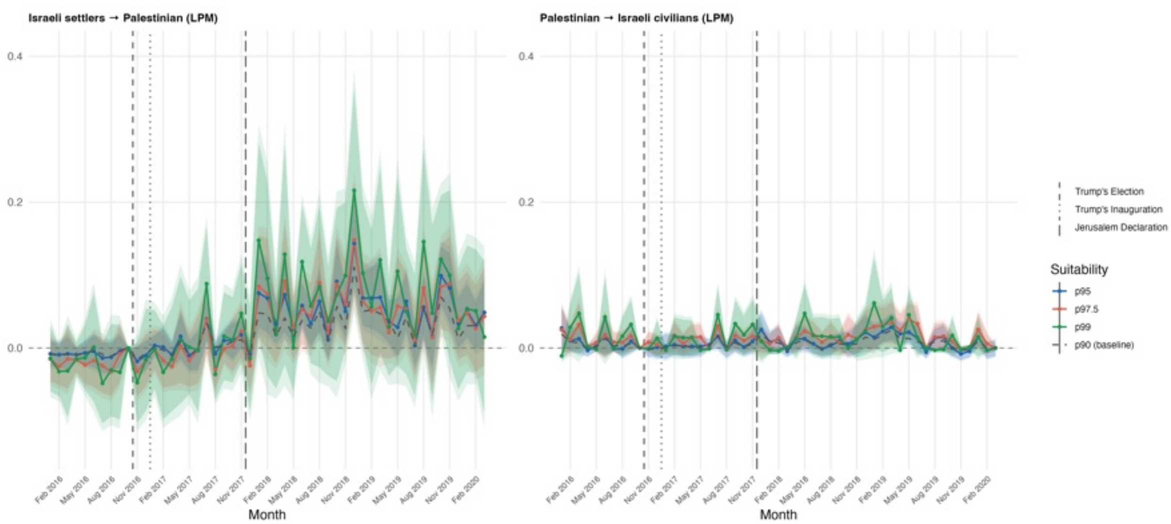

(b) Incidence (LPM)

Notes: Robustness checks with alternative suitability thresholds for settler–Palestinian violence outcomes. The baseline threshold is depicted in red; all other thresholds are in blue.

Figure C.23: Robustness: Buffer Size, Israeli Settler Violence on Palestinians

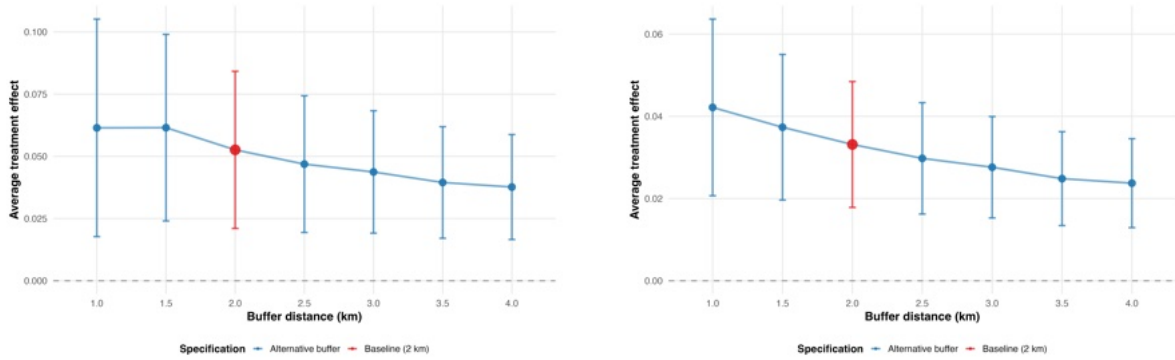

(a) Event counts

(b) Incidence (LPM)

Notes: Robustness checks with different buffer sizes ranging from 1 km to 4 km in steps of 0.5 km. The baseline (2 km) is depicted in red; all other buffer sizes are in blue.

Figure C.24: Robustness: Buffer Size, Palestinian Violence on Israeli Settlers

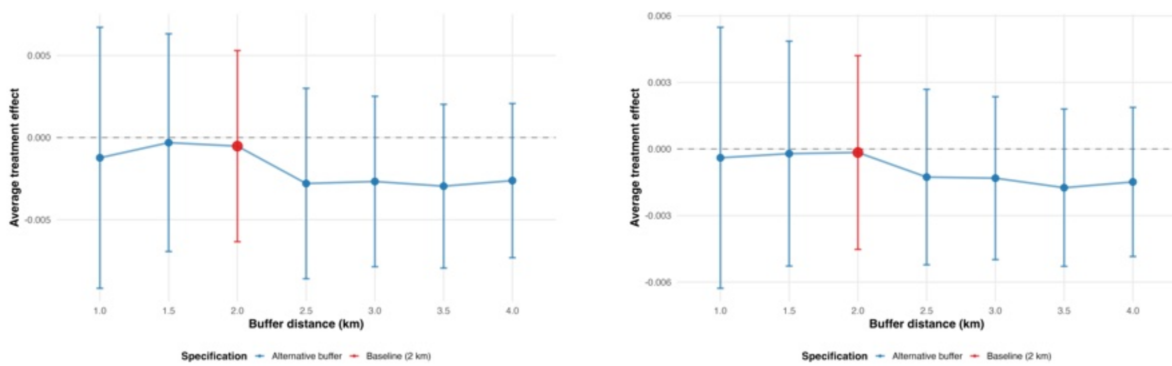

(a) Event counts

(b) Incidence (LPM)

Notes: Robustness checks with different buffer sizes ranging from 1 km to 4 km in steps of 0.5 km. The baseline (2 km) is depicted in red; all other buffer sizes are in blue.

Figure C.25: Robustness: Donut Design, Treatment Assignment Map

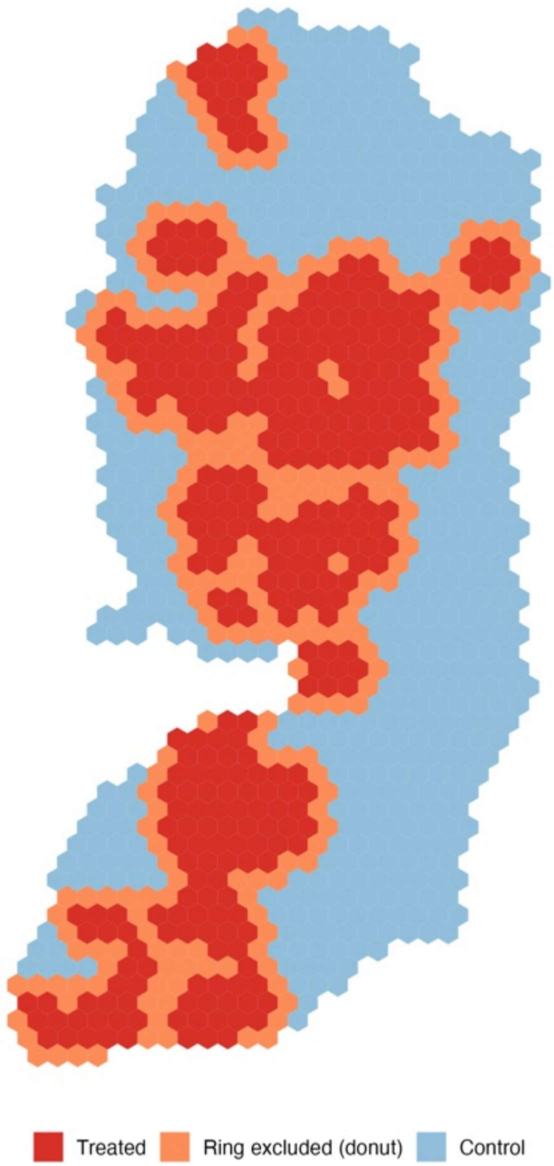

Notes: Map of treatment assignment under Donut design. Treated in red, control in blue and orange for the excluded ring.

Figure C.26: Robustness: Donut Design

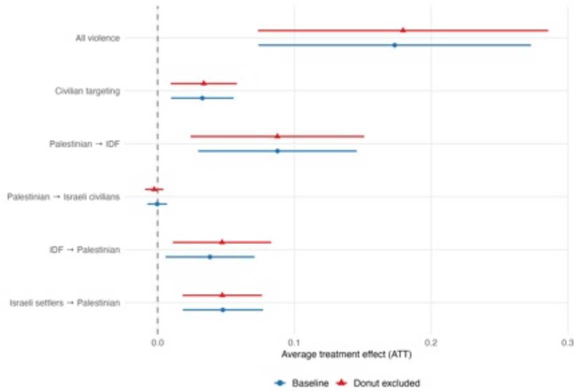

(a) Event counts

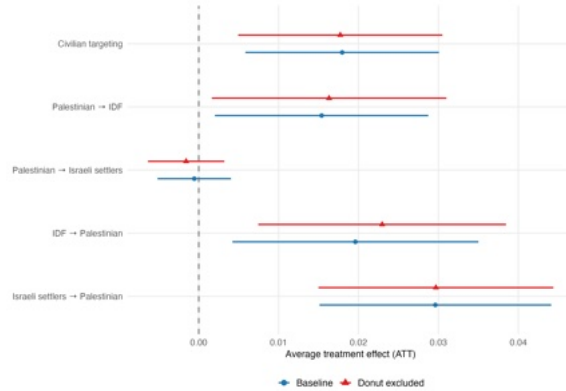

(b) Incidence (LPM)

Figure C.27: Robustness: Placebo Ring, Treatment Assignment Map

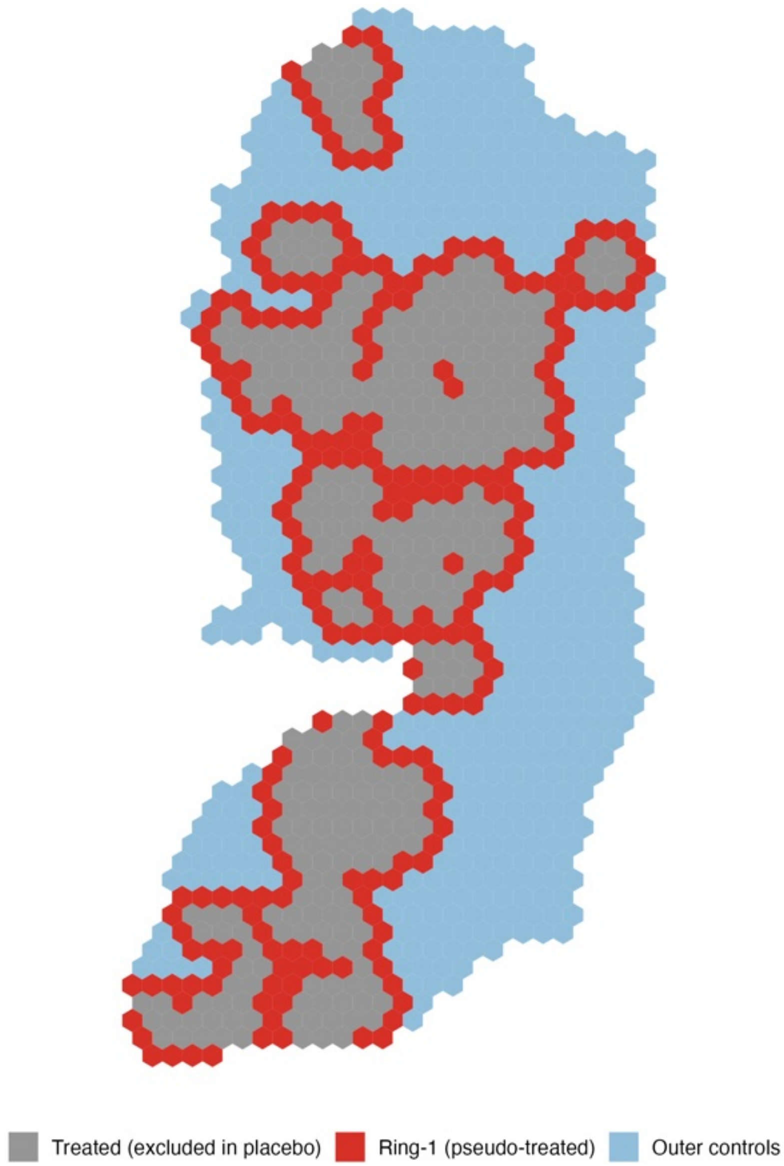

Notes: Map of treatment assignment under the placebo ring design. In red the pseudo treated units, in gray the excluded treated units and in blue the control units.

Figure C.28: Robustness: Placebo Ring

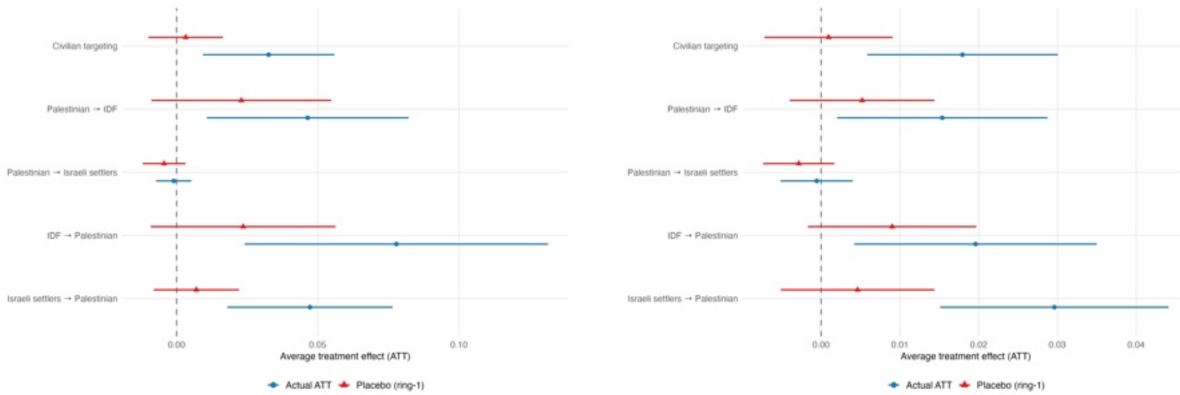

(a) Event counts (b) Incidence (LPM)

Notes: In red the placebo estimates and in blue the baseline estimates.

Figure C.29: Robustness: Leave-out-Regression, Israeli Settler Violence on Palestinians

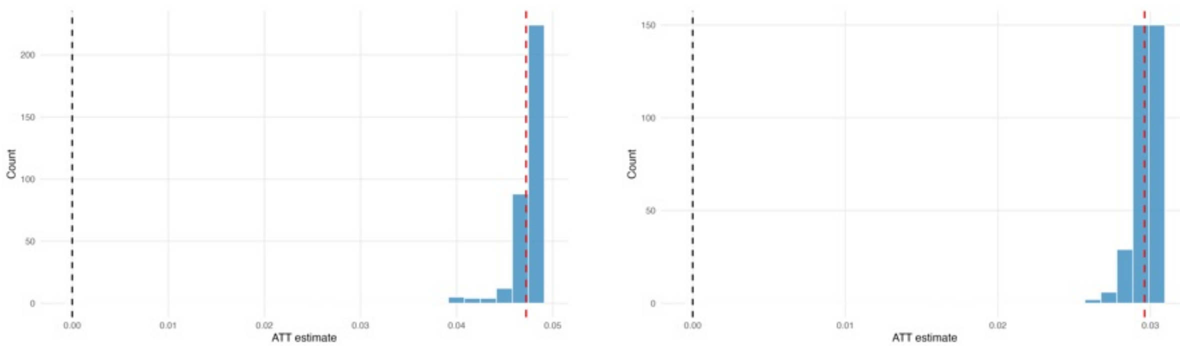

(a) Event counts (b) Incidence (LPM)

Notes: Robustness checks using leave-out regression. Distribution of estimated coefficients in blue, the vertical dashed red line indicates the baseline estimate and the black vertical line indicates the 0.

Figure C.30: Robustness: Leave-out-Regression, Palestinian Violence on Israeli Settlers

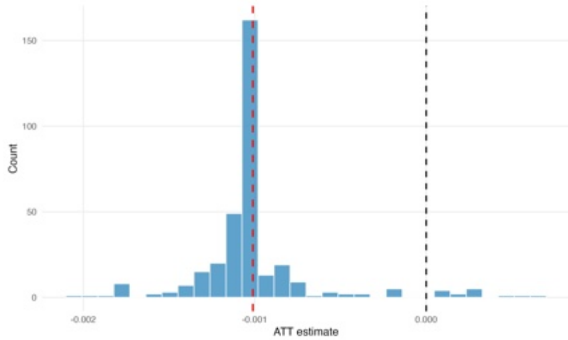

(a) Event counts

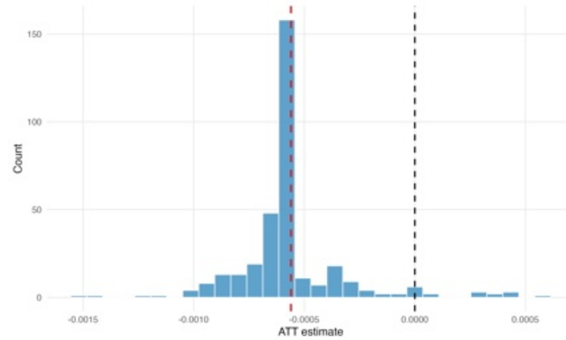

(b) Incidence (LPM)

Notes: Robustness checks using leave-out regression. Distribution of estimated coefficients in blue, the vertical dashed red line indicates the baseline estimate and the black vertical line indicates the 0.

D. Robustness Checks: Tables

Table D.10: Pre/Post-Matching Balance: Geographical matching ($K = 1$, with replacement)

	Pre-matching				Post-matching			
	Control Mean	Treated Mean	Diff	SMD	Control Mean	Treated Mean	Diff	SMD
Matching variables								
Elevation (mean, m)	228.741	554.645	325.904***	1.113	528.074	539.147	11.073	0.048
Slope (mean, deg)	9.913	11.603	1.690***	0.397	11.153	11.558	0.405	0.132
Terrain ruggedness	13.473	15.368	1.895***	0.323	14.817	15.308	0.491	0.116
Distance to road (km)	2.711	1.329	-1.381***	-0.684	1.333	1.369	0.036	0.033
Distance to village (km)	2.889	1.323	-1.565***	-0.622	1.314	1.323	0.009	0.012
Municipal area share	0.009	0.069	0.060***	0.810	0.038	0.036	-0.001	-0.018
Exact-matching variables								
Elevation bin: e1	0.327	0.043	-0.284***	-0.705	0.050	0.050	0.000	0.000
Elevation bin: e2	0.290	0.184	-0.106***	-0.244	0.212	0.212	0.000	0.000
Elevation bin: e3	0.248	0.268	0.020	0.045	0.262	0.262	0.000	0.000
Elevation bin: e4	0.135	0.504	0.370***	0.923	0.477	0.477	0.000	0.000
Municipal area: zero	0.870	0.375	-0.495***	-1.264	0.430	0.430	-0.000	-0.000
Municipal area: medium	0.049	0.193	0.144***	0.501	0.222	0.222	0.000	0.000
Municipal area: low	0.067	0.274	0.206***	0.630	0.315	0.315	0.000	0.000
Municipal area: high	0.014	0.159	0.144***	0.627	0.033	0.033	0.000	0.000
Hex cells	713	347			135†	302		

Notes: Nearest-neighbour Mahalanobis matching (Geographical matching), $K = 1$, with replacement. Post-matching means computed using match weights (consistent with TWFE). †Unique matched control cells. $^{*}p < 0.10$, $^{**}p < 0.05$, $^{***}p < 0.01$ (Welch t-test).

Table D.11: Match-Weighted TWFE: Settler–Palestinian Violence

	Israeli settlers → Palestinians			Palestinians → Israeli settlers		
	(1)	(2)	(3)	(4)	(5)	(6)
Panel A: Event counts						
$E_i \times$ Post	0.029914***	0.027836**	0.027836**	-0.002213	-0.002362	-0.002362
	(0.011532)	(0.011687)	(0.012257)	(0.002464)	(0.002471)	(0.002738)
Pre-treat. mean $\bar{Y}$	0.0076	0.0076	0.0076	0.0055	0.0055	0.0055
Panel B: Event counts $\log(Y+1)$						
$E_i \times$ Post	0.015442***	0.014286**	0.014286**	-0.001634	-0.001749	-0.001749
	(0.005796)	(0.005818)	(0.006325)	(0.001625)	(0.001628)	(0.001821)
Pre-treat. mean $\bar{Y}$	0.0051	0.0051	0.0051	0.0038	0.0038	0.0038
Panel C: Incidence (LPM)						
$E_i \times$ Post	0.014998**	0.013881**	0.013881**	-0.002528	-0.002723	-0.002723
	(0.006307)	(0.006340)	(0.007008)	(0.002209)	(0.002212)	(0.002506)
Pre-treat. mean $\bar{Y}$	0.0069	0.0069	0.0069	0.0053	0.0053	0.0053
Hex FE	✓	✓	✓	✓	✓	✓
Period FE	✓	✓	✓	✓	✓	✓
Targeted controls		✓	✓		✓	✓
Match weights	✓	✓	✓	✓	✓	✓
Std. errors	Clustered (hex)	Clustered (hex)	Conley (5 km)	Clustered (hex)	Clustered (hex)	Conley (5 km)
N	22,287	22,287	22,287	22,287	22,287	22,287

Notes: monthly hex-cell panel, Jan 2016–Mar 2020. Nearest-neighbour Mahalanobis matching (K=1, with replacement). Panel A: raw event counts. Panel B: $\log(1+Y)$. Panel C: linear probability model (LPM). All models use match weights. Post $= \mathbf{1}[t \geq \text{Nov } 2016]$. Specifications (2) and (3) include Oslo-area $\times$ Post and seasonal-proximity interactions. All models include hex and period fixed effects. Spec. (3): Conley spatial SEs (5 km cutoff). $^{*}p < 0.1$, $^{**}p < 0.05$, $^{***}p < 0.01$.

E. Additional Materials

Figure E.31: Outposts, Settlements and Palestinian Communities in the West Bank

(a) Ahiya Outpost, 1997

(b) Nahal Tirza Farm Outpost, 2020

(c) Outposts (red), Settlement (blue) and Palestinian Towns (white)

Notes: Satellite images of different outposts in the West Bank. Resolution: 0.5m. Source: Maxar Technologies (2023).

Figure E.32: West Bank Voting in National Elections

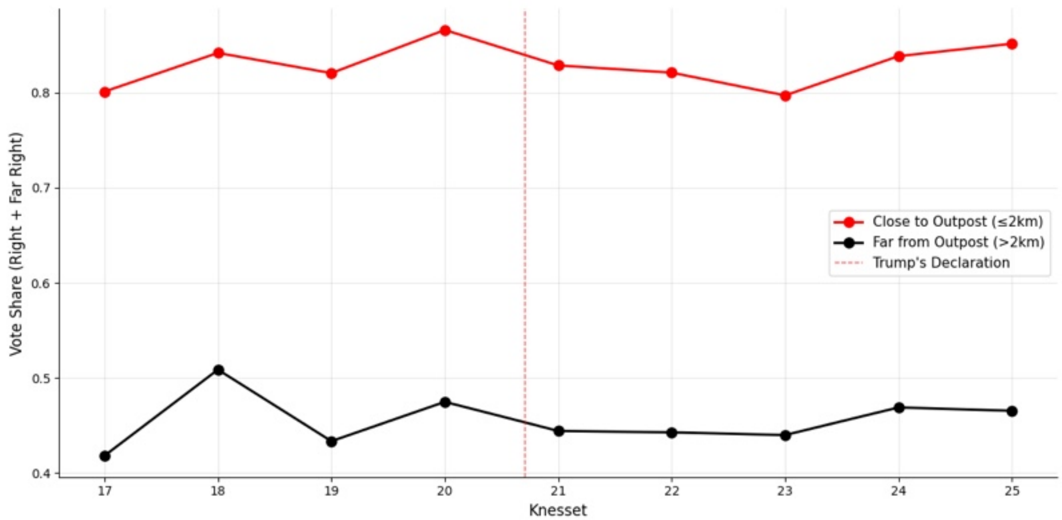

Notes: The figure plots the average vote share of right-wing and far-right parties across Knesset elections for polling stations located within 2 km of an outpost and for polling stations located farther away. Data are obtained from Knesset Election Results Data (2025).

Figure E.33: Outpost Timing Example – Bentayim Farm Outpost

(a) 2016-02-26

(b) 2016-05-16

(c) 2016-06-25

(d) 2017-02-10

(e) High Resolution Image

Notes: Panels E.33a–E.33d show the evolution of the Bentayim Farm outpost from February 2016 to February 2017. Panel E.33e shows the same outpost in 2023. Sources: Copernicus Sentinel-2 Level 2A and Maxar Technologies.

Figure E.34: Settlement Expansion Indicators

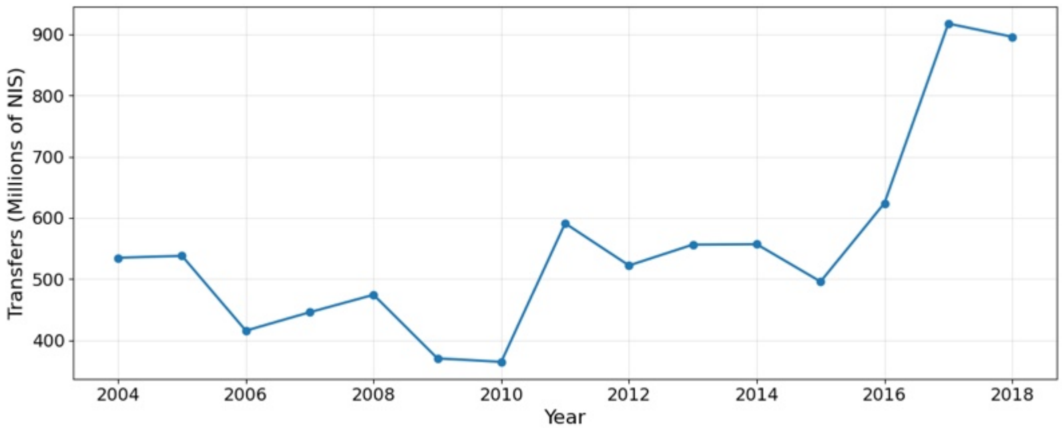

(a) Fiscal Transfers to Settlements

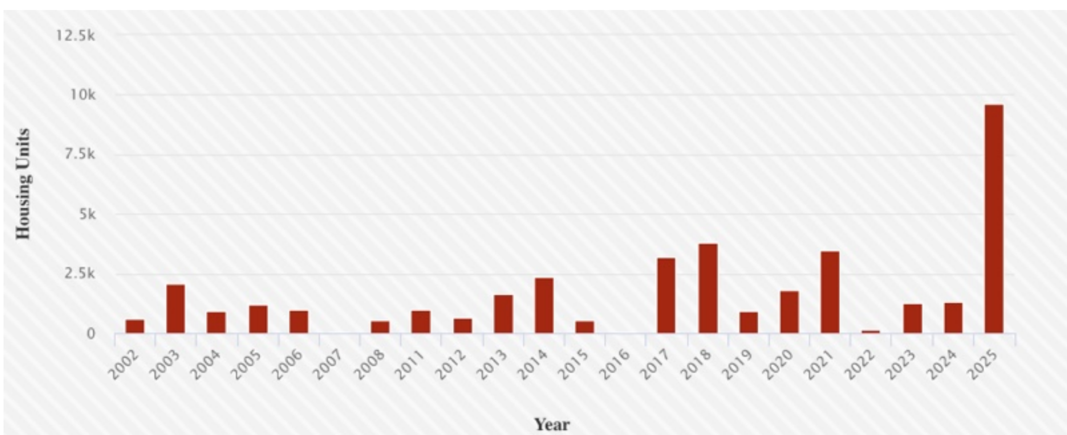

(b) Tenders for Settlement Construction

Notes: Panel (a) reports fiscal transfers to settlements from 2013 to 2018. Since the last data point is from the second quarter of 2018, for each year only the first two quarters are shown. Data are obtained from Israeli Settlement Division reports disclosed through the Movement for Freedom of Information. Panel (b) reports tenders for settlement construction from 2013 to 2025. Data are obtained from Peace Now (2024).

Figure E.35: Descriptive Monthly Trends: Total Violence and Civilian Targeting

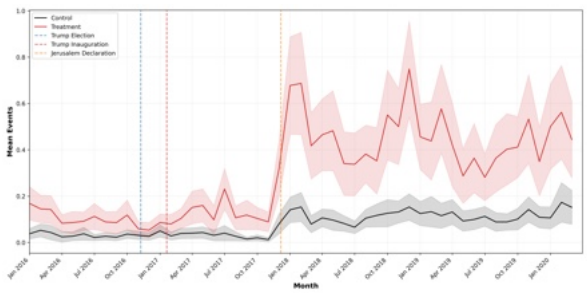

(a) Total violence

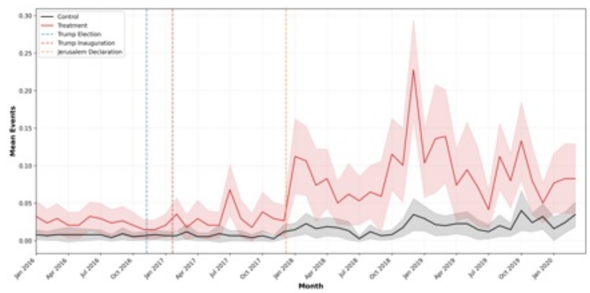

(b) Civilian targeting

Notes: Raw monthly mean violence in treated and control cells. Panel (a) reports total violent events; Panel (b) reports violent events targeting civilians. The treatment group includes cells classified as highly exposed to radical settler activity based on the suitability design; the control group includes all remaining cells. Shaded areas represent 95% confidence intervals around the monthly means. Vertical lines indicate Trump's election, inauguration, and the Jerusalem Declaration. These figures are purely descriptive and are intended to complement the event-study estimates by illustrating the underlying level dynamics. Because treated and control cells differ in baseline levels, these plots should not be interpreted as identification evidence.

Figure E.36: Descriptive Monthly Trends: Israeli Violence against Palestinians

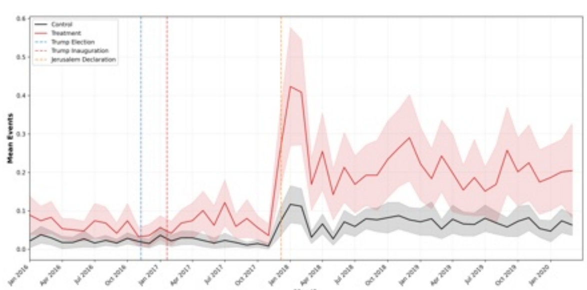

(a) IDF → Palestinian

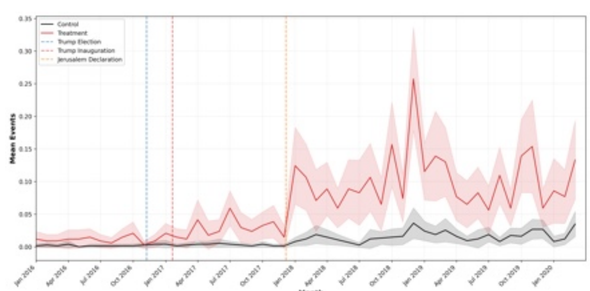

(b) Israeli settlers → Palestinian

Notes: Raw monthly mean violence in treated and control cells. Panel (a) reports IDF violence against Palestinians; Panel (b) reports Israeli settler violence against Palestinians. Shaded areas represent 95% confidence intervals around the monthly means. Vertical lines indicate Trump's election, inauguration, and the Jerusalem Declaration. These figures are descriptive only and are included to show the underlying series corresponding to the event-study estimates. As treated and control cells differ in baseline violence levels, interpretation should focus on the broad evolution of the series rather than on raw level differences.

Figure E.37: Descriptive Monthly Trends: Palestinian Violence

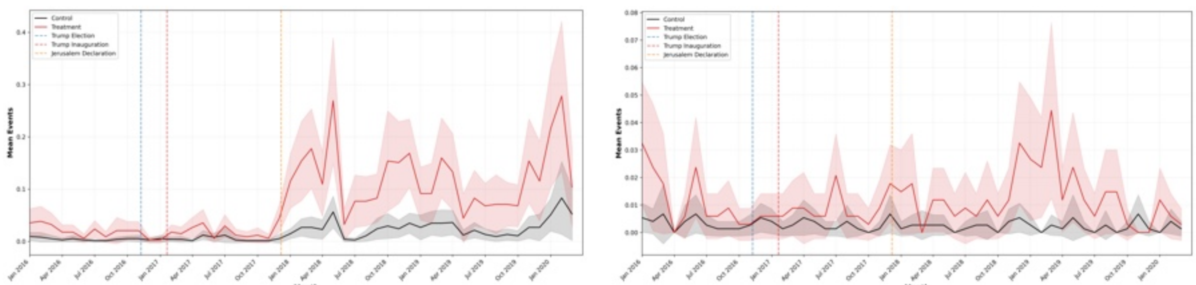

(a) Palestinian → IDF

(b) Palestinian → Israeli civilians

Notes: Raw monthly mean violence in treated and control cells. Panel (a) reports Palestinian violence against the IDF; Panel (b) reports Palestinian violence against Israeli civilians. Shaded areas represent 95% confidence intervals around the monthly means. Vertical lines indicate Trump's election, inauguration, and the Jerusalem Declaration. These plots are descriptive complements to the event-study results and are not meant to identify causal effects. Their purpose is to illustrate the raw monthly evolution of violence across treated and control areas.

F. Theoretical Model

F.1. Overview

This appendix presents a simple reduced-form model of how weaker political and institutional constraints on forbearance can activate violence by radical non-state actors without requiring a change in their underlying preferences. The mechanism is one of state forbearance. Radical actors may already have a preference for force, but violence becomes more attractive when enforcement is expected to weaken. A government, in turn, may tolerate violence by aligned actors when it partially internalizes the political or territorial gains generated by their actions and when the costs of tolerating them are sufficiently low.

The model is intentionally reduced form. It does not attempt to microfound the government's ideology, coalition incentives, or full enforcement capacity. Instead, it isolates one margin: when a government may find it politically useful to relax enforcement and tolerate aggression by politically aligned non-state actors. This abstraction is useful for the empirical setting, where the object of interest is not overt state violence, but the selective tolerance of violence by radical settlers and the resulting escalation of local conflict.

F.2. Model Setup

Consider a setting with N locations, indexed by i. In each location, a radical local actor R_i chooses a level of violence

$$v_i \geq 0.$$

A government or political elite chooses how much to forbear from enforcing against radical actors in each location. Forbearance toward actor R_i is denoted by

$$f_i \in [0, 1],$$

where $f_i = 0$ corresponds to full enforcement and $f_i = 1$ corresponds to full tolerance.

The political and institutional constraints on forbearance are summarized by S. A higher value of S corresponds to weaker constraints, that is, a more permissive environment. This permissiveness may reflect lower diplomatic pressure, weaker expected legal constraints, greater political cover for non-enforcement, or a broader political climate in which radical action is less costly to tolerate.

Each location has a level of local opportunity, denoted by $E_i \geq 0$. This captures the extent to which violence can produce territorial or strategic gains in location i. In the empirical application, E_i corresponds to the pre-determined suitability of a location for radical settler encroachment.

The strategic or territorial return to force is denoted by

$$\pi(E_i),$$

with

$$\pi(E_i) \geq 0, \qquad \pi_E(E_i) > 0.$$

Thus, violence is more productive in high-opportunity locations. Forbearance determines how much of this local opportunity the radical actor can exploit. This is captured by the term

$$f_i \pi(E_i).$$

The advantage of this specification is that the two roles are distinct: E_i determines the productivity of violence, while f_i determines the expected room to act.

Radical actor R_i also receives an intrinsic payoff from violence, denoted by r_i. This captures pre-existing radical motivation and is fixed with respect to S. If the government fully enforces, the actor faces punishment, obstruction, or evacuation cost $L > 0$. With forbearance f_i, the expected enforcement cost becomes

$$(1 - f_i)L.$$

The private cost of violence is denoted by $K_i(v_i)$. I assume that $K_i(0) = 0$, $K_i'(v_i) \geq 0$, $K_i''(v_i) > 0$, and $\lim_{v_i \to \infty} K_i'(v_i) = \infty$.[57] The government partially internalizes the benefits generated by radical action. This is summarized by a reduced-form parameter

$$\lambda \in [0, 1].$$

This parameter captures the extent to which the government values gains produced through violence by aligned non-state actors. It may reflect ideological affinity, coalition incentives, territorial objectives, bureaucratic sympathy, or the political usefulness of

[57] The last condition guarantees a finite interior solution when the marginal benefit of violence is high.

indirect force. When λ is high, the government attaches greater value to the gains generated by radical action. When λ is low, radical action provides little or no political benefit to the government.

I treat λ as fixed with respect to S. Thus, changes in permissiveness need not change the government's preferences or ideological alignment. Instead, S affects the government's problem by changing the cost of tolerating radical action.[58]

The government incurs a cost of forbearance and induced violence denoted by

$$C_i(f_i, v_i; S).$$

This object collects the legal, diplomatic, institutional, domestic, and public-order costs borne by the government when it tolerates radical violence. The two relevant marginal costs are the direct cost of forbearance and the indirect cost generated by the violence that forbearance induces. I assume

$$C_i^f(f_i, v_i; S) \geq 0, \qquad C_i^f(f_i, v_i; S) > 0 \text{ for } f_i > 0, \qquad C_i^v(f_i, v_i; S) \geq 0.$$

Weaker political constraints lower the marginal cost of forbearance:

$$C_i^{fS}(f_i, v_i; S) \leq 0,$$

with strict inequality for $f_i > 0$ in the relevant interior region. It also lowers the marginal backlash cost of visible violence:

$$C_i^{vS}(f_i, v_i; S) \leq 0.$$

The cost functions are continuous and sufficiently smooth for the derivatives used below.

The timing is sequential. First, S is realized. Second, the government chooses forbearance f_i. Third, the radical actor observes f_i and chooses violence v_i. The equilibrium is characterized by backward induction. Forbearance represents an observable enforcement stance that remains operative while the radical actor acts.

[58] Allowing λ to increase with S would reinforce the same comparative static. I keep λ fixed to isolate the cost-of-forbearance channel.

F.3. Radical Actor's Problem

Given f_i, radical actor R_i chooses $v_i \geq 0$ to maximize

$$U_i^R(v_i; f_i) = [r_i + f_i \pi(E_i) - (1 - f_i)L]\, v_i - K_i(v_i). \tag{F.1}$$

Define the net marginal payoff from violence as

$$M_i(f_i) = r_i - L + f_i\, [\pi(E_i) + L]\,. \tag{F.2}$$

The radical actor's problem can then be written as

$$\max_{v_i \geq 0} \{M_i(f_i) v_i - K_i(v_i)\}\,.$$

If $M_i(f_i) \leq K_i'(0)$, the actor chooses no violence:

$$v_i^*(f_i) = 0.$$

If $M_i(f_i) > K_i'(0)$, the solution is interior and satisfies

$$K_i'(v_i^*) = M_i(f_i).$$

Equivalently,

$$v_i^*(f_i) = \begin{cases} 0, & \text{if } M_i(f_i) \leq K_i'(0), \\ (K_i')^{-1}\,(M_i(f_i))\,, & \text{if } M_i(f_i) > K_i'(0). \end{cases} \tag{F.3}$$

The best response is continuous and nondecreasing in f_i on the whole unit interval, because $M_i(f_i)$ is increasing in f_i and $(K_i')^{-1}$ is increasing. In particular, on the active branch, where $v_i^*(f_i) > 0$,

$$v_i^*(f_i) = (K_i')^{-1}\,(M_i(f_i))\,.$$

Since $M_i(f_i) = r_i - L + f_i[\pi(E_i) + L]$, an interior activation threshold, when it exists, is given by

$$\bar{f}_i = \frac{K_i'(0) + L - r_i}{\pi(E_i) + L}. \tag{F.4}$$

When this threshold lies in $(0, 1)$, violence is zero below $\bar{f}_i$ and positive above it.

Forbearance raises the radical actor's net marginal payoff by

$$\frac{\partial M_i(f_i)}{\partial f_i} = \pi(E_i) + L > 0.$$

This marginal payoff effect is stronger in high-opportunity locations because

$$\frac{\partial}{\partial E_i}[\pi(E_i) + L] = \pi_E(E_i) > 0.$$

On the active branch, this translates into

$$\frac{\partial v_i^*}{\partial f_i} = \frac{\pi(E_i) + L}{K_i''(v_i^*)} > 0. \tag{F.5}$$

With quadratic private costs and other primitives held fixed, the violence response to forbearance increases with local opportunity.

F.4. Government's Problem

The government anticipates the radical actor's best response. The total political or territorial output generated by radical violence in location i is

$$f_i \pi(E_i) v_i^*(f_i).$$

The term $f_i \pi(E_i) v_i^*(f_i)$ should be interpreted as realized violent output. Forbearance determines the extent to which violence is allowed to generate durable political or territorial gains. When $f_i = 0$, enforcement prevents violence from being converted into such gains; when $f_i = 1$, radical action can fully exploit local opportunity. The government internalizes a fraction λ of this output and bears the cost $C_i(f_i, v_i; S)$. Its local problem is therefore

$$f_i^* \in \arg\max_{f_i \in [0,1]} \left\{ \lambda f_i \pi(E_i) v_i^*(f_i) - C_i\left(f_i, v_i^*(f_i); S\right) \right\}. \tag{F.6}$$

An optimum exists because the payoff is continuous and the choice set is compact. If several choices maximize the government's payoff, I select the largest.

At an interior optimum on the active branch, the first-order condition is

$$\begin{aligned} \lambda \pi(E_i) \left[v_i^*(f_i) + f_i \frac{\partial v_i^*(f_i)}{\partial f_i} \right] &= C_i^f\left(f_i, v_i^*(f_i); S\right) \\ &\quad + C_i^v\left(f_i, v_i^*(f_i); S\right) \frac{\partial v_i^*(f_i)}{\partial f_i}. \end{aligned} \tag{F.7}$$

At an interior optimum, this condition has a simple interpretation. The government increases forbearance until the internalized marginal benefit of radical action equals the marginal cost of tolerating it. The left-hand side captures the benefit from allowing existing radical action to exploit local opportunity and from inducing additional radical action. The right-hand side captures the direct cost of non-enforcement and the indirect backlash cost generated by visible violence. The two cost terms are not separate assumptions; they are two margins of the same cost function. Corner solutions and discontinuous switches between the dormant and active branches need not satisfy the condition.

The model does not imply that the government abandons the state's monopoly of violence. Rather, it isolates the margin on which a government may find it politically useful to relax enforcement and tolerate violence by radical non-state actors.[59] The relevant question is not whether the state can act directly, but when indirect force becomes politically useful.

F.5. Comparative Statics

Throughout this section, let

$$W_i(f_i; S) = \lambda f_i \pi(E_i) v_i^*(f_i) - C_i\big(f_i, v_i^*(f_i); S\big)$$

denote the government's reduced objective after substituting the radical actor's best response, and let $f_i^*(S)$ denote its largest maximizer on $[0, 1]$. Derivative results characterize regular interior equilibria on the active branch. Corner solutions allow zero responses below the activation threshold or saturation at $f_i = 1$.

Monotonicity. Greater permissiveness makes higher forbearance relatively more attractive to the government: it reduces the additional cost of tolerating more radical action. The government's optimal forbearance is therefore nondecreasing in permissiveness, including at corners and across jumps.[60] Since the radical actor's best response is nondecreasing in forbearance, equilibrium violence is also nondecreasing. This result establishes the monotonicity of aggregate output used in the dynamic extension.

[59] The framework could be extended to distinguish between aligned and non-aligned radical actors, and to allow the state to choose direct force against the latter. This richer setting is beyond the scope of the paper.

[60] The reduced payoff has increasing differences in (f_i, S); its largest maximizer is nondecreasing in S (Milgrom and Shannon, 1994).

The local derivative calculation sharpens this to a strict increase at a regular active interior optimum. Write the first-order condition (F.7) as $H_i(f_i, S) = 0$, where

$$\begin{aligned} H_i(f_i, S) = \lambda\pi(E_i)\left[v_i^*(f_i) + f_i\frac{\partial v_i^*(f_i)}{\partial f_i}\right] \\ - C_i^f\big(f_i, v_i^*(f_i); S\big) - C_i^v\big(f_i, v_i^*(f_i); S\big)\frac{\partial v_i^*(f_i)}{\partial f_i} \\ = W_i^f(f_i; S). \end{aligned}$$

Because λ, E_i, and the radical actor's best response are fixed with respect to S,

$$H_i^S = -C_i^{fS} - C_i^{vS}\frac{\partial v_i^*}{\partial f_i} \geq 0,$$

since $C_i^{fS} \leq 0$, $C_i^{vS} \leq 0$, and $\partial v_i^*/\partial f_i > 0$ on the active branch. The inequality is strict whenever greater permissiveness strictly lowers at least one marginal cost, that is, whenever $C_i^{fS} < 0$ or $C_i^{vS} < 0$. At a regular interior optimum, the second-order condition gives $H_i^f = W_i^{ff} < 0$, and the implicit function theorem yields

$$\frac{\partial f_i^*}{\partial S} = -\frac{H_i^S}{H_i^f} \geq 0, \tag{F.8}$$

with strict inequality whenever $H_i^S > 0$. Since the radical actor's best response is increasing in forbearance on the active branch, the effect of S on violence is

$$\frac{\partial v_i^*}{\partial S} = \frac{\partial v_i^*}{\partial f_i}\frac{\partial f_i^*}{\partial S} \geq 0, \tag{F.9}$$

which is strictly positive whenever $H_i^S > 0$. Hence, weaker political constraints increase violence by increasing government forbearance, and strictly so when permissiveness strictly relaxes at least one relevant marginal cost.

Opportunity. To characterize how the response varies with opportunity, consider quadratic private costs, $K_i(v_i) = \chi v_i^2/2$, with $\chi > 0$, holding all other primitives fixed. In an active location,

$$v_i^*(S, E_i) = \frac{r_i - L + [\pi(E_i) + L]f_i^*(S, E_i)}{\chi}.$$

Along a smooth interior equilibrium,

$$\frac{\partial^2 v_i^*}{\partial S\,\partial E_i} = \frac{\pi_E(E_i)}{\chi}\frac{\partial f_i^*}{\partial S} + \frac{\pi(E_i)+L}{\chi}\frac{\partial^2 f_i^*}{\partial S\,\partial E_i}.$$

Higher opportunity therefore amplifies the response of violence if it does not reduce the government's response to permissiveness:

$$\frac{\partial^2 f_i^*}{\partial S\,\partial E_i} \geq 0. \tag{F.10}$$

This is an additional sufficient condition, rather than a consequence of the baseline assumptions. The amplification is strict where forbearance responds strictly to permissiveness. The comparison concerns active locations with $0 < f_i^* < 1$. Where full tolerance already prevails, no enforcement margin remains to relax.[61]

Activation. Higher opportunity lowers the actor's activation threshold (F.4), holding other primitives fixed. As permissiveness rises, different locations may become active at different points. Within a dormant location, however, positive forbearance is strictly dominated: it imposes additional costs without producing violent output. Equilibrium forbearance therefore remains zero until inducing positive violence becomes worthwhile. The model yields two empirical predictions.

Prediction 1: Political permissiveness weakly increases violence. A more permissive environment weakly increases government forbearance and equilibrium violence. Violence rises when greater tolerance activates a previously dormant actor or increases violence by an already active actor.

Prediction 2: Opportunity can amplify the response to permissiveness. Holding other primitives fixed, violence responds more strongly where territorial gains are more feasible, under quadratic private costs and the stated complementarity condition. This comparison applies to active locations where enforcement can still relax.

F.6. A Parametric Illustration

The basic monotonicity and activation results allow general convex private costs. The following quadratic example also illustrates the conditional opportunity prediction.

[61] The ranking is local; finite-shock comparisons require the conditions throughout the relevant range.

Consider

$$\pi(E_i) = \theta E_i, \qquad K_i(v_i) = \frac{\chi}{2} v_i^2, \qquad C_i(f_i, v_i; S) = \frac{1}{2} c_0 e^{-\phi S} f_i^2 + \frac{\gamma}{2} v_i^2,$$

with $\theta, \chi, c_0, \phi > 0$ and $\gamma \geq 0$. A higher S lowers the direct cost of forbearance, consistent with $C_i^{fS} < 0$. The radical actor's best response is

$$v_i^*(f_i) = \max\left\{0,\ \frac{r_i - L + f_i(L + \theta E_i)}{\chi}\right\},$$

and the activation threshold, when it lies in the unit interval, is $\bar{f}_i = (L - r_i)/(L + \theta E_i)$, which is decreasing in E_i. Substituting the best response into the government's payoff gives the reduced objective

$$W_i(f_i; S) = \lambda f_i \theta E_i v_i^*(f_i) - \frac{1}{2} c_0 e^{-\phi S} f_i^2 - \frac{\gamma}{2} \left(v_i^*(f_i)\right)^2, \qquad f_i^* \in \arg\max_{f_i \in [0,1]} W_i(f_i; S).$$

The radical best response does not shift directly with S; the government's utility curve does, and f_i^* moves to the right. Higher opportunity raises θE_i and lowers $\bar{f}_i$, so a given relaxation in enforcement has a larger behavioral effect and violence becomes active at lower levels of tolerance. The reduced objective is piecewise quadratic in f_i, so f_i^* is computed by exact comparison of the two endpoints, the activation kink $\bar{f}_i$, and the interior stationary point of the active branch when it is admissible, selecting the largest maximizer in case of ties. For the illustrative parameterization underlying Figure F.38 ($\lambda = 0.90$, $\theta = 1.20$, $L = 1$, $r_i = 0.81$, $\chi = 1$, $\gamma = 1.00$, $c_0 = 1.00$, $\phi = 1$; Table F.12), the complementarity condition (F.10) is verified numerically: on a grid of $E_i \in [0.3, 1.5]$ and $S \in [0, 0.8]$, the discrete cross-partial $\partial^2 f_i^* / \partial S\, \partial E_i$ is strictly positive at every grid point whose finite-difference stencil lies entirely within a smooth interior-active region, that is, with the interior stationary point selected and $0 < f_i^* < 1$ at every point the stencil uses, so that no difference crosses an activation or saturation boundary. This is a property of the illustrative parameterization, not a proof of the general condition.

Figure F.38 shows the mechanism. The solid curve reports the radical actor's best response $v_i^*(f_i)$, measured on the left axis. The dashed curve reports the government's utility $W_i(f_i; S)$, measured on the right axis. The vertical dashed line marks the government's equilibrium choice f_i^*.

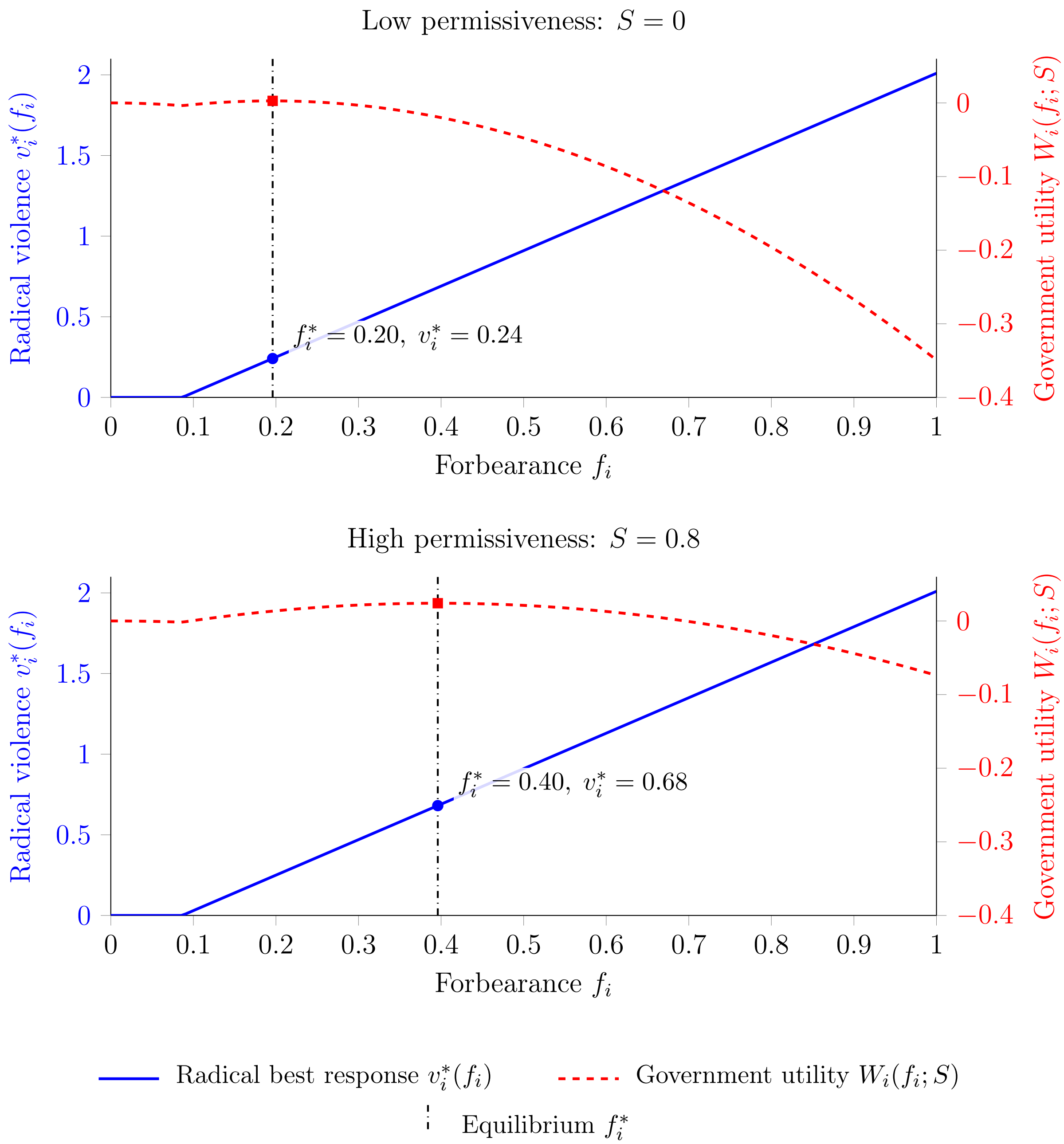

Figure F.38: Equilibrium forbearance and violence under low and high political permissiveness. The solid curve shows the radical actor's best response $v_i^*(f_i)$, measured on the left axis. The dashed curve shows government utility $W_i(f_i; S)$, measured on the right axis. The illustrative parameterization is $\lambda = 0.90$, $E_i = 1$, $\theta = 1.20$, $L = 1$, $r_i = 0.81$, $\chi = 1$, $\gamma = 1.00$, $c_0 = 1.00$, and $\phi = 1$. Moving from $S = 0$ to $S = 0.8$ lowers the cost of forbearance, shifts the government's utility-maximizing choice from $f_i^* = 0.20$ to $f_i^* = 0.40$, and increases equilibrium violence from $v_i^* = 0.24$ to $v_i^* = 0.68$.

F.7. Dynamic Extension: Endogenous Institutional Leverage and Persistence

The static model explains the immediate activation of violence but treats the political environment as exogenous. I now allow tolerated radical action to feed back into the future institutional environment. The purpose of the extension is descriptive: to show how this feedback can generate persistence and, when sufficiently strong, threshold dynamics in which temporary shocks have different long-run consequences.

Setup

Time is discrete, $t = 0, 1, 2, \ldots$. Let $b_t \in [0, 1]$ denote the institutional leverage of the radical settler constituency, and define effective permissiveness as

$$\widetilde{S}_t = S_t + \kappa b_t, \qquad \kappa > 0,$$

where S_t is the external component. In each period the static game is played exactly as above with $\widetilde{S}_t$ in place of S. Leverage, like S_t, enters only the government's cost of tolerating radical action, so λ remains fixed and the static results carry over: by the global monotonicity result, f^*_{it} and v^*_{it} are nondecreasing in $\widetilde{S}_t$, and strictly increasing on an active interior branch with $C_i^{fS} < 0$. Let

$$A_t = \frac{1}{N} \sum_{i=1}^{N} f^*_{it}\, \pi(E_i)\, v^*_{it}$$

denote the aggregate politically productive output of tolerated radical action, the same object the government internalizes location by location. Leverage evolves according to

$$b_{t+1} = (1 - \delta) b_t + \eta (1 - b_t) A_t, \qquad \eta > 0, \quad \delta \in (0, 1). \tag{F.11}$$

The extension therefore adds one state and three parameters: κ governs how strongly institutional leverage relaxes future constraints on forbearance, η how strongly politically productive tolerated action builds leverage, and δ the rate at which leverage depreciates. The factor $(1 - b_t)$ captures diminishing room for further institutional penetration. The period-t government takes the future evolution of b_t as outside its current objective.

Transition Map, Steady States, and Stability

For a fixed external environment S, write

$$A^*(b;S) = \frac{1}{N}\sum_{i=1}^{N} f_i^*(S+\kappa b)\,\pi(E_i)\,v_i^*(S+\kappa b)$$

for aggregate output at the static equilibrium. The dynamics reduce to the one-dimensional map

$$T_S(b) = (1-\delta)b + \eta(1-b)A^*(b;S), \qquad b_{t+1} = T_S(b_t), \tag{F.12}$$

with drift

$$D_S(b) \equiv T_S(b) - b = \eta(1-b)A^*(b;S) - \delta b. \tag{F.13}$$

A steady state satisfies $D_S(b^*) = 0$. Positive drift raises leverage in the next period; negative drift lowers it. The transition map may jump when locations become active.

The static monotonicity result implies that aggregate output is nonnegative and nondecreasing in both institutional leverage and external permissiveness. Let $\bar{A}$ bound aggregate output over the full range of leverage and external environments considered. Assume

$$\eta\bar{A} + \delta \leq 1. \tag{F.14}$$

This restriction keeps leverage within $[0,1]$ and ensures that higher current leverage cannot produce lower leverage next period. It permits kinks and branch switching as locations move between dormant, interior, and corner regimes; no differentiability is required. The restriction is sufficient rather than necessary, and how restrictive it is depends on the parameters.

Lemma 1 (Existence). *Under these conditions, for every fixed S the transition map T_S is an order-preserving self-map of $[0,1]$ and therefore admits at least one steady state.*

Proof. Nonnegativity of A^* gives $T_S(b) \geq 0$, and $A^* \leq \bar{A}$ gives $T_S(b) \leq \eta\bar{A} + b(1 - \delta - \eta\bar{A}) \leq 1 - \delta < 1$ by (F.14). For $b' > b$, monotonicity of A^* in b gives

$$T_S(b') - T_S(b) \geq (b'-b)\big[1-\delta-\eta A^*(b;S)\big] \geq (b'-b)\big[1-\delta-\eta\bar{A}\big] \geq 0,$$

so T_S is order preserving. Since $[0,1]$ is a complete lattice, Tarski's fixed-point theorem implies that T_S has at least one fixed point. ■

Persistence

Proposition 2 (Persistence). *Let b_0 be a steady state under S_0. Suppose $S_t = S_H > S_0$ for $t = 1, \ldots, T$, after which $S_t = S_0$, and suppose*

$$A^*(b_0; S_H) > A^*(b_0; S_0). \tag{F.15}$$

Then $b_{T+1} > b_0$. Hence, immediately after the external environment reverts,

$$\widetilde{S}_{T+1} = S_0 + \kappa b_{T+1} > S_0 + \kappa b_0 = \widetilde{S}_0,$$

so forbearance and violence remain weakly above their pre-shock equilibrium levels. A sufficient condition for (F.15) is that at least one location with $\pi(E_i) > 0$ is on an active interior branch at b_0 and permissiveness strictly lowers at least one relevant marginal cost there, so that $\partial f_i^* / \partial S > 0$.

Proof. The shock arrives at $t = 1$ with $b_1 = b_0$ predetermined. Since $T_{S_0}(b_0) = b_0$, condition (F.15) gives

$$b_2 = T_{S_H}(b_0) = (1 - \delta) b_0 + \eta(1 - b_0) A^*(b_0; S_H) > T_{S_0}(b_0) = b_0.$$

If $b_t \geq b_0$ for some $t \leq T$, then because T_{S_H} is nondecreasing, $b_{t+1} = T_{S_H}(b_t) \geq T_{S_H}(b_0) = b_2 > b_0$. Induction gives $b_{T+1} > b_0$. At $t = T + 1$ the external environment has returned to S_0 but b_{T+1} is predetermined, so $\widetilde{S}_{T+1} > \widetilde{S}_0$; the final claim follows from the global monotonicity result. For the sufficient condition, global monotonicity combined with the strict local increase at b_0 implies that f_i^*, and hence v_i^* and $f_i^* \pi(E_i) v_i^*$, are strictly higher at S_H than at S_0 in that location, while no other location's output falls. ■

The proposition establishes persistence immediately after the external shock ends. Leverage eventually returns toward its baseline level if the post-shock state remains in the baseline steady state's basin of attraction. Otherwise, the model may generate a lasting change in the political environment.

Threshold Dynamics

Remark 3 (Threshold dynamics). *Suppose that, for the baseline environment S_0, the drift has three zeros $b_L < b_U < b_H$ with $D_{S_0}(b) > 0$ on $[0, b_L)$, $D_{S_0}(b) < 0$ on (b_L, b_U), $D_{S_0}(b) > 0$ on (b_U, b_H), and $D_{S_0}(b) < 0$ on $(b_H, 1]$. Suppose the system starts at b_L before the positive shock. If $b_{T+1} \in [b_L, b_U)$, leverage subsequently weakly decreases and remains in that interval. If $b_{T+1} > b_U$, leverage never returns below b_U. If aggregate output is* *also continuous in leverage, these paths converge to b_L and b_H, respectively.*[62]

Proof. If $b_{T+1} \in (b_U, b_H)$, then $D_{S_0}(b_{T+1}) > 0$ gives $T_{S_0}(b_{T+1}) > b_{T+1} > b_U$, while monotonicity of T_{S_0} and $T_{S_0}(b_H) = b_H$ give $T_{S_0}(b_{T+1}) \leq b_H$. If $b_{T+1} \geq b_H$, monotonicity gives $T_{S_0}(b_{T+1}) \geq b_H > b_U$, and $D_{S_0} \leq 0$ on $[b_H, 1]$ gives $T_{S_0}(b_{T+1}) \leq b_{T+1}$. By induction, $b_t > b_U$ for all $t \geq T + 1$; the path is nondecreasing and bounded above by b_H in the first case, and nonincreasing and bounded below by b_H in the second. If instead $b_{T+1} \in [b_L, b_U)$, then $D_{S_0}(b_{T+1}) \leq 0$ and $T_{S_0}(b_{T+1}) \geq T_{S_0}(b_L) = b_L$, so the path weakly decreases and remains in $[b_L, b_U)$. The paths are monotone and bounded. Under continuity, their limits are fixed points, and the drift signs identify the corresponding limits: b_L is the only zero of the drift in $[b_L, b_U)$, and b_H is the only zero in $(b_U, 1]$. ■

The threshold separates regions that the system cannot leave after the shock. Convergence to the corresponding steady states requires the additional continuity condition or separate verification in the numerical illustration.

Numerical Illustration

The numerical exercise is a stylized descriptive illustration. The illustrative parameterization is chosen to display a low steady state, a threshold, and a high steady state; it is not fitted to observed data. Parameter values and period lengths are illustrative and have no quantitative empirical interpretation. Within-period behavior is the parametric specialization of the static model above, unchanged, with $N = 400$ locations that differ only in E_i, evenly spaced on $[0, 1]$. Because the reduced objective is piecewise quadratic in f_i, the government's choice in each location is computed by exact comparison of the two endpoints, the activation kink, and the interior stationary point when admissible, with ties resolved in favor of the largest maximizer. Table F.12 reports the parameters of the static and dynamic illustrations side by side.

Figure F.39 tells the dynamic story in four panels. Panel (a) shows the feedback: mean violence rises with leverage. Panel (b) shows where the steady states come from, as the three crossings of the accumulation term $\eta(1-b)A^*(b; S_0)$ and the depreciation term δb. Panel (c) shows the transition map against the 45-degree line, with the phase line beneath it marking the direction of motion in each interval: toward b_L and b_H, and away from b_U. Panel (d) shows two temporary shocks of equal size but different duration: the

[62]Heterogeneity does not eliminate activation jumps in a finite set of locations.

shorter leaves leverage below b_U and returns toward b_L, while the longer crosses b_U and converges to b_H.

Table F.12: Illustrative Parameterizations of the Static and Dynamic Examples

	Static illustration (Figure F.38)	Dynamic illustration (Figure F.39)
Static primitives		
Government internalization λ	0.90	0.90
Return to opportunity θ in $\pi(E_i) = \theta E_i$	1.20	2.00
Enforcement cost L	1	1
Intrinsic payoff r_i	0.81	0.81
Private cost χ in $K_i(v_i) = \chi v_i^2/2$	1	1
Backlash cost γ	1.00	1.00
Forbearance cost c_0 in $c(S) = c_0 e^{-\phi S}$	1.00	2.60
Cost sensitivity ϕ	1	1
Opportunity E_i	1	$(i - \frac{1}{2})/N$
Number of locations N	1	400
Dynamic feedback		
Leverage-to-permissiveness κ	–	1.00
Accumulation η	–	0.30
Depreciation δ	–	0.15
External environment and shocks		
Baseline S_0	0	0
High permissiveness S_H	0.8	0.3
Shock durations T (periods)	–	2 (short), 4 (long)
Bound $\bar{A} = A^*(1; S_H)$	–	≈ 1.252
$\eta\bar{A} + \delta$	–	≈ 0.526
Solution and selection rule		
Government choice	exact comparison of $\{0, \bar{f}_i, \tilde{f}_i, 1\}$	
Tie-breaking	largest maximizer	
Baseline steady states (b_L, b_U, b_H)	–	$\approx (0.054,\ 0.258,\ 0.557)$

Notes: $\bar{f}_i$ is the activation threshold (F.4) and $\tilde{f}_i$ the interior stationary point of the active-branch objective when admissible. The complementarity check for the static illustration uses the grid $E_i \in [0.3, 1.5]$, $S \in [0, 0.8]$. Parameter values and period lengths are illustrative and have no quantitative empirical interpretation.

The extension separates immediate activation from longer-run political feedback. In the static model, radical actors are objects of forbearance. In the dynamic extension, successful tolerated action can increase their leverage over the institutions that determine future tolerance. A temporary external shock can therefore have effects that outlast the shock itself and, when the feedback is sufficiently strong to generate multiple steady states, can move the system to a persistently more permissive equilibrium. The post-2021 pattern—settler violence that does not immediately revert under the Biden administration or the Bennett–Lapid government, and figures aligned with the radical

Figure F.39: Dynamic Extension: Feedback, Multiple Steady States, and Temporary Shocks

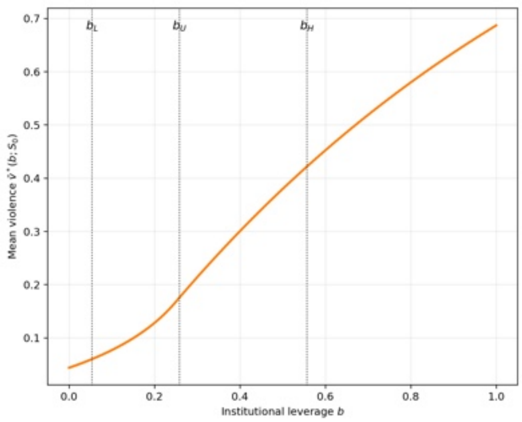

(a) Feedback: violence rises with leverage b

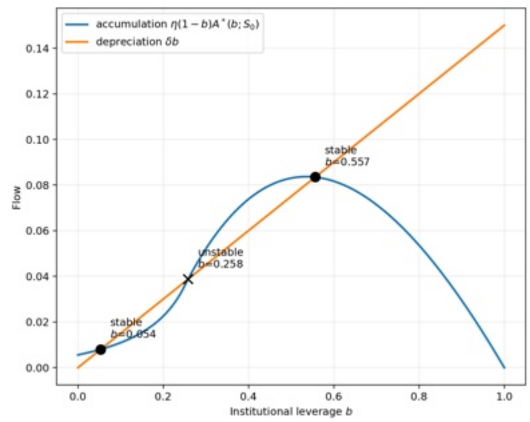

(b) Steady states: accumulation vs. depreciation

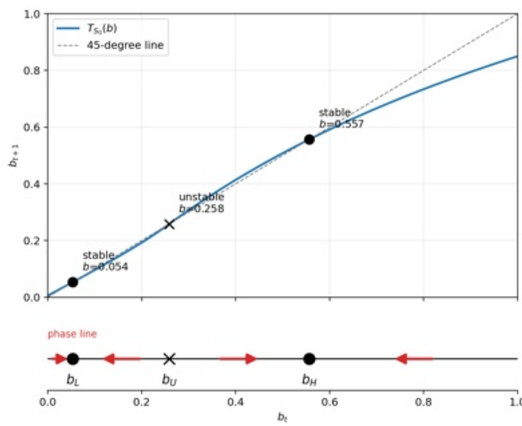

(c) Transition map and phase line

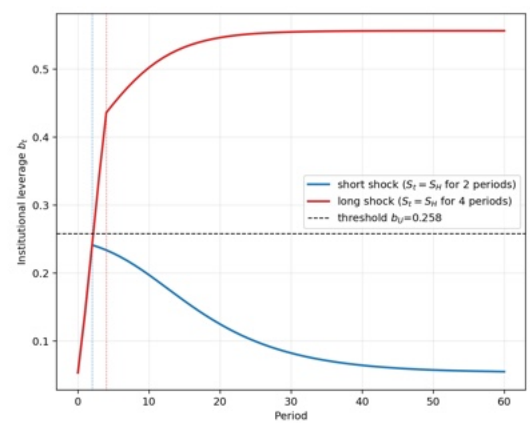

(d) Short shock returns toward b_L; long shock tips to b_H

Notes: Stylized illustration of the dynamic extension, not fitted to observed data. Locations differ only in territorial opportunity E_i, evenly spaced on $[0, 1]$ ($N = 400$); all other primitives are common, and within-period behavior is the parametric specialization of the static model. The illustrative parameterization is chosen to generate three steady states, each verified numerically as a zero of the baseline drift: a low steady state $b_L \approx 0.054$, a threshold $b_U \approx 0.258$, and a high steady state $b_H \approx 0.557$. Convergence toward b_L and b_H and divergence from b_U are verified by simulation from perturbed initial conditions. In Panel (d), a short shock ($S_t = S_H$ for 2 periods) leaves leverage below the threshold and returns toward b_L, while a long shock ($S_t = S_H$ for 4 periods) crosses the threshold and converges to b_H. Parameter values and period lengths are illustrative and have no quantitative empirical interpretation; they are reported in Table F.12.

settler movement entering portfolios directly relevant to policing and settlement policy—is compatible with this mechanism. The dynamic extension is descriptive, however, and the historical pattern does not identify the feedback channel empirically.[63]

[63]The feedback is related to models of endogenous institutional change (Acemoglu et al., 2015) and of delegation of violence to aligned actors (Bisin et al., 2026), but differs in that leverage changes the cost of forbearance rather than the government's objective and requires no initial delegation of decision rights.

G. Methodology for LLM-Assisted Classification

The following prompt was fed to GPT-5-mini and used to classify the violent events in the ACLED dataset:

> *You are coding violent events in the West Bank for academic research.*
>
> *Your task is to classify the event described below according to strict definitions. Follow the rules carefully. When information is unclear, apply conservative coding.*
>
> *EVENT DESCRIPTION:*
> *{event_text}*
>
> *DEFINITIONS*
>
> *1) PERPETRATOR*
>
> *Identify the actor who INITIATED the violent action.*
>
> *Use ONLY the following categories:*
>
> *- Palestinian Civilians: individual Palestinians acting without explicit organizational affiliation.*
> *- Palestinian Militias: organized armed groups (e.g., Hamas, Islamic Jihad, Al-Aqsa Martyrs Brigades, etc.). Use ONLY if explicit organizational affiliation is mentioned in the description.*
> *- Israeli Settlers/Civilians: Israeli civilians or settlers acting outside official military structures.*
> *- Israeli Military: IDF soldiers, Israeli security forces, border police, or other officially deployed Israeli forces.*
> *- Palestinian National Authority: official Palestinian Authority security forces.*
> *- Other: actors that clearly do not fall into any of the categories above.*
>
> *Rules:*
>
> *- Identify the actor who FIRST initiated the violent action. Initiating actions include, but are not limited to: military raids, arrest operations, airstrikes, shootings, stabbings, stone-throwing, arson, use of explosive devices, physical assault, and destruction of property.*

- A military or police raid into an area counts as the initiating action. If the opposing side responds with violence during or immediately after a raid, code the raiding force as the perpetrator.
- If one actor initiates violence and another actor retaliates, ONLY the initiating actor is the perpetrator.
- If affiliation is NOT explicitly stated, assume civilian (not militia).
- Do NOT infer militia status from weapons, organization, tactics, or coordination.

Ambiguous initiation rule:

- If the description clearly involves multiple actors but it is NOT possible to determine who initiated the violence (e.g., "clashes erupted", "both sides exchanged fire"), classify the perpetrator as a COMBINATION of actors involved.
- In that case, include all actor categories mentioned in the description as a list.

Example:
["Israeli Settlers/Civilians", "Palestinian Civilians"]

2) TARGET

Identify the PRIMARY intended target of the attack.

Use the same actor categories listed above.

Rules:

- The target is the group being attacked, NOT actors who retaliate later.
- If multiple actors participate in violence, but the primary target is clear, code the intended target.
- If the target cannot be determined, assign "Other".

3) CASUALTIES

Casualties include BOTH killed and injured individuals.

Rules:

- Count ONLY individuals explicitly reported as killed or injured.
- If no casualties are reported for a group, assign 0.
- Do NOT infer or estimate numbers.

- Do NOT count arrests, detentions, or property damage as casualties.

- If an attacker is killed or injured, count them as a casualty within their own actor category.

OUTPUT FORMAT

Return ONLY a JSON object that matches the required schema.
Do NOT include explanations or additional text.

The model was therefore asked to identify the main perpetrator of the event, the main target, and the number of casualties among Palestinian civilians, Israeli settlers/civilians, Palestinian militants, and Israeli military personnel. The allowed actor categories were Palestinian Civilians, Israeli Settlers/Civilians, Palestinian Militias, Israeli Military, Palestinian National Authority, and Other. When multiple actors were involved and it was not possible to determine who initiated the violence, the perpetrator was coded as a combination of actors. Targets could also be coded as a combination when appropriate. The model was explicitly instructed to classify militia involvement only when organizational affiliation was directly stated in the event description, and otherwise to default to civilians.
As for casualties, the model was instructed to count only individuals explicitly reported as killed or injured. If no casualties were reported for a group, the value was set to 0. Arrests, detentions, and property damage were not counted as casualties. The output of the classification is shown in Figures G.40 and G.41: Figure G.40 displays bar charts of the yearly distribution of violent events by perpetrator and target type, while Figure G.41 shows the corresponding monthly time series.
Prior to the main analysis, I perform a deduplication exercise on the ACLED dataset to remove redundant records that correspond to the same real-world incident. The procedure computes sentence-transformer embeddings for all event descriptions and flags same-day pairs that occur within 500 meters of each other and have a cosine similarity above 0.5. Each flagged pair is then verified by GPT-4o-mini, which is asked to judge whether the two records describe the same incident. This yields 145 confirmed duplicate event IDs across the full dataset, which are excluded before constructing the analysis panel.
Furthermore, to validate the results, I randomly sampled 200 events and manually classified them. The output of the validation is displayed in Figures G.42 and G.43. It is important to note that labels are considerably more difficult to assign, even for a human

Figure G.40: Main Actors of Violence in the West Bank

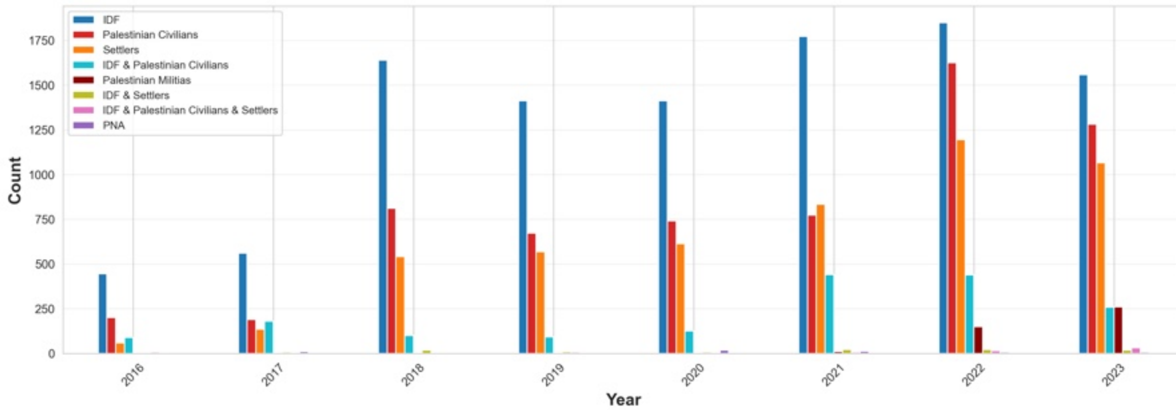

(a) Perpetrators of Violence

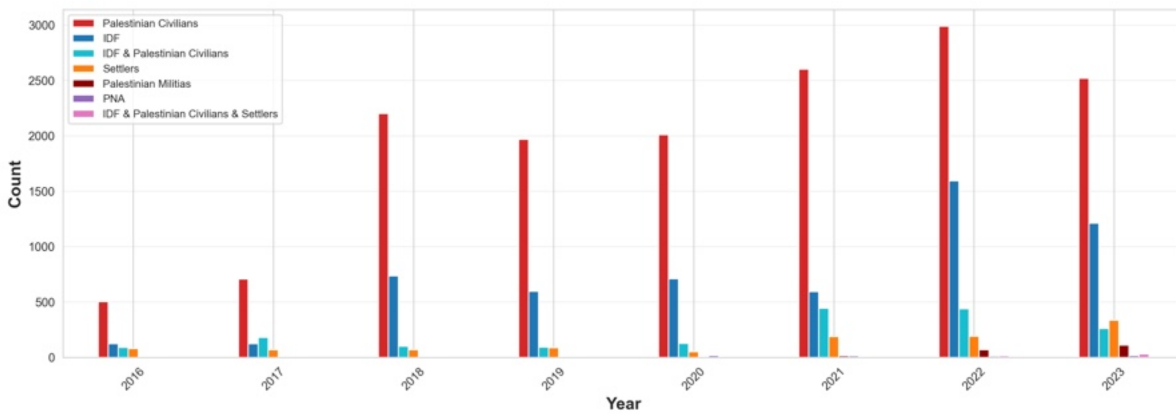

(b) Targets of Violence

Notes: Bar charts showing the distribution of violent events by perpetrator and target over time as classified by ChatGPT 5-mini. The graph only excludes events where Palestinians civilians targeted the IDF and viceversa. Source: ACLED (2024b).

coder, when the perpetrator or target involves a combination of different actors. Therefore, I only consider cases in which the classification did not include combinations. The perpetrator accuracy is 98.0%, the target accuracy is 98.5%, with a mean label accuracy of 98.2%. Figure G.43 additionally displays the confusion matrix for perpetrator–target pairs jointly. Overall, the classification appears to be very accurate and reliable.

Figure G.41: Violence Time Series: Perpetrators and Targets

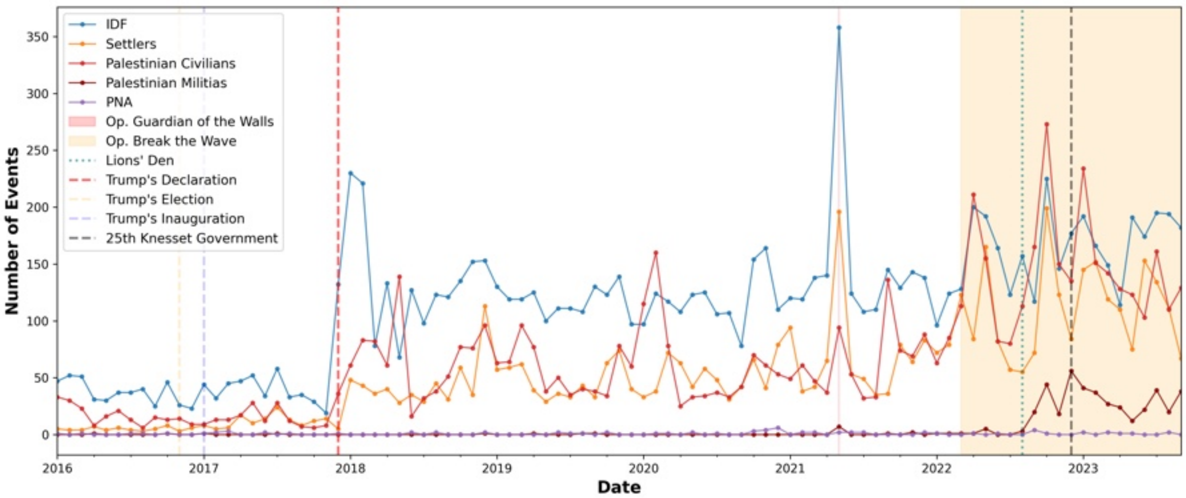

(a) Perpetrators

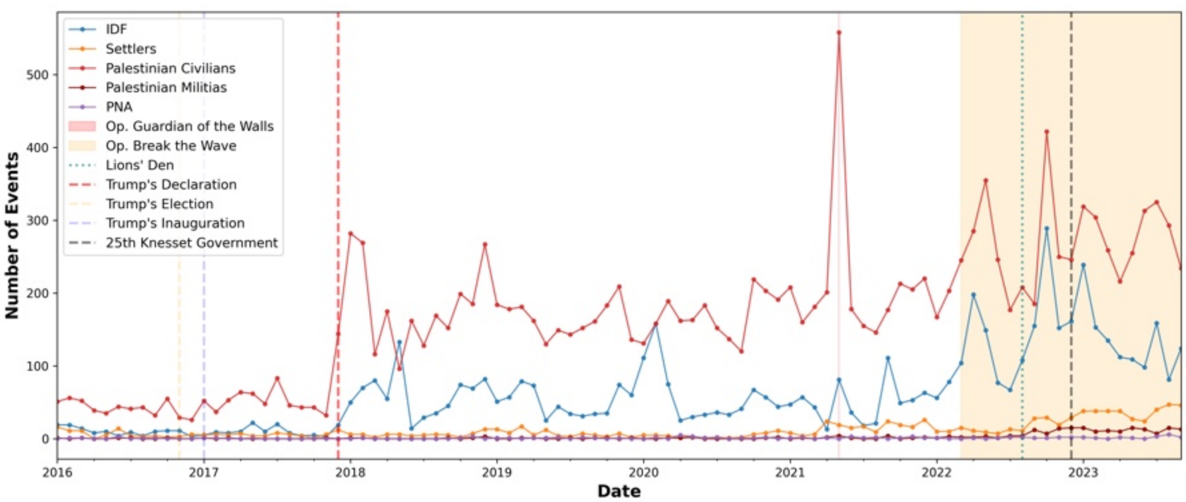

(b) Targets

Notes: Monthly time series of violent events by perpetrator type (Panel a) and target type (Panel b). The graph shows the classification output for all violent events in the data using ChatGPT 5-mini, as explained in Section 4. The dashed vertical lines indicate key dates in the political shock sequence: Trump's election (Nov 2016), inauguration (Jan 2017), and the recognition of Jerusalem (Dec 2017). Shaded areas depict important events following the Jerusalem Declaration, such as Operation Guardian of the Walls and Operation Break the Wave, as well as the birth of the Palestinian militia Lion's Den.

Figure G.42: Confusion Matrices for Perpetrators and Targets

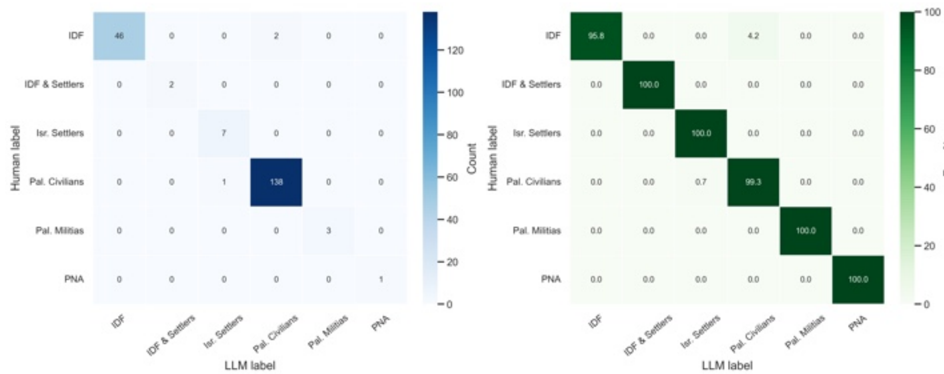

(a) Target

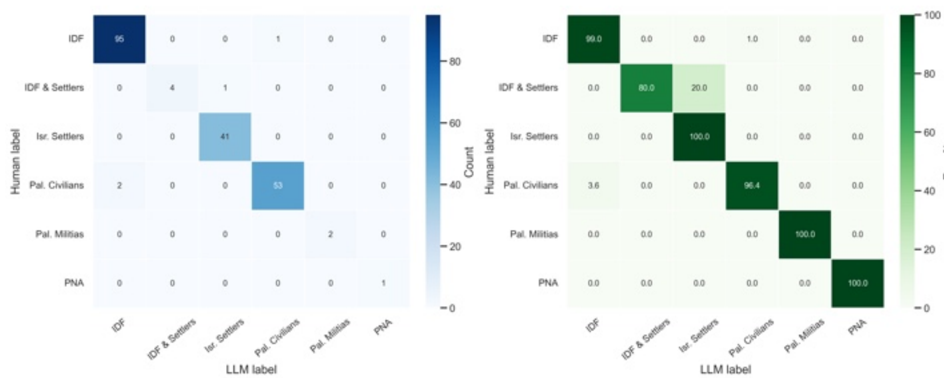

(b) Perpetrator

Notes: Confusion matrices for the classification of targets and perpetrators. Only cases in which the classification did not include combinations are considered.

Figure G.43: Confusion Matrix for Perpetrator–Target Pairs

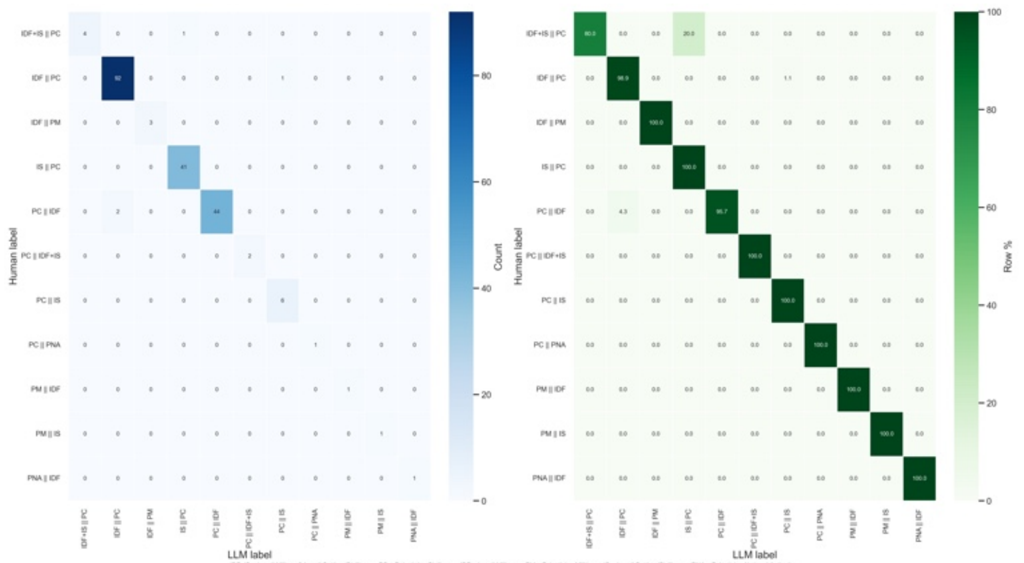

Notes: Confusion matrix for the joint classification of perpetrator–target pairs. Only cases in which neither the perpetrator nor the target classification included combinations are considered.

H. Knesset Speeches Annotation and Classification

This appendix describes the classification procedure used to measure parliamentary responses to fatality events. The objective is not to estimate forbearance directly, but to classify how topic-relevant Knesset speeches refer to fatal violence involving settlers and Palestinians. In particular, the procedure identifies whether a speech discusses the focal fatality event, the same victim–perpetrator pair, a different concrete incident, or general Israeli–Palestinian conflict, and whether it contains focal-side condemnation, enforcement demands, opposite-side deflection, or perpetrator defense.

Input data and event windows The procedure combines two inputs: a corpus of Knesset speeches and a list of fatality events involving settlers and Palestinians. Each fatality event is assigned an event index, date, label, perpetrator group, target group, and short event summary. For each event, I construct a post-event window containing all Knesset speeches delivered after the event date and within the following 15 days:

$$t_e < t_s \leq t_e + 15,$$

where t_e is the fatality-event date and t_s is the speech date. A speech can enter multiple event windows if it falls within 15 days of multiple fatality events. For this reason, the classification is performed at the speech–event level rather than only at the speech level.

Pass 1: topic-relevance filtering Before focal-event classification, I first pass it speeches to gpt-4o-mini, asking it to assess whether a speech discusses physical violence between Israelis and Palestinians. If the speech is not relevant to the topic, it is excluded from further analysis.

Pass 2: focal-event classification The second pass classifies each topic-relevant speech–event pair. Because the same speech may fall into several fatality-event windows, the cache key is defined as `speech_uid|event_idx`. Thus, the same speech is classified independently for each focal event. This is necessary because a speech may be focal with respect to one event, refer to a same-pair incident with respect to another, or be unrelated to a third.

The focal-event classification uses the model `gpt-5-mini`. The prompt version used in the analysis is `v3`. The system prompt is reported verbatim below.

System prompt

```
You are analyzing Israeli Knesset speeches in Hebrew.
```

```
You will receive:
1. A focal fatality event (date, type, victim group,
   perpetrator group, summary).
2. One Knesset speech delivered shortly after that event.

Your task: decide whether the speech discusses the focal event,
a similar type of violence, a different concrete incident,
or only general conflict.

--- Rules -----------------------------------------------------------
FOCAL EVENT IDENTIFICATION:
- Do not classify a speech as focal_event unless it contains
  identifying information: victim name, village/location,
  date/timing, specific outpost, stabbing/shooting specifics,
  or an unmistakable reference to this incident.
  Vague mentions of 'settler violence' or 'conflict in the
  territories' do not qualify.

FOCAL EVENT CONFIDENCE LEVELS (apply strictly):
- high: speech names the victim, location, or gives
  unmistakable details.
- medium: speech likely refers to the focal event but does
  not name it explicitly.
- low: uncertain. If low, also set
  focal_event_mentioned = false.

RELATIONSHIP CATEGORIES (mutually exclusive, use the most
  specific valid one):
  1. focal_event    -- discusses this specific incident
  2. same_pair_type -- same victim/perpetrator type but not
                       this exact incident
  3. different_incident -- a different concrete violent incident
  4. general_conflict   -- Israeli-Palestinian violence
                           discussed in general terms
  5. unrelated          -- different theater, historical,
                           or clearly off-topic
  6. unclear
If the speech qualifies for focal_event, do not use
same_pair_type.
```

```
INCIDENT TYPE (incident type and perpetrator-defense framing
  are separate fields):
  settler_on_palestinian / palestinian_on_israeli /
  israeli_civilian_on_palestinian /
  idf_police_on_palestinian / general_security /
  general_conflict / other_violence / unclear

CONDEMNATION:
- explicit_condemnation = true only if the speaker explicitly
  condemns a killing or attack.
  Procedural complaints (e.g., objecting to an arrest)
  do not count.
- condemnation_target: who is being condemned
  (the perpetrator group)?

ENFORCEMENT DEMAND:
- enforcement_demand = true if the speaker calls for
  investigation, prosecution, arrest, punishment,
  evacuation of outposts, or legal enforcement action.
- enforcement_target: who is the enforcement demand
  directed against?

PERPETRATOR DEFENSE:
- perpetrator_defense_or_self_defense_frame = true if
  the speaker defends, excuses, minimizes, or reframes
  the perpetrator's actions as justified or self-defense.
- defended_actor_group: which group's perpetrator is
  being defended?

DEFLECTION TYPE:
- Choose one: none /
  deflects_to_palestinian_violence /
  deflects_to_settler_or_israeli_violence /
  deflects_to_idf_or_state_violence /
  defends_focal_or_same_side_perpetrator /
  defends_opposite_side_perpetrator /
  generalizes_without_accountability / unclear.

ALTERNATIVE INCIDENT:
```

```
- If the speech discusses a different concrete incident
  (not the focal event), provide a brief English description
  in alternative_incident_summary.
  Use 'None' if the speech is about the focal event or
  general conflict.

- Return ONLY valid JSON. No markdown, no explanation
  outside the JSON.
```

The user message is constructed separately for each speech–event pair by inserting the focal-event metadata and the speech text into the following template. The template is reported verbatim below.

Derived rhetorical outcomes The raw model outputs are transformed into the rhetorical outcomes used in the analysis. First, I define a high-confidence focal mention as a case where the speech mentions the focal event and the model assigns high confidence:

$$HighConfFocal_{se} = \mathbf{1}\big\{FocalMention_{se} = 1,\ Confidence_{se} = \texttt{high}\big\}.$$

Second, I define a broader focal-or-same-pair indicator:

$$FocalOrSamePair_{se} = \mathbf{1}\big\{Relationship_{se} \in \{\texttt{focal\_event}, \texttt{same\_pair\_type}\}\big\}.$$

This variable captures speeches that either discuss the exact fatality event or discuss the same victim–perpetrator pair without identifying the exact event.

The main accountability variables require both a focal-or-same-pair relationship and correct targeting of the focal perpetrator side. For Palestinian-killed-by-settler events, the focal perpetrator side is coded as settler, Israeli civilian, or Israeli state. For settler-killed-by-Palestinian events, the focal perpetrator side is coded as Palestinian. Strict focal-side condemnation is therefore defined as:

$$StrictCondemnation_{se} = FocalOrSamePair_{se} \times ExplicitCondemnation_{se} \times CorrectCondemnationTarget_{se}.$$

Strict focal-side enforcement is defined analogously:

$$\begin{aligned}StrictEnforcement_{se} = FocalOrSamePair_{se} &\times EnforcementDemand_{se} \\ &\times CorrectEnforcementTarget_{se}.\end{aligned}$$

The script also constructs a broader focal-side enforcement measure that does not require the speech to be classified as focal-or-same-pair, but does require an enforcement demand against the focal perpetrator side.

Finally, I define opposite-side attention. Unlike the condemnation and enforcement measures, opposite-side attention does not require the speech to be classified as focal or same-pair. A speech is coded as opposite-side attention if it redirects discussion toward violence committed by the other side—regardless of whether it engages with the focal event. For Palestinian-killed-by-settler events, a speech is coded as opposite-side attention if it redirects attention to Palestinian violence or defends the opposite-side perpetrator. For settler-killed-by-Palestinian events, a speech is coded as opposite-side attention if it redirects attention to settler or Israeli violence, IDF or state violence, or defends the opposite-side perpetrator. For example, after a settler kills a Palestinian, a speech that discusses Palestinian attacks on Israelis or defends settler actions without addressing the focal incident would be coded as opposite-side attention. This captures cases in which the speech moves away from accountability for the focal perpetrator side and toward violence by the other side.

The perpetrator-side defense measure is constructed analogously and, like opposite-side attention, does not require the speech to be classified as focal or same-pair. A speech is coded as perpetrator-side defense if it defends, excuses, minimizes, or reframes as justified the actions of the focal perpetrator side. It therefore captures defense of the focal perpetrator side anywhere in the post-event window, not necessarily defense of the specific perpetrator in the focal fatality.

Aggregation After classification, the data are aggregated to the event × bloc level. The denominator is the number of unique topic-relevant speeches in event e and bloc g:

$$N_{eg} = \#\left\{\text{topic-relevant speeches in event } e \text{ and bloc } g\right\}.$$

For each rhetorical feature k, I compute the corresponding count C_{eg}^k and share:

$$Y_{eg}^k = \frac{C_{eg}^k}{N_{eg}}.$$

These event–bloc shares are the outcomes used in the parliamentary-response regressions. The aggregation also records the total number of speeches in the event window before topic filtering, allowing the analysis to distinguish the size of the speech window from the number of topic-relevant speeches.

Validation and diagnostic outputs The script exports three diagnostic objects. First, it saves a speech-level file containing the classification for each speech–event pair. Second, it saves an event–bloc panel containing the aggregated counts and shares. Third, it produces a per-event text summary reporting, for each fatality event, the number of speeches in the window, the number of topic-relevant speeches, focal-event mentions, high-confidence focal mentions, and bloc-level counts of focal attention, condemnation, enforcement, and perpetrator defense. In addition, the script exports a human-validation sample stratified by relationship-to-focal-event category and event type, with up to 15 observations per stratum and a target size of 500 rows. This validation sample is used to manually assess the quality of the LLM classifications.

Figures & Tables

Figure H.44: Number of Daily Violent Events in the West Bank

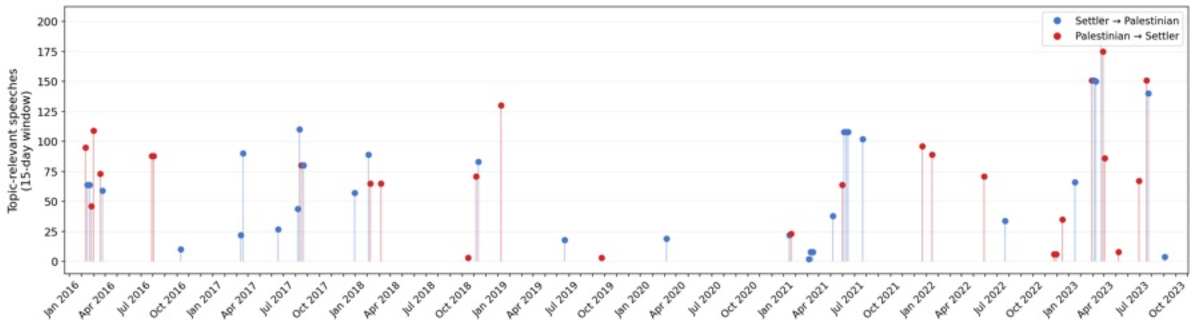

Notes: Fatalities over time in the West Bank and number of relevant speeches in the Knesset about said events. The figure only considers events in which Palestinians killed Settlers or viceversa. The y-axis is the number of relevant speeches on political violence in the West Bank in a 15-day window from every single event. The speeches need not speak explicitly about the specific event.

Figure H.45: LLM Output: Relationship to Focal Event Categories

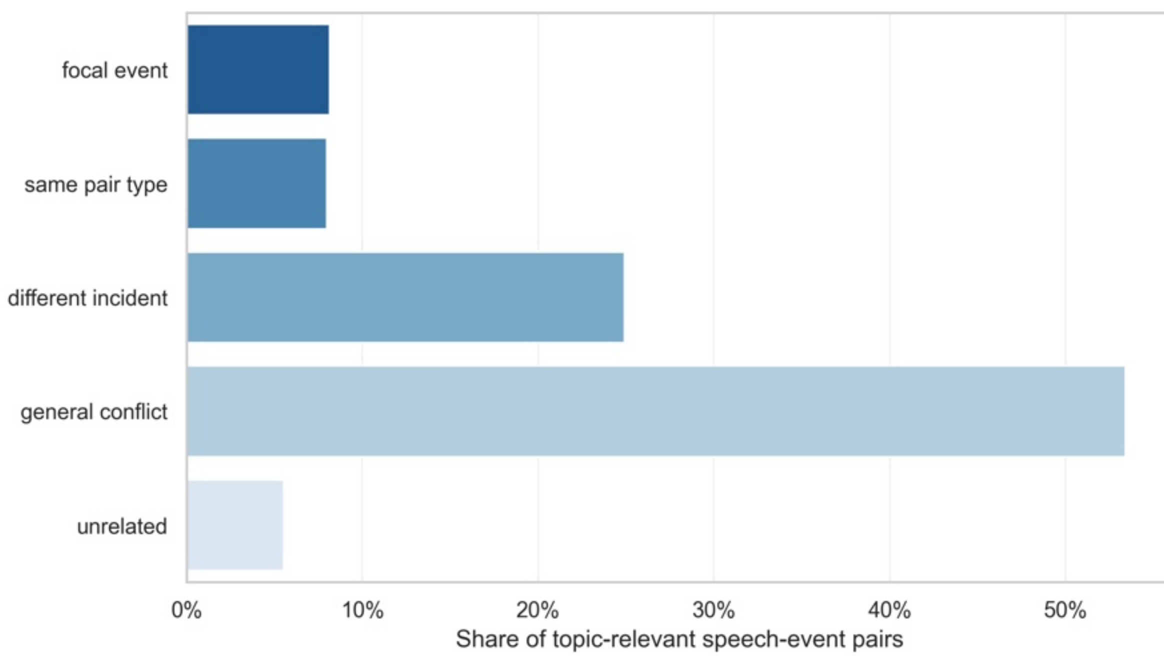

Notes: Distribution of LLM-classified mutually exclusive relationship categories of the filtered speeches. They can be classified as: 1) focal event, 2) same pair type, 3) different incident, 4) general conflict, 5) unrelated, and 6) unclear.

Figure H.46: Selective Accountability

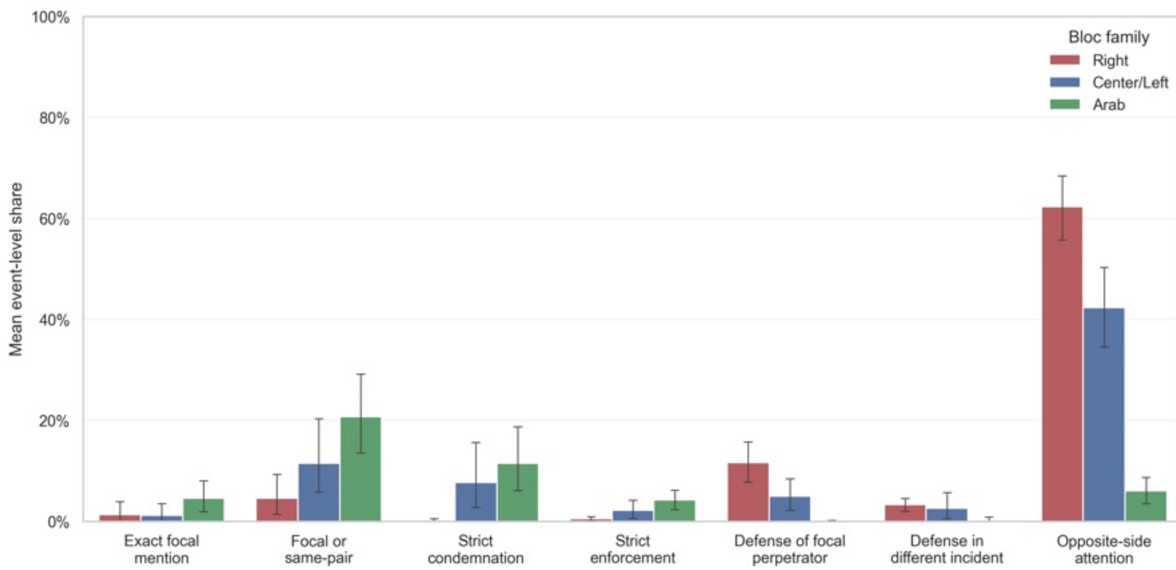

(a) After Palestinians Are Killed by Settlers

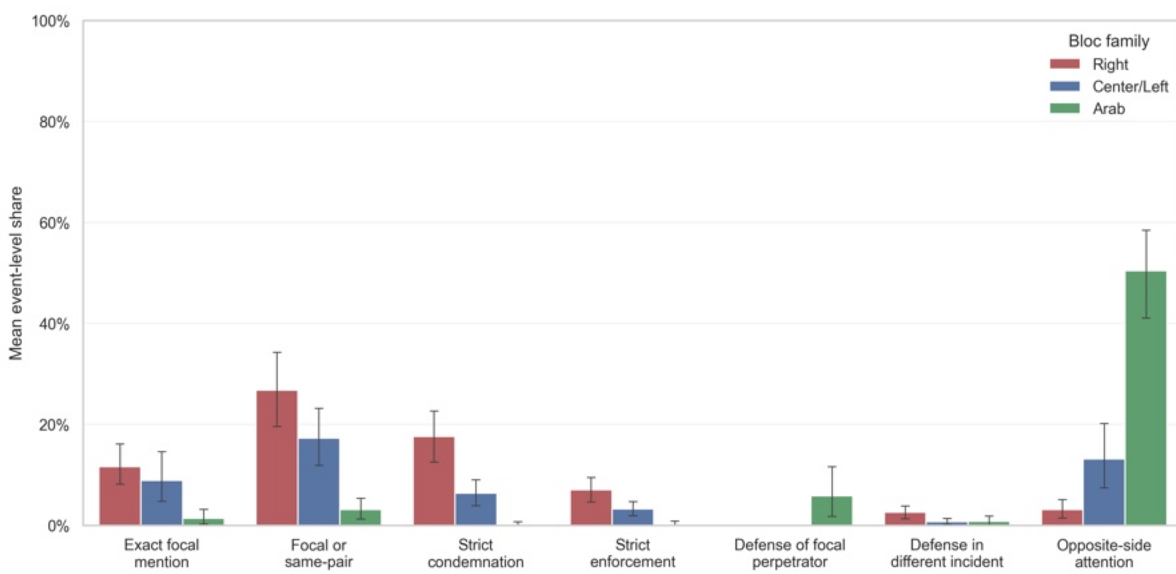

(b) After Settlers Are Killed by Palestinians

Notes: Mean event-level share of LLM-classified accountability categories in Knesset speeches following violent events, by political bloc (Right, Center/Left, Arab). Categories range from exact focal mention to opposite-side attention. Error bars indicate 95% confidence intervals.

Table H.13: Israeli Knesset parties classified by political bloc

Right	**Center**	**Arab**
Ahi	Blue and White	Arab Democratic Party
Aliyah – Our People for a Renewed Israel	Gesher	Arab National Party
Tzomet	Center Party	Ta'al
Derekh Eretz	Yiud	Hadash–Ta'al
Herut – The National Movement	Gil (Pensioners' Party)	Balad
Independent MK Amichai Chikli	Kulanu	National Unity – National Progressive Alliance
Yisrael BaAliyah	Kadima	Ra'am–Ta'al
Yamin Yisrael	Shinui	United Arab List
Likud	The Movement	Joint List
National Union – Yisrael Beiteinu	National Unity	Joint List – Balad
New Hope	The Third Way	**Religious Zionist**
Yamina	Yesh Atid	National Religious Party
Yisrael Beiteinu	Yesh Atid–Telem	National Union
Far Right	**Left**	The Jewish Home
Moledet	Independence	**Orthodox**
Jewish Power	Labor	Agudat Yisrael
Strength for Israel	Labor–Meretz	Degel HaTorah
	One Nation	Independent MK Yosef Ba-Gad
	Meretz	Shas
	The Democratic Choice	United Torah Judaism
	Mapai	**Far Left**
		Hadash

Notes: Bloc–party classification as in Goldin et al. (2024).